AD-A243 900

92-00171

DEPARTMENT OF THE AIR FORCE
AIR UNIVERSITY

AIR FORCE INSTITUTE OF TECHNOLOGY

Wright-Patterson Air Force Base, Ohio

92 1   2 142

AFIT/GAE/ENY/91D-6

DTIC
ELECTE
JAN 0 3 1992
S D
D

THE EFFECT
OF ANGLE OF INCIDENCE AND REYNOLDS NUMBER
ON HEAT TRANSFER
IN A LINEAR TURBINE CASCADE

THESIS

Steven Meschwitz
Captain, USAF

AFIT/GAE/ENY/91D-6

AFIT/GAE/ENY/91D-6

THE EF.-ECT OF ANGLE OF INCIDENCE AND REYNOLDS NUMBER

ON HEAT TRANSFER IN A LINEAR TURBINE CASCADE

THESIS

Presented to the Faculty of the School of Engineering

of the Air Force Institute of Technology

Air University

in Partial Fulfillment of the

Requirements for the Degree of

Master of Science in Aeronautical Engineering

Steven G. Meschwitz, B.S.A.E, M.S.I.E.

Captain, USAF

December 1991

Approved for public release; distribution unlimited

Acknowledgments

I would like to thank all of those who have helped during the course of this effort. The guidance of my advisor, Dr Paul King, has provided me with the ability to separate fact from fiction. The craftsmanship of the AFIT model shop has provided me with the finest of fabrications. The expertise of the AFIT aeronautical engineering technician staff has provided me with everything else. Without their help, I would not have succeeded.

I would especially like to thank my wife, Allison, for her patience and understanding and my daughter, Emily, for reminding me that there was more to life than AFIT.

Table of Contents

List of Figures

List of Tables

Roman Symbols

Symbol	Definition
c	Specific Heat ($J/kg \cdot °K$)
C_P	Pressure Coefficient
D	Diameter of a Cylinder (m)
E	Potential ($volts$); Energy ($Joules$)
f	Frequency (Hz)
h	Convective Heat Transfer Coefficient ($W/m^2 \cdot °K$)
I	Electrical Current ($Ampere$)
k	Thermal Conductivity ($W/m \cdot °K$); correction factor
N	Total Number
Nu	Nusselt Number
n	Frequency (Hz)
p or P	Pressure (kPa)
Pr	Prandtl Number
q	Dynamic Pressure or "Head" (kPa)
$\dot{q}$ or q''	Heat Flux (W/m^2)
R	Resistance (Ω/m^2)
Re	Reynolds Number
R_E	Eulerian Time Correlation (s)
St	Stanton Number
T	Temperature ($°K$)

Tu	Turbulence Intensity
u or U	Velocity (m/s)
V	Velocity (m/s); Voltage
x	Distance (m)

Greek Symbols

Symbol	Definition
α	Thermal Diffusivity (m^2/s); Seebeck Coefficient
ϵ	Emissivity
λ	Microscale (m)
Λ	Integral Scale (m)
μ	Dynamic Viscosity $(kg/m \cdot s)$
ν	Kinematic Viscosity (m^2/s)
ρ	Density (kg/m^3); Resistivity $(\Omega - m)$
σ	Stefan-Boltzman Constant $(W/m^4 \cdot {}^\circ K^4)$
τ_E	Eulerian Micro Time Scale (s)

Abstract

The AFIT linear Turbine Cascade Test Facility (TCTF) was used to study the effect of the small changes in the angle of incidence on turbine blade convective heat transfer. Other parameters in the study were the model Reynolds number and the freestream turbulence level. Characterization tests were performed to determine the feasibility of the study, followed by a series of tests designed to separate the effects of the angle of incidence, Reynolds number, and freestream turbulence level on the convective heat transfer.

For any given freestream turbulence level or angle of incidence, there is an increase in the heat transfer coefficient for an increase in the Reynolds number. For the low freestream turbulence (0.5%) configuration at a given Reynolds number, there is a decrease in the convective heat transfer coefficient with an increase in the angle of incidence, partially a result of the decrease in the cascade passage velocity and partially a result of the variation in the boundary layer behavior. For the high freestream turbulence configuration (10%) at any Reynolds number, there is an obvious increase in the convective heat transfer coefficient over that for the low turbulence configuration; however, the transitional or fully turbulent boundary layer makes it difficult to observe any relation between the convective heat transfer coefficient and the angle of incidence.

I Introduction

1.1 General

The objective of this thesis was to determine the effect of the angle of incidence to a linear turbine cascade blade row on the turbine blade surface convective heat transfer. Included were the effects due to the variation in the model Reynolds number and the freestream turbulence level.

The linear turbine cascade has been used as an experimental device for predicting and analyzing the behavior of operational turbines for almost 100 years. Because of their simplicity, flexibility, relative low cost, and over 100 years of validation, the linear turbine cascade allows the user to perform a variety of experiments with confidence in the results. The Air Force Institute of Technology (AFIT) linear Turbine Cascade Test Facility (TCTF) was the testbed for this series of experiments. Described in detail in Chapter III, the TCTF is a flexible device, allowing variation in a number of turbine cascade parameters.

Heat transfer from a turbine blade in a turbine cascade has been shown to be a function of many parameters, including the freestream turbulence intensity, the model Reynolds number, the blade geometry, and the cascade geometry. Many experimental efforts, including those of Galassi (Galassi, 1989) and Acree (Acree, 1990) using the TCTF, have explored the effects of the aforementioned parameters on the turbine blade heat transfer. Each effort has built onto the wealth of knowledge concerning turbine blade heat transfer, but no effort has supplied all of the answers. Every turbine cascade is different, and the influence of the individual cascade arrangement, secondary end-wall effects, initial conditions, and other specifics prevent "an experiment to end all experiments"; in addition, advances in instrumentation and analysis techniques continually warrant the reexamination of many issues.

1.2 Objective

The objective of this effort is to build onto that wealth of turbine blade convective heat transfer knowledge by examining the turbine blade heat transfer behavior at off-design conditions. The principal off-design parameter chosen was the turbine blade cascade angle of incidence. In order to separate the effects of turbulence and model Reynolds number, a test plan was developed to isolate and identify the influence of all turbine cascade parameters.

Unlike an axial compressor with a variable inlet guide vane and variable stators, an axial turbine is designed to operate effectively and efficiently at one operating condition which may be characterized by a number of parameters, including the model Reynolds number, freestream turbulence, and angle of incidence; however, the turbine is not always operating at the design condition. For this reason, the off-design performance is just as important as the on-design performance and deserves the same experimental and analytical considerations.

By determining the behavior of the turbine blade heat transfer at specified and controlled design and off-design conditions, the complicated heat transfer mechanisms may be more easily understood, predicted, and managed.

1.3 Method

An opportunity was available to build on the works of Galassi (Galassi, 1989) and Acree (Acree, 1990) using the TCTF where the majority of the hardware, software, and theory was in place. In order to accommodate a variable angle of incidence, the TCTF was modified upstream of the cascade test section; in addition, extensive changes were incorporated into the calibration, data acquisition, and data reduction software.

After completing the characterization of the TCTF, a test plan was developed which allowed variations in the model Reynolds number, freestream turbulence level, and angle of incidence. No attempt was made to vary the amplitude or frequency nature of the turbulence. The data was then analyzed and compared to the efforts of others, where possible and relevant.

II Theory

2.1 General

The theory required for the performance of this thesis was that of linear turbine cascade flow, heat transfer, and turbulence. Since the objective of this thesis was limited to the heat transfer behavior, the cascade theory and turbulence theory will be limited to the topics which aid the heat transfer analysis.

2.2 Cascade Theory

The bulk of the linear turbine cascade theory deals with the performance of the cascade as determined by the behavior of the flow through the cascade. No cascade "performance" theory is required for this thesis other than that needed for character-ization of the cascade flow. A well behaved cascade will exhibit certain flow properties upstream, downstream, and in the cascade passages. Without these certain flow properties, it is difficult to extrapolate the heat transfer results to real turbine behavior.

Periodicity. In general, a well behaved cascade will exhibit periodic static pressure and velocity (magnitude and direction) profiles both upstream and downstream of the cascade. The amplitude and shape of the periodicity will vary with model Reynolds number, the angle of incidence, and the turbulence level. It is beyond the scope of this work to predict the periodic profiles for the TCTF; however, periodicity is a key a characterization requirement.

Pressure Coefficient. The only other aspect of cascade theory required deals with the behavior of the flow in the cascade as determined by the nondimensional blade pressure coefficient, C_p, defined as:

$$C_p = \frac{p_i - p_\infty}{\frac{1}{2}\rho_\infty U_\infty^2} \qquad (2.1)$$

where p_l is the local static pressure on the blade surface

$\bar{p}_\infty$ is the freestream static pressure

ρ_∞ is the freesteam density

U_∞ is the freestream velocity

The term freestream here refers to the upstream cascade conditions and the quantity $\frac{1}{2}\rho_\infty U_\infty^2$ is also known as the freestream q or q_∞, commonly called the tunnel "head".

The behavior of the blade surface C_p distribution is a good indication of the overall cascade behavior. When plotted as a function of position along the chord, a turbine blade pressure distribution is formed. As the cascade parameters are varied, the pressure distribution changes and can be observed and analyzed for characterizing the cascade flow.

In addition to providing information about the general cascade behavior, manipulation of C_p yields the blade local velocity, an important parameter in evaluating the heat transfer. According to Bernoulli's equation for incompressible flow along a streamline,

$$p_l + \frac{1}{2}\rho_l U_l^2 = p_\infty + \frac{1}{2}\rho_\infty U_\infty^2 \tag{2.2}$$

where U_l is the local velocity. Combining the definition of C_p and Bernoulli's equation, the local velocity U_l can be determined:

$$U_l = \left[\frac{2q_\infty}{\rho_l}(1 - C_p) \right]^{\frac{1}{2}} \tag{2.3}$$

The local density ρ_l is determined based on the film temperature T_f

$$T_f = \frac{T_l + T_\infty}{2} \qquad (2.4)$$

where T_l is the local blade surface temperature

T_∞ is the freestream temperature

The values of U_l and ρ_l combine with the viscosity, μ, and a geometric parameter such as the surface distance, s, on an airfoil to form the local Reynolds number Re defined as:

$$Re = \frac{\rho U s}{\mu} \qquad (2.5)$$

a nondimensional quantity important for both cascade flow analysis and heat transfer analysis.

2.3 Heat Transfer Theory

Turbine blade heat transfer requires the understanding of the conductive, convective, and radiative heat transfer processes. In an actual turbine, heat is convected, conducted, and radiated from the hot combustion gases into the turbine blade surface. In the TCTF, heat transfer is studied by heating the foil surface of a specially fabricated turbine blade; in this case the heat generated in the thin foil surface is convected and radiated into the freestream and conducted into the interior of the blade, as illustrated in Figure 2.1. Whatever the situation, heat transfer into or out of the blade, nondimensional analysis allows valid comparison.

In the general case, the heat transfer to or from an object is the sum of the conductive, convective, and radiative heat fluxes:

$$\dot{q} = q''_{cond} + q''_{conv} + q''_{rad} \qquad (2.6)$$

where $\dot{q}$ is the total heat flux (W/m^2)

q''_{cond} is the conductive heat flux

q''_{conv} is the convective heat flux

q''_{rad} is the radiative heat flux

Total Heat Flux. For the TCTF, the heat flux $\dot{q}$ is the heat generated in the blade foil surface as a result of current passing through it and can be calculated based on the resistance of the foil:

$$\dot{q}_{foil} = I^2_{foil} R_{foil} \tag{2.7}$$

where I_{foil} is the current passing through the foil surface

R_{foil} is the resistance of the foil per unit area

The resistivity of the foil ρ_{foil} is a function of the local foil surface temperature and has been determined (Acree, 1990) to be

$$\rho_{foil}(\Omega - m) = 2.223 \cdot 10^{-10} T(degF) + 8.446 \cdot 10^{-7} \tag{2.8}$$

and

$$R_{foil} = \frac{\rho_{foil}}{w^2 t} \tag{2.8a}$$

where w = width of foil = 0.0508 m

t = thickness of foil = 0.0000508 m

Conductive Heat Transfer. The conductive heat flux q''_{cond} is determined from Fourier's Law of cooling:

$$q''_{cond} = -k \frac{\partial T}{\partial x} \qquad (2.9)$$

where k is the thermal conductivity and $\partial T / \partial x$ is the temperature gradient in the direction of the heat flow.

Conductive heat transfer is a process involving molecular collisions in gases and liquids and lattice vibration and free electron transport in solids; therefore, the value of k is a function of the heat transfer medium and is dependent on the material composition and temperature. For gases in particular, k varies widely with temperature. When combined with the material's density, ρ, and specific heat, c, the material's temperature dependent thermal diffusivity, α, is obtained:

$$\alpha = \frac{k}{\rho c} \qquad (2.10)$$

The magnitude of α is a good indicator of the conductive heat transfer ability of the material and a large α will conduct heat faster than a small α.

Convective Heat Transfer The convective heat flux q''_{conv} is determined from Newton's law of cooling:

$$q''_{conv} = h(T_l - T_\infty) \qquad (2.11)$$

where h is the convection heat transfer coefficient, an experimentally determined value. The convection coefficient h and the thermal conductivity k can be combined with a geometrical parameter such as the diameter of a cylinder D to form the nondimensional Nusselt number Nu defined as:

$$Nu = \frac{hD}{k} \qquad (2.12)$$

Widely used in convective heat transfer analysis, the Nu has been determined both analytically and empirically for many convective heat transfer situations, including the turbine blade. Calculation of the Nu will be explored in detail later.

Radiation Heat Transfer. The radiation heat flux q''_{rad} is based on the Stefan-Boltzmann law of thermal radiation:

$$q''_{rad} = \epsilon \sigma (T_l^4 - T_\infty^4) \qquad (2.13)$$

where ϵ is the emissivity of the surface

 σ is the Stefan-Boltzmann constant $= 5.669 x 10^{-8} \frac{W}{m^2 K^4}$

In summary, the overall heat transfer equation for the TCTF heat transfer turbine blade is

$$I_{foil}^2 R_{foil} = -k_{foam}\frac{\partial T}{\partial x} + h(T_l - T_\infty) + \epsilon_{foil}\sigma(T_l^4 - T_\infty^4) \qquad (2.14)$$

The objective of the heat transfer experiment is to obtain h, the convective heat transfer coefficient:

$$h = \frac{I_{foil}^2 R_{foil} + k_{foam}\frac{\partial T}{\partial x} - \epsilon_{foil}\sigma(T_l^4 - T_\infty^4)}{T_l - T_\infty} \qquad (2.15)$$

The Nu can then be calculated, along with another nondimensional heat transfer parameter, the St, defined as:

$$St = \frac{h}{\rho c U_\infty} = \frac{Nu}{RePr} \qquad (2.16)$$

where Pr is the Prandtl number = ν / α

$\bar{\nu}$ is the kinematic viscosity

Several empirical means exist for calculating the Nu and St numbers for a wide variety of convective heat transfer situations. Convective heat transfer is a boundary layer mechanism, highly dependent on the behavior of the boundary layer. For that reason, empirical relationships are often presented in pairs: one relationship for the laminar boundary layer case and one relationship for the turbulent boundary layer case.

<u>Turbine Blade Heat Transfer</u>. The most simplified analysis of turbine blade heat transfer approximates the curved turbine blade surface with a flat plate. For the TCTF configuration, the heated turbine blade would be approximated by a constant heat flux flat plate. A laminar analytical solution, based on boundary layer theory, is given as a function of the Re and the Pr, a common convention:

$$Nu_x = \frac{hx}{k} = 0.453 \, Re_x^{\frac{1}{2}} Pr^{\frac{1}{3}} \tag{2.17}$$

Experimental studies have verified the analytical solution above. A turbulent analytical solution, based on superposition theory, is given by,

$$Nu_x = \frac{hx}{k} = 0.03078 \, Re_x^{.8} Pr^{\frac{1}{3}} \tag{2.18}$$

A more accurate approximation of the curved turbine blade is that of a body of arbitrary shape. These analytical solutions are more complex than the flat plate, requiring simplifying assumptions, yet yield very good results. For laminar flow over an arbitrary surface, a solution is given by Eckert (Kays and Crawford, 1980):

$$St = 0.418 \frac{\mu^{\frac{1}{2}} \rho_\infty^{0.435} U_\infty^{0.435}}{[\int\limits_0^\infty \rho_\infty^{1.87} U_\infty^{1.87} dx]^{0.5}} \qquad (2.19)$$

For the turbulent case, a procedure by Ambrok (Kays and Crawford, 1980) yields

$$St = 0.0287 Pr^{-0.4} \frac{(T_l - T_\infty)^{0.25} \mu^{0.2}}{\left[\int\limits_0^x (T_l - T_\infty)^{1.25} \rho_\infty U_\infty\right]^{0.2}} \qquad (2.20)$$

Regardless of which approximation is used, the flat plate or body of arbitrary shape, the flow across the leading edge of the turbine blade can be represented as flow across a cylinder, an important case of heat transfer used in heat exchanger theory. For laminar flow across a cylinder, the Nu takes a familiar form:

$$Nu_R = 0.81 Re_R^{\frac{1}{2}} Pr^{0.4} \qquad (2.21)$$

where Re_R is calculated using the cylinder radius R and the upstream velocity.

2.4 Turbulence Theory

"Turbulent fluid motion is an irregular condition of flow in which the various quantities show a random variation with time and space coordinates, in that *statistically distinct* average values can be discerned" (Hinze, 1959). The ability to calculate distinct average values of the flow properties allows for comparative analysis based on these values.

An instantaneous turbulent property X is represented as

$$X = \overline{X} + x' \qquad (2.22)$$

where

$$\overline{X} = \frac{1}{T} \int_0^T X \, dt \qquad (2.23)$$

or, for discrete data,

$$\overline{X} = \frac{1}{N} \sum_{i=1}^{N} X_i \qquad (2.24)$$

and x' represents the instantaneous turbulent fluctuation such that

$$\overline{x'} = 0 \qquad (2.25)$$

The primary measure of turbulence used in this thesis is the relative intensity Tu, defined (for the u velocity component) as

$$Tu = \frac{u'_{rms}}{\overline{U}} \qquad (2.26)$$

where, for discrete data,

$$u'_{rms} = \left[\frac{1}{N} \sum_{i=0}^{N} u'^2_i \right]^{\frac{1}{2}} \qquad (2.27)$$

In a coordinate system where $\overline{V} = \overline{W} = 0$, the relative turbulence intensity Tu is

$$Tu = \frac{\left[\frac{(\overline{u'^2} + \overline{v'^2} + \overline{w'^2})}{3} \right]^{\frac{1}{2}}}{\overline{U}} \qquad (2.28)$$

When $u'_{rms} = v'_{rms} = w'_{rms}$, the turbulence is said to be isotropic, where the turbulent properties are independent of coordinate axes rotation.

Other measures used in this thesis for comparative purposes only are the turbulence microscale and integral scale. These scales represent the sizes of the largest and smallest eddies in the turbulent flow. The methods of calculating these scales are detailed in Appendix A.

III Apparatus

3.1 Turbine Cascade Test Facility

This investigation was performed in the AFIT Turbine Cascade Test Facility (TCTF) located in Building 19 at Wright-Patterson Air Force Base. Designed, built, and originally located at the United States Air Force Academy, the TCTF is an open circuit, draw-down tunnel powered by a 20 Hp, 18-inch diameter centrifugal blower permitting test section speeds up to 90 m/s. The tunnel speed is controlled by a variable vane arrangement at the blower inlet.

The TCTF layout is illustrated in Figure 3.1. The bell-mouth inlet directs the flow through a 21-inch square, 8-inch deep honeycombed-type flow straightener. The flow continues on through a 7:1 contraction ratio curved-wall converging nozzle to the 4.5-inch x 16-inch stilling chamber. The 12-inch deep stilling chamber, a new addition to the TCTF for this series of experiments, has been outfitted with hand cranks allowing the user to manually adjust the inlet sideboard for a variable angle of incidence to the linear cascade, illustrated in Figure 3.2. The installation of the chamber required the fabrication of longer inlet sideboards, potentially improving the cascade inlet flow.

The stilling chamber is followed by the 24-inch diameter linear turbine cascade test section. Although not utilized for this series of experiments, the test section can be rotated, also allowing a variable angle of incidence to the linear blade array. Both the stilling chamber and the test section have plexiglass top covers allowing visual observation of the experiments. For turbulence generation, a removeable tube grid can be inserted into the flow upstream to the test section, parallel to the row of blades. The turbulence grid consists of eight 1/4-inch diameter tubes that span the height of the cascade assembly placed 1-inch apart on center.

After passing through the cascade, the flow is diffused and continues on through the blower, exiting to atmosphere. The open-circuit design results in test section pressures below atmospheric but with acceptable Reynolds numbers. The drawbacks of the open-circuit design are high noise levels and the ingestion of dust and insects, harmful to the delicate test section instrumentation.

3.2 Linear Turbine Cascade

The 4-blade linear turbine cascade arrangement is illustrated in Figure 3.3. The reaction stage blade profile is identical to that used in several studies (Langston et al., 1977; Moore and Ransmayr, 1984) and is listed in Appendix B. With a chord of 4.5 inches, a span of 4.5 inches, and an aspect ratio of 1, secondary flow effects limit the instrumentation area to the middle two-thirds of the blade; however, the large blades allow conventional pressure and temperature instrumentation techniques. Blades #1 and #4 were machined from solid aluminum at the USAFA. Blades #2 and #3 are eurethane foam, fabricated at AFIT from molds of the original blades. Blades #1, #3, and #4 are uninstrumented.

Blade #2 is the heart of the cascade, instrumented for both surface static pressure and temperature, and equipped with a constant-current heat transfer surface as illustrated in Figure 3.4. A 2-inch wide strip of very thin (0.002 inches) stainless steel shim foil was fitted to the surface contour of the blade, beginning 1/4-inch from the trailing edge of the suction surface, continuing forward and around the leading edge, and ending 1/4-inch from the trailing edge on the pressure side. The electrical taps are connected to the underside of the foil and pass through the center of the blade and exit through the bottom endwall. Power for the heat transfer surface is supplied by a Hewlett Packard HP6456B direct current power supply.

Heat transfer temperature measurements are obtained with 23 type J thermo-couples-soldered to the underside of the foil, and 23 static pressure taps are located along a 1/2-inch wide band adjacent to the foil at the same thermocouple axial locations. Both the thermocouple leads and the pressure lines pass through the center of the blade and exit through the bottom endwall. The pressure tap/thermocouple locations are listed in Appendix C.

3.3 Instrumentation

<u>Requirements</u>. The instrumentation for this series of experiments consisted of temperature, pressure, velocity, electrical power measuring devices. The measurement requirements were as follows:

temperature	-blade surface, 23 locations
	-blade interior, 5 locations
	-tunnel air, 1 location
	-room air, 1 location
pressure	-blade surface, 23 locations
	-tunnel static, 1 location
	-tunnel total, various locations
	-room static, 1 location
velocity	-tunnel, various locations
power	-voltage across the heat transfer surface
	-current through the heat transfer surface

<u>Temperature Measurements</u>. The blade #2 heat transfer surface was outfitted with 28 type J thermocouples: 23 along the surface and 5 embedded in the blade

interior, along the blade centerline as shown in Figure 3.5. For tunnel temperature, a single type J thermocouple was placed in the freestream, and a single type J thermocouple was place in the room alongside the TCTF for room temperature.

Pressure Measurements. For blade surface pressure measurements, 23 static pressure taps were installed on blade #2 at the same axial locations as the thermocouples. The tunnel freestream total and static pressures were obtained with a pitot-static pressure tube located upstream of the cascade at mid span z = 2.25 inches. A pitot tube was used to obtain the total pressure at any location in the cascade. Access to the cascade test section was obtained through the circular plexiglass cover. For this experiment, the cover was modified for accurate and simple total pressure scanning. Two grooves were cut in the cover along the leading and trailing edges of the cascade, as well as 4 access ports to the cascade passages. Machined aluminum blocks held the total pressure tube in place while data acquisition took place. The configuration is illustrated in Figure 3.6.

The 23 blade static pressures, the tunnel total/static pressures, and atmospheric pressure were measured with a 48 port Scanivalve pressure transducer equipped with a +/- 2 psi pressure module, referenced to atmosphere. The Scanivalve pressure transducer received excitation and signal amplification from an Endevco model 109 power supply/model 106 conditioner unit. A Scanivalve CTRL2P/S2 solenoid controller allowed sequential port stepping or immediate return to home port 0 and a Scanivalve OED2 odd-even decoder provided port location digital readout. The complete Scanivalve port assignments are listed in Appendix D.

For tunnel speed setting and monitoring, the freestream pitot-static tube also was connected to a Trimount Instrument U-tube water manometer providing 1.5 digits of accuracy. This configuration allowed setting the tunnel speed to within 1 m/s of the desired speed. The pressure system schematic is detailed in Figure 3.7.

Velocity Measurements. Velocity measurements were obtained with a 2-channel constant temperature hot wire anemometer. An x-wire of the arrangement in Figure 3.8 was used to gather both streamwise and normal velocity components at any location in the cascade. A TSi IFA-100 Intelligent Flow Analyzer provided the controlling circuits for the x-wire. Depicted Schematically in Figure 3.9, the IFA-100 combines the constant temperature x-wire bridge and controlling circuits, the amplifier, and the signal conditioner. The entire system is controlled from the front panel of the IFA-100, providing bridge compensation, gain and filtering, and fault (broken-wire) indication.

Power Measurements. Power to the heat transfer surface was estimated based on the local resistivity of the foil and the current through the foil. The local resistivity of the foil is a function of the local temperature as measured by the thermocouples and was determined by Acree (Acree, 1990) with a foil resistivity experiment. The current through the foil was measured with a Weston Electric model 430 DC ammeter and the voltage across the foil was measured with a Hewlett Packard HP3438A digital multimeter. Although not required for power estimation, the voltage across the foil was measured to detect any current leaks. The blade power schematic is illustrated in Figure 3.10.

3.4 Data Acquisition Equipment

The heart of the data acquisition system was the Hewlett Packard HP3852A Data Acquisition and Control Unit equipped with three 24-channel high-speed FET multiplexers (slots 0, 2, and 3), an 8 channel relay module (slot 1), a high-speed voltmeter (slots 4 and 5), and an integrating voltmeter (slot 6) as illustrated in Figure 3.11. The

HP3852A acquired all analog transducer signals and performed the analog to digital conversion. The HP3852A was remotely programmed and controlled by a Zenith 386 PC via a National Instruments General Purpose Interface Bus (GPIB) as illustrated in Figure 3.12.

All thermocouples were connected to the 24-channel multiplexers in slots 0 and 2 and the signals were measured by the integrating voltmeter. The multiplexers allowed direct temperature measurements in degrees Celsius through temperature compensation. A secondary room temperature was monitored through a type J thermocouple and Omega Trendicator. The output from the model 106 conditioner was connected to channel 221 in the slot 2 multiplexer and the signal was measured with the integrating voltmeter. The Scanivalve scanning solenoid was controlled by the relay module, allowing incremental scanning by relay channel 101 or instant return to port 0 by relay channel 100. The high-speed voltmeter (100,000 measurements per second) was used for the hot-wire anemometer velocity measurements. The output from the TSi IFA-100 signal conditioners was connected to channels 321 (wire1) and 322 (wire2) in the slot 3 multiplexer. The IFA-100/high-speed voltmeter combination allowed hot-wire scanning rates up to 100KHz. A complete HP3852A channel assignment listing is contained in Appendix E.

3.5 Software

3.5.1 Requirements

In order to acquire, catalogue, and reduce the large amounts of data anticipated, the TCTF was automated in the areas of data acquisition and data reduction and, to a small degree, experiment control. All software was written in Microsoft QuickBASIC version 4.5 (QB). The software package, listed in its entirety in Appendix F, is divided

into 3 task oriented subsections: calibration, data acquisition, and data reduction, illustrated in Figure 3.13. The tasks (calibration, data acquisition, and data reduction) are described in detail in Chapter IV.

The calibration and data acquisition software primarily instructs the HP3852A data acquisition unit through the GPIB. In fact, the HP3852A instructions are basic-like programs within the QB calibration and data acquisition programs. For more information on programming the HP3852A through the PC and GPIB, consult the HP3852A and GPIB user's manuals. Unlike the calibration and data acquisition programs, the data reduction programs operate independently of the HP3852A; therefore, all data reduction can be performed with any QB equipped PC.

3.5.2 Calibration Software

The function of a calibration program is to aid the user in calibrating a measurement device and produce the calibration results in the form of calibration constants. Since no thermocouple calibrations were required (see Section 4.2), the only calibration programs required and developed were PRESSCAL.bas for the Scanivalve pressure transducer calibration and XWIRECAL.bas for the hot-wire anemometer calibration. Both calibration programs were initially written by Galassi (Galassi, 1989) and then modified by Acree (Acree, 1990), but further refinements were incorporated to improve and simplify the calibration process. Exact details about the program steps can be found in the program comments.

Pressure Transducer Calibration Software. The PRESSCAL.bas program directs the user through the Scanivalve pressure transducer calibration process. The program originally only acquired the calibration data in the form of pressures and associated Scanivalve pressure transducer voltages; however, the program was modified and the

current menu-driven PRESSCAL.bas program reduces the calibration data and writes the calibration data and calibration constants to files which are accessed by the data acquisition and reduction programs.

Hot-Wire Anemometer Calibration Software. The XWIRECAL.bas program directs the user through the hot-wire calibration process. As with the PRESSCAL.bas program, the original XWIRECAL.bas program only acquired the hot-wire calibration data in the form of velocities and associated voltages for the 2 wires; the program also was modified to reduce the calibration data and write the calibration data and calibration constants to files; additionally, an x-wire alignment subroutine was added to the menu-driven XWIRECAL.bas program. The subroutine allows the user to somewhat simply align the x-wire in the calibration stand, ensuring a repeatable and accurate calibration.

3.5.3 Data Acquisition Software

Originally, the TCTF data acquisition program both acquired and reduced the experimental data. Although very useful for real-time confirmation of data validity, the automated data reduction aspect of the program was time consuming; furthermore, a well thought out test plan is preferred over a "let's see what happens". For this experiment, data acquisition was confined to one user-friendly program and data reduction to other user-friendly programs.

The majority of the data acquisition is performed by the menu-driven data acquisition program ACQUIRE.bas. Functions of the menu driven program include acquiring the blade pressure and temperature data and the cascade flow turbulence data and displaying real-time blade temperature and tunnel velocity information.

Temperature Data Acquisition Software. The blade temperature data is acquired with the subroutine TEMPACQ. The TEMPACQ subroutine instructs the HP3852A to momentarily interrupt the power to the heat transfer surface using a relay channel, and

then scan the 30 thermocouples with high-speed FET multiplexers. The HP3852A automatically converts the thermocouple voltages to temperatures in degrees Celsius and the 30 thermocouple data points are transferred to the PC in the form of ASCII data files. Once stored, the temperatures are then listed on the screen for a validity check.

Pressure Data Acquisition Software. The blade and tunnel pressure data is acquired with the subroutine PRESSACQ. In addition to instructing the HP3852A to acquire the Scanivalve pressure transducer voltage data through one multiplexer channel, the program also instructs the HP3852A "call the Scanivalve home" and to step the Scanivalve through ports 0 - 28 through relay channels. Unlike the thermocouple readings, the Scanivalve pressure transucer voltages are not converted to pressures; instead, the voltages are transferred to the PC in an ASCII data file. Once stored, the voltages are then plotted as a function of their pressure tap location, allowing the user to check for an obvious error. The pressure data acquisition and storage process takes approximately 2 minutes, mainly due to the port stepping speed.

Hot-Wire Anemometer Data Acquisition Software. The x-wire data acquisition is the most complex and time consuming data acquisition process, requiring extensive revisions to the original x-wire data acquisition subroutine. Since the x-wire voltages are acquired with a "dedicated" high-speed multiplexer/high-speed voltmeter combination, special data acquisition, transfer, and storage considerations were required. The VELACQ subroutine instructs the HP3852A to acquire a specified number of x-wire voltages at a specified frequency with the multiplexer/voltmeter combination. The unusually large amount of sequential (almost simultaneous) wire1/wire2 data is transferred to the PC for temporary storage.

After the data transfer is complete, the subroutine then reads in the data from the temporary storage files, sorts the wire1 and wire2 readings, removes the IFA-100 signal

processor gain and offset, and then rewrites the voltage data to the binary data files, ready for data reduction. Binary data files were used since each data file would require over 500kb of storage in ASCII format. As an error check, the first 5 and last 5 voltages from each data file are printed to the screen. Depending upon the number of data points acquired, (16,384 per channel maximum), the x-wire data acquisition, transfer, and storage process can take up to 5 minutes.

Real-Time Data Display Software. To aid the user in the data acquisition process, the real-time display subroutines TSET and VSET were included in the data acquisition program ACQUIRE.bas. The subroutine TSET displays a bar graph of the room temperature from thermocouple 29 and the 5 blade internal temperatures from thermocouples 24 - 28. This display is useful during the heat transfer data acquisition process when the tunnel speed and turbulence is changed, altering the steady-state conditions. The VSET subroutine is similar to the x-wire alignment routine in XWIRECAL.bas, allowing the user to properly align the x-wire in the flow through a real-time display of the x-wire voltages and the streamwise and normal velocity components.

3.5.4 Data Reduction Software

There are 2 levels of data reduction; low level, consisting of the conversion of raw data, usually in the form of voltages, to useful data by means of the calibration constants; and high level, where the useful data is manipulated using the theory of Chapter II to tell the user something about what is going on in the experiment.

Temperature Data Reduction Software. The low level temperature data reduction is simplified by the HP3852A, which presents thermocouple data in the form of temperatures automatically. Further low level temperature data reduction is performed by TREDUCE.bas which, using the thermocouple location file CHORD.dat, produces a

screen plot of the temperatures and writes the thermocouple locations and associated temperatures to files for plotting purposes. High level temperature data reduction is performed by HTXFER.bas, described below.

Pressure Data Reduction Software. The low level and some high level pressure data reduction is performed by PREDUCE.bas. This program reads in the raw pressure data files and the calibration data file produced by PRESSCAL.bas and produces a file of static pressures listing the static pressure in kPa for each of the 28 ports; additionally, the program calculates the pressure coefficient for each point and, using the CHORD.bas file, produces a screen plot of the pressure coefficient profile and writes the pressure tap locations and associated pressure coefficients to a file for plotting purposes.

Hot-Wire Anemometer Data Reduction Software. Like the hot-wire data acquisition subroutine VELACQ, the hot-wire data reduction program VELREDUC.bas is the most complex of the data reduction programs, with 5 subroutines for performing both the low level and the high level data reduction. The low level subroutines REDUCE and STATS convert the hot-wire voltages to velocities and convert the velocities to a mean value, a standard deviation, and a turbulence level. For the high level data reduction, the subroutines RealFT, Four1, and SCALES utilize Fast Fourier Transform (FFT) analysis and the theory of Chapter II to calculate the Energy Spectrum, the integral scale, and the microcscale of the turbulence. As with the other data reduction programs, the processed data is printed to the screen. The x-wire data reduction process is time consuming and can take up to 5 minutes.

Heat Transfer Data Reduction Software. Another high level of data reduction is performed by HTXFER.bas, which uses the temperature data files and the pressure data files to calculate the heat transfer properties of the instrumented blade.

Duplicating the procedures of TREDUCE.bas and PREDUCE.bas, HTXFER.bas uses the pressure calibration data and the thermocouple position data in files CHORD.dat, S.dat, and DELTAL.dat, the temperature and pressure data to obtain temperature and pressure values for each of the 23 heat transfer surface data locations. The data is further reduced, using the heat transfer theory of Chapter II, to obtain the Reynolds numbers, heat transfer coefficients, Nusselt numbers, and Stanton numbers for each of the 23 thermocouple locations. The program prints the raw and reduced data to the screen and writes the reduced data to a data reduction file which can be accessed for plotting purposes.

IV Procedures

4.1 General

This section describes the operational procedures followed for this series of experiments. The procedures are intended to be a guide for performing experiments using the TCTF with the aforementioned instrumentation and data acquisition equipment. Recommendations for changes to these procedures are listed in Chapter VI. As with the classification of the software, the experiment itself is divided into 3 distinct elements or tasks: calibration of instrumentation, data acquisition, and data reduction.

4.2 Instrumentation Calibration

The most important element of any experiment is properly calibrated instrumentation. Proper calibration will verify that the instrument is operating correctly and will insure that the experiment will yield repeatable results.

Thermocouple Calibration. A thermocouple is a junction of 2 dissimilar metals which generates a temperature-dependent thermoelectric potential, E_{AB}, as a result of the Seebeck effect, illustrated in Figure 4.1a. For small changes in temperature, E_{AB} is linearly proportional to the junction temperature:

$$E_{AB} = \alpha T \qquad (4.1)$$

where α is the Seebeck coefficient

T is the junction temperature

For a given pair of metals at a given junction temperature, the thermoelectric potential will always be the same, eliminating a calibration requirement; however, measuring E_{AB} results in the introduction of several more junctions, illustrated in Figure 4.1b, which now must be compensated for. The HP3852A multiplexer/voltmeter

combination is configured for this compensation by measuring the temperature of the terminal-block, schematically illustrated in Figure 4.1c, and factoring in the appropriate correction electronically in real-time.

Inexpensive type J thermocouples were chosen for this experiment. The iron(+)/constantan(-) combination has a high Seebeck coefficient and excellent performance over the expected temperature range. The only calibration procedural requirement for thermocouples is configuring the HP3852A to measure temperature with type J thermocouples (see HP3852A handbook).

Pressure Transducer Calibration. Unlike the thermocouples, the pressure transducer must be calibrated over its expected range of operation. The Scanivalve system employs a diaphram-type pressure transducer which uses a piezoresistive element to measure the "pressure" applied to the diaphram to which it is bonded. This diaphram/piezoresistive element must be calibrated, yielding a relationship between the pressure and the bridge voltage. Since the bridge voltage is not referenced to ground, a requirement for the HP3852A, the signal passes through the Endevco operational amplifier where it is amplified and referenced to ground.

Calibration of the pressure transducer requires applying a known pressure to the transducer and recording the associated voltage. A properly designed pressure transducer will exhibit a linear pressure/voltage relationship over the designed range; therefore, the calibration data reduces to a linear equation:

$$P = V_o + mV \tag{4.2}$$

where V_o is the transducer voltage as atmospheric pressure

   m is the pressure/voltage curve slope

A detailed pressure transducer calibration procedure is included in Appendix G.

Hot-Wire Anemometer Calibration. A hot-wire probe operates on the principles of convective heat transfer. When placed in a flowing fluid, the rate of convective heat transfer from a heated cylinder is proportional to the velocity of the fluid. This relationship is described by King's Law,

$$h = A + BV^{1/2} \qquad\qquad (4.3)$$

where h is the heat transfer coefficient

A and B are constants

V is the fluid velocity

A constant temperature hot-wire anemometer operates by maintaining a heated probe at a constant temperature. The probe is constructed of a very fine piece of material which has a high temperature coefficient of resistance. When used in the bridge circuit of Figure 3.9, the temperature maintenance circuits generate a fluctuating bridge voltage which can be measured and correlated to the heat transfer. This correlation can be calibrated, using known velocities, yielding the relationship

$$E^2 = A + BV^n \qquad\qquad (4.4)$$

where E is the bridge voltage

A and B are calibration constants

V is the fluid velocity

n is the power which gives the best linearization

The exponent n is a function of the fluid and its value is determined when the data is linearized, usually using a least-squared error reduction technique. Several references have determined that for air $n \approx 0.45$.

When the x-wire of Figure 3.8 is placed in a flowing fluid, each wire is subjected to both a normal and tangential flow component; in this case, V in equation 4.4 is replaced by the effective velocity V_{eff},

$$V^2_{eff} = V^2_N + k^2 V^2_T \qquad (4.5)$$

where V_N is the velocity component normal to the wire

   V_T is the velocity component tangential to the wire

   k is a yaw correction factor

The values of V_N and V_T are determined from the freestream V and the angle

between V and the wire. The correction factor k is a function of the wire geometry and varies linearly with the length/diameter ratio of the probe wire. Details of the hot-wire calibration are included in Appendix G.

4.3 Data Acquisition

General. The data acquisition procedure involves 2 steps: configuring the TCTF for a specific experiment and acquiring the required data. In order to perform each of the 2 steps, the user must develop a test plan which states the desired TCTF configuration and the desired data requirements.

TCTF Configuration. For a fixed cascade, the variables in the TCTF configurations are the model Reynolds number, the freestream turbulence level, and the cascade angle of incidence. Changing a given configuration usually requires shutting down the TCTF for a brief period; starting the TCTF back up again requires a settling period, allowing the TCTF to arrive at steady-state conditions, ready for data acquisition. For these reasons, a well thought out test matrix prepared in advance is necessary for accomplishing the desired TCTF test in any reasonable period of time. The test matrix chosen for this heat transfer experiment is illustrated in Table 4.1.

Table 4.1 TCTF Test Configurations

TEST NO.	ANGLE of INCIDENCE	MODEL REYNOLDS NUMBER	FREESTREAM TURBULENCE INTENSITY
1	-2.5	low	low
2	-2.5	med	low
3	-2.5	high	low
4	-2.5	low	high
5	-2.5	med	high
6	-2.5	high	high
7	0.0	low	low
8	0.0	med	low
9	0.0	high	low
10	0.0	low	high
11	0.0	med	high
12	0.0	high	high
13	2.5	low	low
14	2.5	med	low
15	2.5	high	low
16	2.5	low	high
17	2.5	med	high
18	2.5	high	high
19	5.0	low	low
20	5.0	med	low
21	5.0	high	low
22	5.0	low	high
23	5.0	med	high
24	5.0	high	high

Steady State Conditions. Prior to acquiring any data, the TCTF steady-state conditions must be insured. The steady-state requirement also applies to the data acquisition equipment. Of primary concern is the period required for data acquisition

equipment warm-up. Figure 4.2 illustrates the warm-up behavior of the Scanival-ve/HP3852A combination and clearly indicates a minimum 2 hour warm-up period for the data acquisition equipment.

Although not illustrated here, the time required for the TCTF to arrive at a steady-state flow condition is approximately 5 minutes; however, when using the heat-transfer blade, the time required for the heat-transfer surface to arrive at a steady-state condition increases the waiting period dramatically.
Figure 4.3 illustrates the blade behavior from power-on at time 0 to a reasonable steady-state condition at time = 30 minutes. A change in the heat-transfer surface due to altering the TCTF flow conditions, such as the freestream velocity or turbulence level, exhibits a similar stabilizing behavior; therefore, a reasonable steady-state waiting period between heat transfer data acquisitions was determined to be approximately 30 minutes.

The experimental data is acquired in three sets: TCTF flow characterizaton data, heat transfer temperature and pressure data, and TCTF flow turbulence data. Acquiring the data in this order allows the user to identify and correct any instrumentation, data acquisition, or flow condition discrepancies.

Cascade Flow Characterization Data. Characterizing the flow consisted of obtaining turbine blade static pressure scans and performing velocity magnitude/direction and total pressure scans along the leading and trailing edges of the cascade. The blade static pressure scans were recorded automatically using ACQUIRE.bas; however, since the leading and trailing edge scanning process required manually moving the probes to the desired locations and aligning the probes with the flow, that data was recorded manually on specially prepared data sheets. For the velocity magnitude/direction data, the x-wire probe was aligned with the streamwise velocity vector,

effectively nulling any normal components; the program VSET.bas displayed the real-time-velocity magnitude and the angle was recorded from the fixture mounted protractor. For the total pressure data, the total pressure probe was aligned with the flow direction as determined from the inlet and exit sideboards; the program TOTPRESS.bas displayed the real time Scanivalve voltages for conversion to pressures from the calibration coefficients.

Heat Transfer Data. Unlike the flow characterization data acquisition, the heat transfer temperature and pressure data acquisition is fully automated, initiated by executing the menu-driven ACQUIRE.bas data acquisition program and selecting the appropriate menu choice. The raw data is automatically recorded, stored, and displayed, ready for data reduction.

Turbulence Data. The turbulence data was collected after all characterization and heat transfer data was collected. Since the hot-wire probe operates on the principle of correlating a probe temperature/resistance to the flow velocity, the turbulence data could not be acquired while the blade was heated. A more advanced probe calibration procedure may be able to compensate for the changing freestream temperatures.

The turbulence data acquisition is the most time consuming process, due to both the large number of data points acquired for each measurement and the number of measurements. This time and data constraint limited the turbulence data acquisition to the low and high blade Reynolds number TCTF configurations. The fully automated data acquisition process was initiated by the appropriate menu selection in the ACQUI-RE.bas program; the data was automatically recorded, stored, and displayed, ready for data reduction.

4.4 Data Reduction

Although very little real-time data reduction was performed, the bulk of the data collected was evaluated at the end of the day it was acquired, allowing adjustments to the test schedule, if necessary. For the most part, raw data reduction was simple, using the software described in Section 3.5.

The manually recorded velocity and total pressure characterization data was manually entered in a QUATTRO PRO spreadsheet for evaluation while the blade static pressure characterization data was processed with PREDUCE.bas. The end products were various plots of the data, discussed in Chapter V, Results.

The raw heat transfer data, consisting of temperature and blade static pressure scans, was processed with the low level TREDUCE.bas and PREDUCE.bas data reduction programs. The products of these programs, blade surface temperature and static pressure plots, were not intended to reveal anything about the heat transfer; instead, they were used to show behaviors and indicate faulty data. High level data reduction was performed by the HTXFER.bas program which provided the heat transfer results in the form of the nondimensional Nusselt number and Stanton number.

The time consuming turbulence data reduction was performed with VELRE-DUC.bas. Unlike the temperature and pressure scans, reducing the data of one turbulence scan did not provide enough information for plotting. Ten turbulence scans were required for each TCTF configuration. VELREDUC.bas was written to batch process the turbulence data, providing results that could be plotted and further evaluated.

V Results and Discussion

5.1 Tunnel and Cascade Flow Characterization

Prior to conducting any heat transfer data experiments, it was necessary to characterize the flow through the cascade. Although both Galassi (Galassi, 1989) and Acree (Acree, 1990) had characterized the flow for their experimental configurations, the installation of the longer variable-angle inlet sideboards called for another look at the flow behavior to ensure proper cascade flow for all experimental configurations.

5.1.1 Cascade Inlet Velocity Profiles

General. A basic indicator of the cascade behavior is the cascade inlet velocity (magnitude and direction) profile. Since, for this experiment, the TCTF was limited to a four-blade cascade, it was important to verify the proper periodic profile for inlet velocities. Unlike previous efforts with the TCTF, the velocity profile measurement was limited to a scan across the cascade inlet; it was assumed that any inconsistency in the velocity profile further upstream would show up at the cascade entrance.

Low and High Freestream Velocity Profiles. The inlet velocity profiles for both low and high freestream turbulence levels at a single model Reynolds number are illustrated in Figures 5.1a and 5.1b. Although the magnitude and direction of the freestream velocity were measured, only the normalized velocity component normal to the cascade inlet is displayed; this convention combines the direction and magnitude information. Normalizing by the velocity measured at the leading edge of the instrumented blade eliminates any variations in the profile caused by variations in the freestream velocity.

The velocity profiles indicate that the flow upstream of the cascade is well-behaved. It appears that the profile for the high turbulence configuration may be slightly higher than the low configuration, probably caused by the local high and low velocity areas caused by the tubes of the turbulence grid. The odd behavior on the

ends of the turbulent profiles in Figure 5.1b is due to the changing space between the turbulence grid and the inlet sideboards. As the angle of incidence (AOI) to the blade row was either increased or decreased by adjusting the sideboards, the spacing between the sideboards and the fixed, non-adjustable grid either increased or decreased, causing a region of local acceleration or deceleration. Since this irregularity did not seem to effect the region of interest, it was ignored.

5.1.2 Pressure Coefficient Profiles

General. A blade static pressure scan was performed for each of the 24 configurations listed in Table 4.1 and a typical low freestream turbulence pressure coefficient (C_p) plot is illustrated in Figure 5.2. Since C_p is nondimensionalized by the same upstream quantities p_∞ and q_∞, the C_p plots for the various configurations listed in table 4.1 can be compared to each other for determining flow differences due to the changing configurations.

Most importantly, a well-instrumented blade will immediately reveal the location of the stagnation point. By Bernoulli's equation for incompressible flow:

$$p_l + q_l = p_\infty + q_\infty \tag{5.1}$$

along a stream line. At the stagnation point $U_l = 0$ and

$$p_l = p_\infty + q_\infty \tag{5.2}$$

or, substituting for C_p

$$C_p = \frac{p_\infty - q_\infty - p_\infty}{q_\infty} = 1 \tag{5.3}$$

By Figure 5.2, the stagnation point occurs at about point 2. This point determines the dividing-line between the suction surface and the pressure surface, important for calculating the local heat transfer quantities.

The shape of the C_p curve also illustrates the behavior of the local velocity of the flow around the blade. Again by Bernoulli's equation

$$U_l = f(1 - C_p) \tag{5.4}$$

For increasing C_p there is an adverse pressure gradient and decreasing local velocity and for decreasing C_p there is a favorable pressure gradient and increasing local velocity.

On the pressure surface of Figure 5.2, the <u>overall</u> general trend is decreasing C_p corresponding to a favorable pressure gradient and acceleration of the flow along the surface to the "throat" of the cascade passage and the trailing edge of the turbine blade, illustrated in Figure 5.3. On the suction surface of Figure 5.2, the favorable pressure gradient accelerates the flow as it approaches the throat and then an adverse pressure gradient decelerates the flow in the diffuser region near the trailing edge of the blade, illustrated in Figure 5.3.

<u>Acceleration Parameter</u>. The acceleration and deceleration of the flow along the turbine blade surface can be described by the acceleration parameter K:

$$K = \frac{\nu}{U_\infty^2} \frac{dU_\infty}{ds} \tag{5.5}$$

It is has been experimentally shown (Kays et al., 1970) that a turbulent boundary layer tends to relaminarize for $K > 2.5 \times 10^{-6}$ as the "viscous sublayer thickens so as to engulf the entire boundary layer" (Kays and Crawford, 1980); in this situation, "the local

heat transfer coefficients are suppressed" (Priddy and Bayley, 1985). Figure 5.4 illustrates the behavior of K for the 0 degree AOI TCTF configuration. Starting from zero at the stagnation point, the flow is highly accelerated on either side of the leading edge, representative of flow around a cylinder. On the suction surface, K drops below the critical value and remains nearly constant; on the pressure surface, however, K exceeds the critical value from tap 5 - 8, where the boundary layer was observed to be reattached. Suppressed heat transfer coefficients are expected in this region.

Flow Separation. Combined with flow visualization experiments, C_p analysis may also indicate the presence of deviations from the expected flow behavior, such as local regions of flow separation. On the pressure surface of Figure 5.3, there is a small adverse pressure gradient and an area of flow acceleration and deceleration between taps 2 and 4, followed by a gradual acceleration to the trailing edge. Extensive oil drop flow visualization experiments have verified flow separation and reattachment in this region for low freestream turbulence; in addition, others with similarly-shaped turbine blades (Hippensteele et al., 1985; Consigny and Richards, 1982) have observed comparable flow behavior in this region. On the suction surface of Figure 5.3, the oil drop experiments have indicated flow separation and reattachment from taps 18 to 16 for low freestream turbulence, also confirmed by the works of others (Priddy and Bayley, 1985; Consigny and Richards, 1982).

Effect of Model Reynolds Number. Based on the turbine blade model true chord, the model Reynolds numbers are 2×10^5, 4×10^5, and 5×10^5 using the tunnel freestream velocities and 4×10^5, 8×10^5, and 10×10^5 using the cascade exit velocities.

Since C_p is nondimensionalized, C_p curves for the same cascade configuration at different Reynolds numbers are expected to be the same, assuming no flow anomalies. This is confirmed in Figure 5.5a, where the C_p curves for three different Reynolds numbers are nearly identical. Although the C_p are identical, the q_∞ are not and the local velocities are proportional to the model Reynolds number, illustrated in Figure 5.5b.

Effect of Freestream Turbulence. When the turbulence grid is inserted, increasing the turbulence level from 0.5% to 10%, the flow along the suction surface appears to gain a little speed, illustrated in Figures 5.6a and 5.6b. The oil drop experiments show that the region of separation on the suction surface from taps 18 - 16 has disappeared and the flow transitions smoothly from accelerating flow near the leading edge to decelerating flow near the trailing edge. The freestream turbulence has "energized" the boundary layer, making it adhere to the blade surface and delay or eliminate separation. The oil drop experiments have also indicated that the increased freestream turbulence has not eliminated the region of separation between taps 2 and 4 on the pressure surface.

Effect of AOI. As the AOI is increased from -2.5 degrees to 5 degrees, several phenomena occur, illustrated in Figures 5.7a and 5.7b. The stagnation point is expected to move towards the pressure side as the AOI is increased. Since the pressure taps are at fixed locations, the location of the stagnation point could not be tracked; however, both Figures 5.7a and 5.7b illustrate that at 5 degrees AOI the stagnation point is at tap 2 but moves slightly toward tap 1 and the suction side as the AOI decreases, as indicated by the behavior of taps 1 and 3. As the AOI increases, Figure 5.8 illustrates that the velocity at tap 1 increases and the velocity of tap 3

decreases, indicative of the movement of the stagnation point of flow around a cylinder. As mentioned, the oil drop experiments confirm the flow separation regions on both surfaces at all AOIs for the low freestream turbulence configurations.

Cascade Passage Streamwise Velocity. A more obvious behavior is the apparent "shift" of the pressure field as the AOI changes, indicating a decrease in the local velocity on the pressure and suction surfaces with an increase in the AOI, illustrated in Figure 5.8. As the AOI increases, the velocity decreases due to the movement of the stagnation point and the requirement of the flow to turn through a greater angle, incurring more losses and losing energy and speed. This effect is further illustrated in Figures 5.9a and 5.9b which show the behavior of the midpassage streamwise velocity as the AOI increases for both the low and high freestream turbulence configurations. After an initial velocity rise as the flow enters the cascade, the velocity decreases near the regions of maximum curvature, perhaps due to the suspected regions of separation and turbulence. The overall favorable pressure gradient then accelerates the flow to a maximum velocity at the cascade exit. For both the low and high Reynolds number configurations, the streamwise velocity at a given point increases for a decrease in the AOI; in addition, the small increase in the surface velocities for the high turbulence configuration observed in Figure 5.6b is further manifested as a small increase in the cascade passage streamwise velocities of Figures 5.9b.

Similar to the variation in the streamwise velocity through the cascade passage, there is a streamwise variation in the turbulence levels through the cascade passage, illustrated in Figures 5.10a and 5.10b. For the high turbulence configurations, the variation in the turbulence level is opposite that of the streamwise velocity, decreasing when the velocity is increasing and vice-versa. For the low turbulence configurations, the variation in the turbulence levels are not as obvious, generally increasing from 0.5%

to 1.5%.

The velocity information of Figures 5.9a and 5.9b and the turbulence information of Figures 5.10a and 5.10b can be combined to determine the behavior of the fluctuating component of velocity. By combining equation 2.28 and the assumption of isotropic turbulence (confirmed by data), the product of the mean velocity and turbulence intensity is

$$\bar{U} T u = u'_{rms} \tag{5.6}$$

where u'_{rms} represents the fluctuating component of the velocity. Priddy and Bayley

(Priddy and Bayley, 1988) have shown that "the absolute amplitude of the turbulent fluctuations is little changed through the passages, certainly when compared with the observed changes in the local turbulence intensity." Although the behavior of the turbulence intensities in this experiment is not comparable to the observed "monotonically" decreasing turbulence intensities of the Priddy and Bayley experiment, Figures 5.10c and 5.10d support the observations that the fluctuating components remains nearly constant through the cascade passage. In all cases, low and high freestream turbulence, low and high Reynolds numbers, the value of u'_{rms} is nearly constant from location 2 through location 4, which represents the cascade passage. Location 1 is the freestream and location 5 is beyond the trailing edges of the turbine blades. Figures 5.10c and 5.10d further illustrate that the values of u'_{rms} at a point appear nearly constant over a range of AOIs.

Although the C_p plots are very useful, they do not necessarily reveal particulars

about the boundary layer, such as whether it is laminar, transitional, or turbulent; however, the C_p and heat transfer data combination provides information not available from either set of data alone.

5.2 Convective Heat Transfer

Since the inlet velocity profiles and the turbine blade C_p plots demonstrated acceptable cascade behavior for all TCTF configurations, the heat transfer experiment was carried out according to the test plan of Table 4.1. A typical "raw" temperature scan is illustrated in Figure 5.11 (see Figure 3.5 for thermocouple locations). Since thermocouples 9 - 12 were located very close to the copper bus bars feeding the power to the foil surface, it was determined that those temperature readings were not representative of "normal" surface temperatures as indicated by the remaining surface thermocouples; therefore, the temperature readings from thermocouples 9 - 12 were omitted from the heat transfer analysis.

The temperature scan of Figure 5.11 illustrates the variation in temperatures over the surface and in the interior of the blade; however, the temperatures alone are not indicative of the local convective heat transfer rates since the heat transfer rates are the result of a combination of heat transfer effects. By including the conductive and radiative heat transfer effects as outlined in Chapter II, the local convective heat transfer coefficients can be determined.

5.2.1 Low Turbulence Convective Heat Transfer

General. A typical low turbulence convective heat transfer coefficient h curve, generated from the temperature data of Figure 5.11, is illustrated in Figure 5.12. This plot illustrates the behavior of the heat transfer and, combined with the C_p plot for the configuration, reveals the cascade flow / heat transfer mechanisms.

Pressure Surface. As expected, the heat transfer is very high at the stagnation point (tap 2) due to the very thin boundary layer. On the pressure surface (negative s/c) the heat transfer rate drops rapidly due to the observed flow separation and rises to small peak as the flow reattaches.

In Figure 5.12, following the reattachment peak at s/c = -0.3, the heat transfer coefficient appears to slowly rise as the flow proceeds to the trailing edge. The analysis of the acceleration parameter K predicted boundary layer relaminarization and a suppressed heat transfer coefficient in this region; however, the heat transfer coefficient is increasing, indicating a transitional or fully turbulent boundary layer. Figure 5.13 illustrates the experimental behavior of the local Nusselt number on the pressure surface in comparison to that predicted for a flat plate and an arbitrary surface using equations 2.19 and 2.20. In the region from tap 5 to tap 8 the experimental Nusselt number values more closely match the turbulent predictions indicating a turbulent boundary layer and not a relaminarized boundary layer as expected.

Leading Edge. In Figure 5.12, a peculiarity exists in the leading edge region of the suction surface where the heat transfer rate decreases at tap 1 and then increases again for taps 23 and 22, the most densely instrumented region of the turbine blade. Neither the C_p plots nor oil-drop flow visualization experiments indicate the existence of a small region of flow separation and nothing could be found in the literature on turbine blade heat transfer resembling this behavior; however, a check and recheck of the blade surface, instrumentation, and data acquisition and reduction systems with the unheated blade indicated that the temperature reading of thermocouple #1 may be 2 - 3 degrees C higher than it should be, yielding an unusually low heat transfer coefficient. In reality, the temperature of thermocouple #1 probably lies in between the temperatures of thermocouple #2 and thermocouple #23. In this case, the behavior of the heat

transfer coefficient at the leading edge would resemble that observed in similarly shaped-blades (Consigny and Richards, 1982; Daniels and Browne, 1981; Priddy and Bayley, 1985) and would appear as in Figure 5.14. The loss of this data point limits the ability to confirm the location of the stagnation point and to study in deta. .he leading edge heat transfer.

Suction Surface. On the suction surface of Figure 5.12, the heat transfer rate drops appreciably after tap 22, typical of laminar boundary layer heat transfer behavior. The heat transfer rate continues to steadily drop to tap 17 where it rapidly rises from tap 16 to tap 13. The rapid rise in the heat transfer coefficient is characteristic of a reattaching boundary layer; a smooth transition to a turbulent boundary layer exhibits a more gradual rise. Figure 5.15 illustrates the experimental behavior of the local Nusselt number on the suction surface in comparison to that predicted for a flat plate and an arbitrary surface using equations 2.19 and 2.20. The experimental Nusselt number values follow the laminar predictions to the region of separation and reattachment, where it rises to a level between laminar and fully turbulent, almost meeting the Ambrok turbulent prediction. It is possible the boundary layer is in a transitional state in that region.

Effect of Model Reynolds Number. By Figure 5.16, the heat transfer coefficients increase with increasing Reynolds number and the suspected regions of separation and reattachment remain as indicated by the jumps in the heat transfer coefficient on the suction and pressure surfaces. The influence of the model Reynolds number on laminar boundary layer heat transfer is demonstrated in the Nusselt number plots of Figures 5.17a and 5.17b. As with the heat transfer coefficient, an increase in the local Reynolds number yields an increase in the Nusselt number since, by equation 2.17:

$$Nu = f(Re^{0.5}) \tag{5.7}$$

For a change in the laminar boundary layer Nusselt number that is due solely to a change in the local Reynolds number, the values of $Nu/Re^{0.5}$ will be identical for a given location. On the pressure surface in Figure 5.17b, the curves do not coalesce further reinforcing the absence of a laminar boundary layer; however, also in Figure 5.17b along the suction surface from 0.2 < s/c < 0.7 the curves for all three model Reynolds numbers completely coalesce, confirming an extensive region of laminar boundary layer heat transfer.

Another effect of the variation in the model Reynolds number appears in the regions of separation and reattachment. For all three model Reynolds numbers, the pressure and suction surface regions of flow separation and reattachment remain; however, for the low model Reynolds number configuration in Figure 5.16, the reattachment on the suction surface at s/c = 0.7 appears more gradual, indicating more of a transition than a reattachment jump.

Effect of AOI. As the AOI is increased from -2.5 degrees to 5.0 degrees, the primary observation of Figures 5.18a is the decrease in the heat transfer coefficient with an increase in AOI. At first glance, it would appear that variation in the heat transfer coefficient is simply a result of the variation in the local velocity or local Reynolds number, observed in Figure 5.8 and illustrated in Figure 5.18b and 5.18c where the influences of the local Reynolds number are visible. On both the pressure and suction surfaces, the decrease in the local Nusselt number is associated with a decrease in the local Reynolds number; however, by the same analysis of Figures 5.17a and 5.17b, Figures 5.19a and 5.19b illustrate that the variation in the Nusselt number is not simply a result of the variation in the local Reynolds number. Unlike the illustration of Figure 5.17b, the Nusselt number curves for the suction surface in Figure 5.19a do not coalesce in Figure 5.19b, indicating some effects in addition to the variation in the local

Reynolds number.

For convenience, the heat transfer coefficients for the -2.5 degree AOI and the +5.0 degree AOI configurations are illustrated in Figure 5.20. On the pressure surfaces at s/c = -0.1 and on the suction surfaces at s/c = 0.7, the effect of the flow separation appears to have a greater influence for the 5.0 degree AOI configuration. The jump in the heat transfer associated with the reattaching flow decreases with increasing AOI despite the nearly equal heat transfer at the leading and trailing edges.

5.2.2 High Turbulence Convective Heat Transfer

General. A typical high freestream turbulence convective heat transfer coefficient curve is illustrated with the low turbulence curve for comparison in Figure 5.21. The primary observation is the obvious across the board increase in the heat transfer coefficient. It was noted that increasing the freestream turbulence level apparently affected the boundary layer and the distribution of the velocity around the blade. These changes are further manifested in the distribution of the heat transfer coefficient. For the high turbulence configuration, the heat transfer coefficient appears almost constant along the aft pressure and suction surfaces, very much unlike the dips and rises observed in the low turbulence configuration.

Pressure and Suction Surfaces. In comparison to the low turbulence configuration, the nearly constant heat transfer coefficients for the high turbulence configuration of Figure 5.21 appear to correspond to turbulent boundary layer throughout both surfaces. On the pressure surfaces of Figure 5.21, the values of the heat transfer coefficients at the trailing edges are nearly equal, supporting the belief that the pressure surface boundary layer for the low turbulence configuration is transitional and approaching fully turbulent near the trailing edge. Again, Figure 5.22a illustrates that the experimental Nusselt numbers are best approximated by the turbulent predictions.

Figure 5.22b indicates that the suction surface boundary layer is somewhere between transition and fully turbulent with the experimental Nusselt number values rising steadily in between the laminar and turbulent predictions.

Figure 5.21 illustrates that the increased freestream turbulence may have slightly delayed the flow separation and reattachment process on the pressure surface at -0.3 < s/c <0.0. On suction surfaces of Figure 5.21, it is difficult to locate any obvious regions of separation and reattachment. The oil drop flow visualization experiments indicated that the high freestream turbulence eliminated the separation observed on the suction surface for low freestream turbulence; however, the experiments also indicated turbulence did not eliminate the separation observed near the leading edge of the pressure surface.

Effect of Model Reynolds Number. As with the low freestream turbulence configuration, an increase in the Reynolds number yielded an increase in heat transfer coefficient, illustrated in Figure 5.23; however, unlike the low freestream turbulence configuration, manipulation of the Nusselt number using equation 2.17 did not force the pressure and suction surface curves to coalesce, illustrated in Figures 5.24a and 5.24b. This confirms the elimination of the suction surface laminar boundary with an increase in the freestream turbulence.

Effect of AOI. Unlike the low turbulence configuration, there appears to be no obvious connection between the heat transfer coefficient and the AOI, illustrated in Figures 5.25a, 5.25b, and 5.25c. Whereas for the low turbulence configuration there was a distinct decrease in the heat transfer coefficient with an increase in the AOI, there is no such behavior for the high turbulence configuration. It is apparent that the freestream turbulence is affecting the boundary layer in such a way as to eliminate the distinct variations observed for the low turbulence configurations. "Normalization" of the

local Nusselt numbers are by $Re^{0.5}$ in Figures 5.26a 5.26b provides no useful information. The curves appear to coalesce near the leading edge of the pressure surface, but this is a known region of flow separation and reattachment.

The low and high turbulence Nusselt numbers are illustrated together in Figures 5.27a and 5.27b. On the pressure surface of Figure 5.27a, the increase in the freestream turbulence level appears to translate into an across the board increase in the local Nusselt number. On the suction surface of Figure 5.27b, the increase in the freestream turbulence level appears to eliminate the region of laminar heat transfer and the boundary layer separation, with the level of heat transfer near the trailing edge equal to the low turbulence values.

In the final analysis of the low and high freestream turbulence heat transfer, the correlation given by Simonich and Bradshaw (Simonich and Bradshaw, 1978),

$$St = St_o(1 + 5Tu) \qquad (5.8)$$

where St_o is the low freestream turbulence Stanton number, was applied to this

experiment as illustrated in Figures 5.28a - 5.28h. For most high Reynolds number configurations, the predicted curve agrees with the experimental curve remarkably well except in the known regions of boundary layer separation on the pressure and suction surfaces; however, for the low Reynolds number configurations, there is little agreement between the measured and predicted. This would indicate that, despite the seemingly irregular behavior of the high freestream turbulence heat transfer, the Simonich and Bradshaw correlation would allow a reasonable prediction of the high freestream turbulence heat transfer based on the low freestream turbulence values for the high Reynolds number configurations.

VI Conclusions and Recommendations

6.1 Conclusions

There are many analytical, experimental, and computational studies dealing with the convective heat transfer to or from a turbine blade. Convective heat transfer is a process which is a function of properties of the heat transfer medium. For forced convection, the most important properties have to do with the behavior of the boundary layer. In general, the behavior the boundary layer is a function of freestream, or edge, properties. In a turbine cascade, the edge, or passage, flow properties are a function of the physical aspects of the linear cascade which include the profile of the blade, the span, and the spacing. Background research for this experiment included reviewing many publications on previous analytical, computational, and experimental efforts. The bottom line is that every experiment is different and the results of one experiment may not provide general guidance for all experiments.

The primary objective of this effort was to determine the effect of the angle of incidence to a linear turbine blade cascade on the turbine blade convective heat transfer. In order to separate the effects of variations in the model Reynolds number and freestream turbulence, a test matrix was developed which included these factors as configuration parameters. An attempt was made to confirm intermediate conclusions by comparison with previous efforts. Since this was not possible in all cases, the following conclusions apply to the linear turbine cascade as installed in the TCTF.

1. For the low turbulence configuration, the pressure surface experimental Nusselt number values exceed the turbulent boundary layer predictions yet the convective heat transfer coefficient indicates a transitional or fully turbulent boundary layer. Relaminarization of the boundary layer as predicted by the acceleration parameter does not seem to occur. The suction surface heat transfer matches the laminar predictions to the point

of separation, after which the heat transfer lies between the laminar and turbulent predictions. ·

For the high turbulence configuration, the pressure surface heat transfer appears fully turbulent and the entire suction surface heat transfer lies between the laminar and turbulent predictions.

2. For any TCTF configuration, the convective heat transfer increases as the Reynolds number increases. This is no surprise since it can be shown that, for both laminar and turbulent boundary layers, the heat transfer is proportional to the local Reynolds number. Localized boundary layer behavior, such as separation, may vary with the Reynolds number.

3. For any TCTF configuration, the convective heat transfer increases as the freestream turbulence level increases. The primary effect of increased freestream turbulence was the apparent elimination of a region of boundary layer separation on the suction surface, dramatically increasing the heat transfer. It was observed that the high freestream turbulence heat transfer may possibly be predicted with reasonable accuracy from the low freestream turbulence using the Simonich-Bradshaw correlation.

4. For a given low turbulence Reynolds number, the convective heat transfer decreases as the AOI increases. This appears to be partially a result of the decrease in the streamwise passage and local velocity for increasing AOI and partially a result of the local and regional behavior of the boundary layer. It was demonstrated through laminar boundary layer heat transfer analysis that the variation in heat transfer was not solely a result of the variation in the local Reynolds number.

5. For a given high turbulence Reynolds number, the effects of increasing the AOI were less pronounced and difficult to isolate. Unlike for the low freestream turbulence configuration, the variation in the heat transfer with the AOI was not obvious and appeared more or less random.

6. The results of the pressure coefficient scans and the oil drop flow visualization experiments became just as important as the results of the heat transfer experiments in determining and understanding the behavior of the heat transfer for changes in the angle of incidence, model Reynolds number, and freestream turbulence level. Any attempt to make conclusions based on the heat transfer data alone will result in unreliable and unsubstantiated conclusions. The heat transfer, pressure coefficient, and oil drop data combination provides an almost complete package of undisputable information.

6.2 Recommendations

6.2.1 TCTF

1. Fabricate a new test section plexiglass cover. After being used by 3 graduate students, the present cover looks like Swiss cheese. The ideal cover would provide access for the necessary instrumentation to the necessary locations. The concentric circle configuration developed by Capt Acree (Acree, 1990) provided limited access to almost any location in the cascade. Since for this series of experiments data was required only for specific locations, this cover was removed and replaced with a cover providing rapid and accurate fixed location access. The Acree cover could possible be reutilized and reconfigured to provide total access to any location in the cascade, including upstream and downstream.

2. Fabricate a new turbulence generation grid. Since adjusting the AOI changed the effective spacing between the tubes, a new turbulence grid with adjustable tube spacing should be installed in the TCTF. The new grid should be designed such that parameters of the turbulence, such as amplitude and frequency, are variable. A "squirrel cage" turbulence generation device has been successfully used in a turbine cascade (Bayley and Priddy, 1981).

6.2.2 Turbine Cascade

1. Fabricate a new heat transfer instrumented turbine blade with more pressure taps and thermocouples, particularly around the leading edge. A more densely instrumented blade would reveal more particulars about the heat transfer processes. With the current thermocouple and pressure tap arrangement, it is sometimes difficult to follow the movement of the stagnation point and regional flow anomalies. The heat transfer surface should be useable throughout, avoiding areas of unknown current density.

2. Fabricate a heated (not necessarily instrumented) blade with a temperature sensitive liquid crystal coating for heat transfer visualization purposes. Experiments with the temperature sensitive liquid crystal material (Hippensteele et al, 1985) have demonstrated the feasibility of the material for calculating heat transfer coefficients. On a simpler scale, in the uncalibrated mode the material displays cooler and warmer regions as different colors, revealing flow and heat transfer patterns not visible with fixed location thermocouples and pressure taps. The addition of the liquid crystal data to the pressure, temperature, and oil flow visualization data would provide all the information needed for the heat transfer analysis.

6.2.3 Instrumentation

1. Replace the Scanivalve with a pressure data acquisition system similar to that used in the 5 ft wind tunnel. The Scanivalve, although relatively inexpensive, is very

slow and somewhat unreliable. A new pressure data acquisition system, combined with a more densely instrumented turbine blade, would greatly improve the experimental value of the TCTF

2. Install another high speed voltmeter in the HP3852A, allowing simultaneous wire1 and wire2 readings. This would allow 100,000 Hz x-wire readings, necessary for accurate calculation of the turbulence scales through the Eulerian time correlation (see Appendix A), and it would allow a greater number of data points since each voltmeter has its own memory. There is a high speed voltmeter in the 5 ft wind tunnel HP3852A, and if is not being used to acquire hot-wire data, it is being underutilized.

3. Fabricate a total pressure rake for both the cascade entrance and exit. A total pressure rake for each AOI of interest would speed up the total pressure data acqui-sition process and insure repeatable data. The current total pressure data acquisition procedure requires adjusting the total pressure tube angle and moving the tube to a location marked on the test section plexiglass cover. This method results in unreliable and unrepeatable data. Connected to the new pressure data acquisition system, total pressure information could be acquired rapidly, repeatably, and reliably.

6.2.4 Procedures

1. Utilize the most advanced x-wire calibration scheme available at AFIT. There was no mechanism to factor in the ambient temperature to the hot-wire calibrations. During the course of a typical summer day, the temperature in Bldg 19 may go from 70 degrees to 95 degrees. The current calibration procedure calls for performing a calibration for every 5 degrees F. This convention complicates the data acquisition and reduction procedure since a different calibration file must be accessed for a change in temperature. A single calibration file would eliminate the possibility of acquiring or reducing data with an incorrect calibration file.

2. The software provides almost fully automated data acquisition and reduction; however, several more weeks of work on the software would provide a complete, idiot-proof, fully automated data acquisition system for the TCTF. For this series of experiments, the data reduction process was removed from the data acquisition process due to the complexity of the software at that time. Due to the large amount of data acquired for a typical test, recombination of the data acquisition and reduction software in a user-friendly package may reduce the time required for data acquisition and reduction.

6.2.5 Follow-On or Supporting Efforts

1. Support the experimental effort with a computational effort. I've always preferred "building and testing" over "modeling"; however, a good model of the TCTF would help in formulating conclusions. Many of the references compared their experimental results with predictions.

2. Perform an experiment with a variable turbulence level. By being able to vary the turbulence level from 0.5 % to 10%, the somewhat erratic heat transfer behavior observed for the turbulent configurations in this experiment may be eliminated to the point where the effect of the AOI may be observed.

3. Most importantly, perform a complete study of the behavior of the flow through the cascade passage, including the turbine blade boundary layer. In order to fully understand the convective heat transfer mechanisms for a given configuration, the behavior of the flow must be fully understood. Although others have studied the flow through a turbine cascade, their results do not help in completely understanding what is going on in the TCTF.

VII References

Acree, 1990. Acree, J.L., "Turbulence Scales in the Passage of a Linear Turbine Cascade," AFIT, 1990.

Cebeci and Smith, 1974. Cebeci, T. and A.O. Smith, Analysis of Turbulent Boundary Layers, New York: Acedemic Press, 1974.

Champagne, 1965. Champagne, F.H., "Turbulence Measurements with Inclined Hot Wires," Boeing Scientific Research Labs, Flight Science Laboratory, Report No. 103, 1965.

Consigny and Richards, 1982. Consigny, H. and B.E. Richards, "Short Duration Measurements of Heat-Transfer Rate to a Gas Turbine Rotor Blade," Journal of Engineering for Power, Vol 104, July 1982, pp. 542 - 551.

Daniels and Browne, 1981. Daniels, L.D. and W.B. Browne, "Calculation of Heat Transfer Rates to Gas Turbine Blades," International Journal of Heat and Mass Transfer, Vol. 24, No. 5, 1981, pp. 871 - 879.

Gallasi, 1989. Gallasi, L., "Turbulence Scale Effects on Heat Transfer in a Linear Turbine Cascade", AFIT, 1989.

Hinze, 1959. Hinze, J.O., Turbulence, New York: McGraw Hill, 1959.

Hippensteele et al., 1985 Hippensteele et al., "Local Heat Transfer Measurements on a Large Scale Model Turbine Blade Airfoil Using a Composite of a Heater Element and Liquid Crystals," Journal of Engineering for Gas Turbines and Power, Vol. 107, October 1985, pp. 953 - 960.

Kays et al., 1970. Kays, W.M. et al., Journal of Heat Transfer, Vol 92, 1970, pp. 499 - 505.

Kays and Crawford, 1980. Kays, W.M. and M.E. Crawford, <u>Convective Heat and Mass Transfer</u>, New York: McGraw Hill, 1980.

Langston et al., 1977. Langston, L.S., "Three-Dimensional Flow Within a Turbine Cascade Passage," <u>Journal of Engineering for Power</u>, Vol. 99, January 1977, pp. 21-28.

Moore and Ransmayr, 1984. Moore, J. and A. Ransmayr, "Flow in a Turbine Cascade: Part I - Losses and Leading Edge Effects." <u>Journal of Engineering for Gas Turbines and Power</u>, Vol. 106, April 1984, pp. 400 - 408.

Priddy and Bayley, 1985. Priddy W.J. and F.J. Bayley, "Effects of Free Stream Turbulence on the Distibution of Heat Transfer Around Turbine Blade Sections," <u>International Journal of Heat and Fluid Flow</u>, Vol. 6, No. 3, September 1985, pp. 181 - 192.

Priddy and Bayley, 1988. Priddy W.J. and F.J. Bayley, "Turbulence Measurements in Turbine Blade Passages and Implications for Heat Transfer," <u>Journal of Turbomachinery</u>, Vol. 110, January 1988, pp. 73 - 79.

Simonich and Bradshaw, 1978. Simonich J.C. and P. Bradshaw, "Effect of Free Stream Turbulence on Heat Transfer Through a Turbulent Boundary Layer," <u>ASME Journal of Heat Transfer</u>, Vol. 100, No. 4, November 1978.
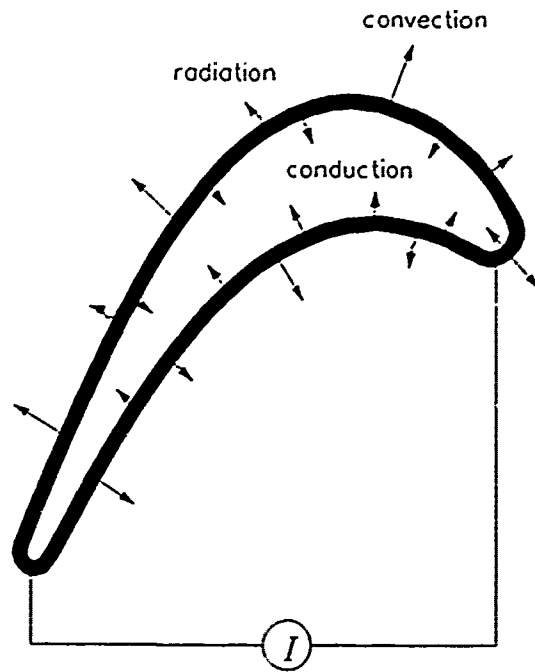
Figure 2.1. Turbine Blade Heat Transfer Model
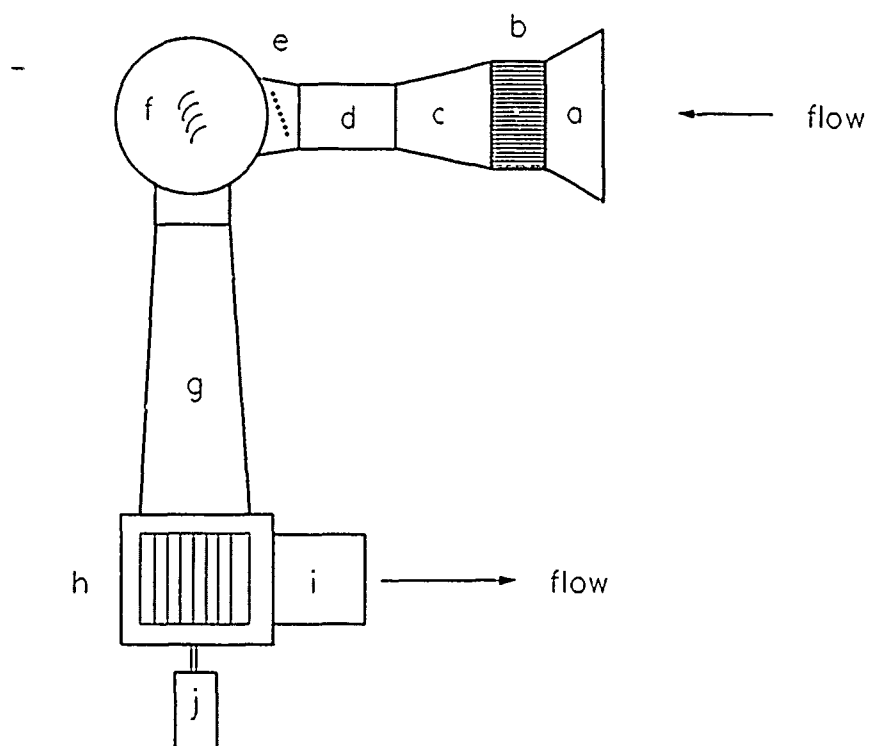
a. bell mouth tunnel inlet
b. honeycombed flow straightener
c. 7:1 contraction ratio converging nozzle
d. settling chamber
e. removeable turbulence grid
f. 23" diameter test section
g. diffuser
h. 18" diameter centrifugal blower
i. tunnel exhaust
j 20 hp motor

Figure 3.1 Turbine Cascade Test Facility (TCTF) Layout

adjustable inlet sideboards
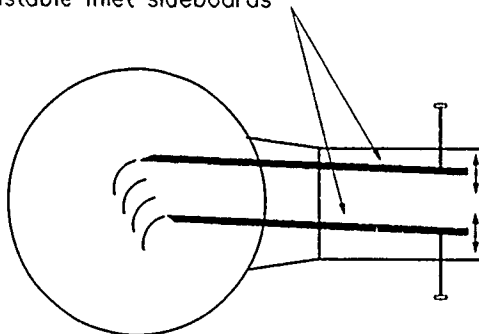
Figure 3.2 Adjustable Inlet Sideboards

blade #4

blade #2

3.5"

blade #2 (instrumented)

45 deg

blade #1

25 deg
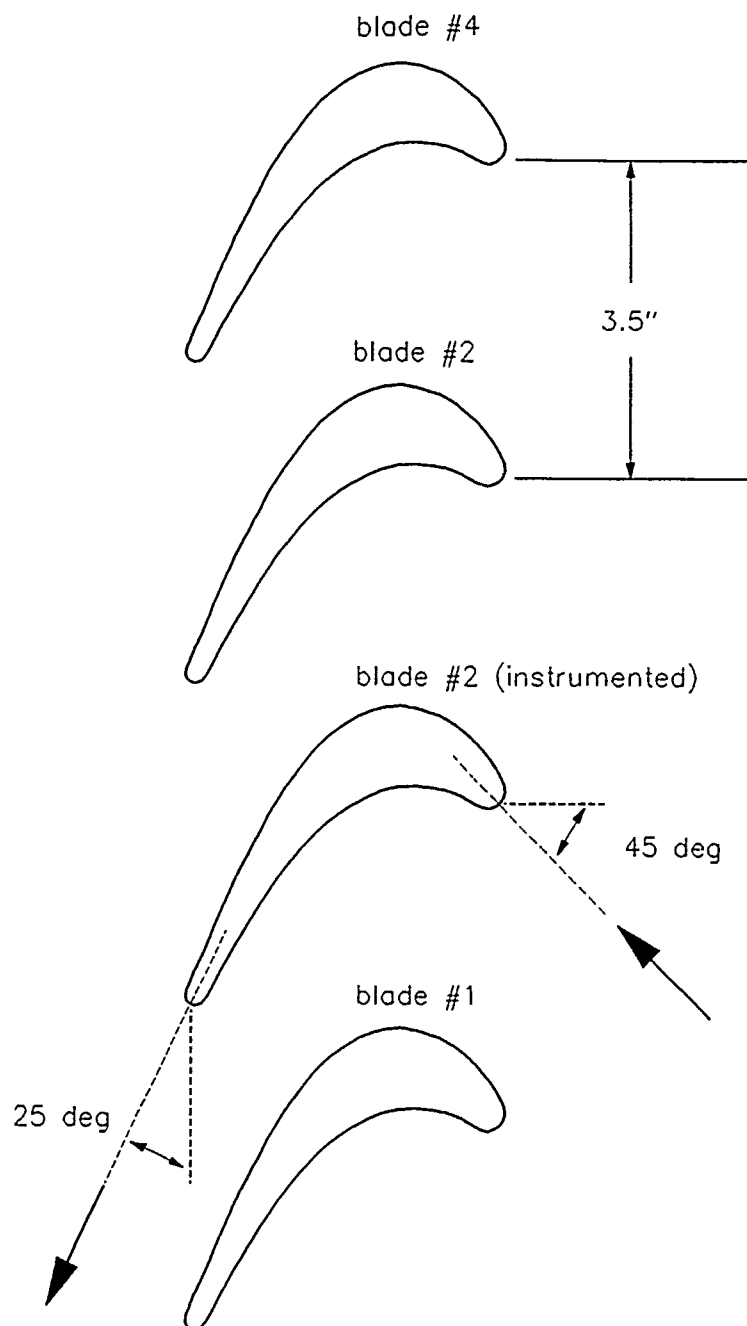
Figure 3.3 Linear Turbine Cascade

3D view

top

chord line
c = 4.5"

top

z = 4.5"

Heat
transfer
surface

pressure tap band

bottom
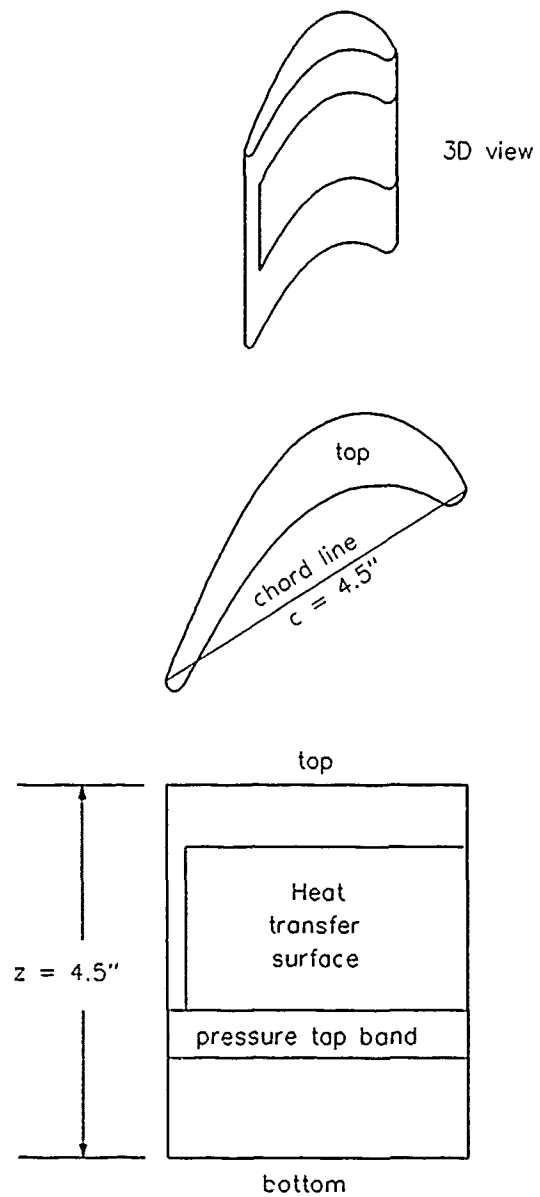
Figure 3.4 Details of Instrumented Blade
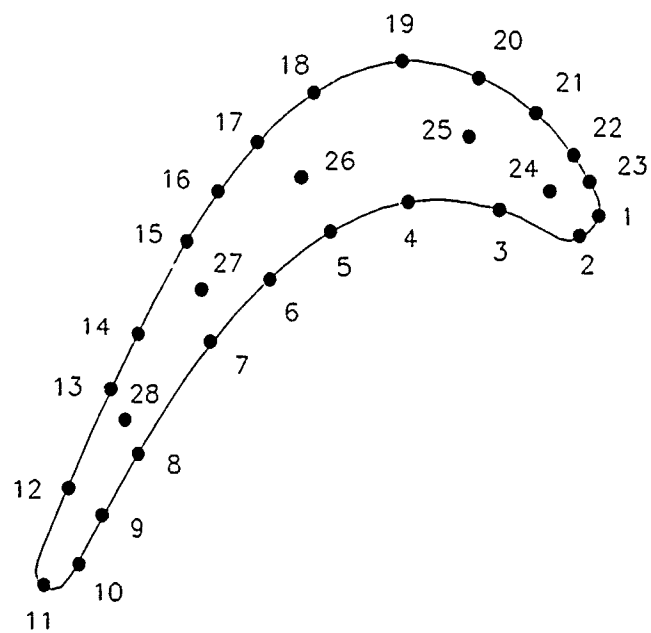
Figure 3.5 Thermocouple Locations

15.5" diameter plexiglass cover

sensor fixture

access slots and holes

protractor and pointer
for angle measurements

shaft for pressure
tubes and X-wire
probes

detail of sensor fixture
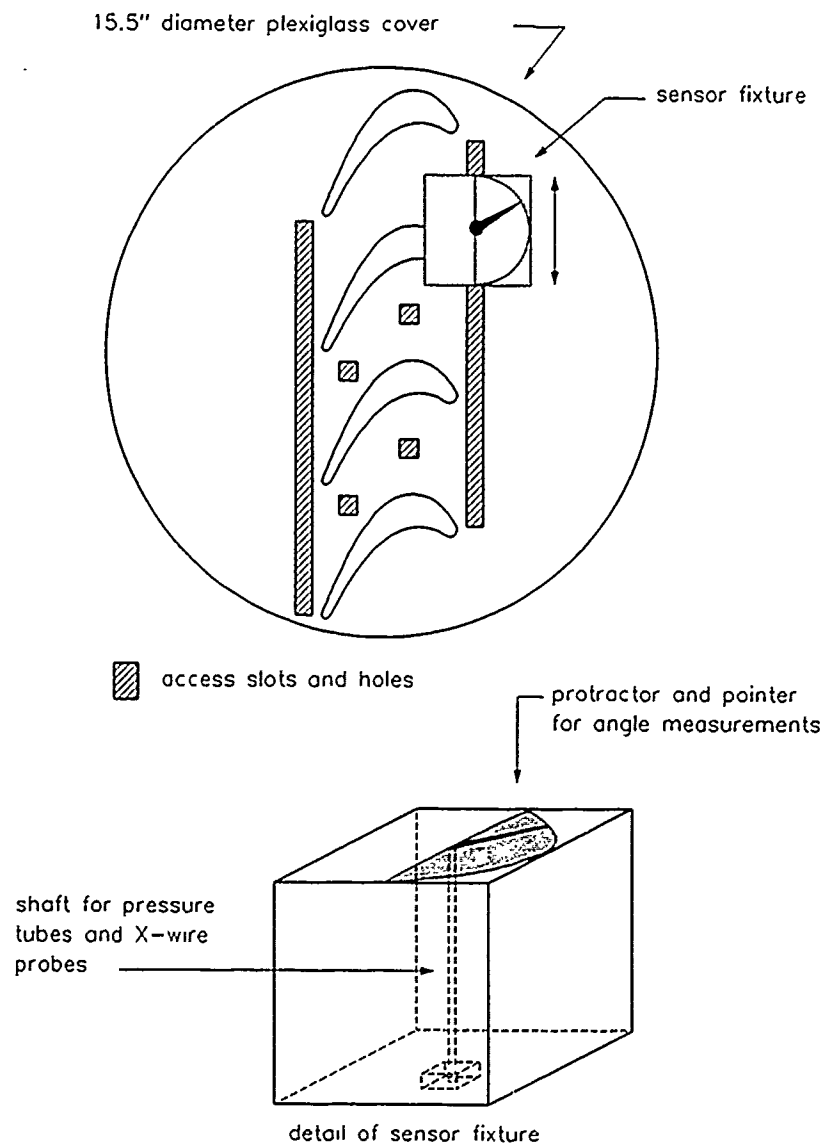
Figure 3.6 Test Section Access Configuration

36 Port Scanivalve

total pressure tube

Blade #2

U-tube manometer

pitot-static tube
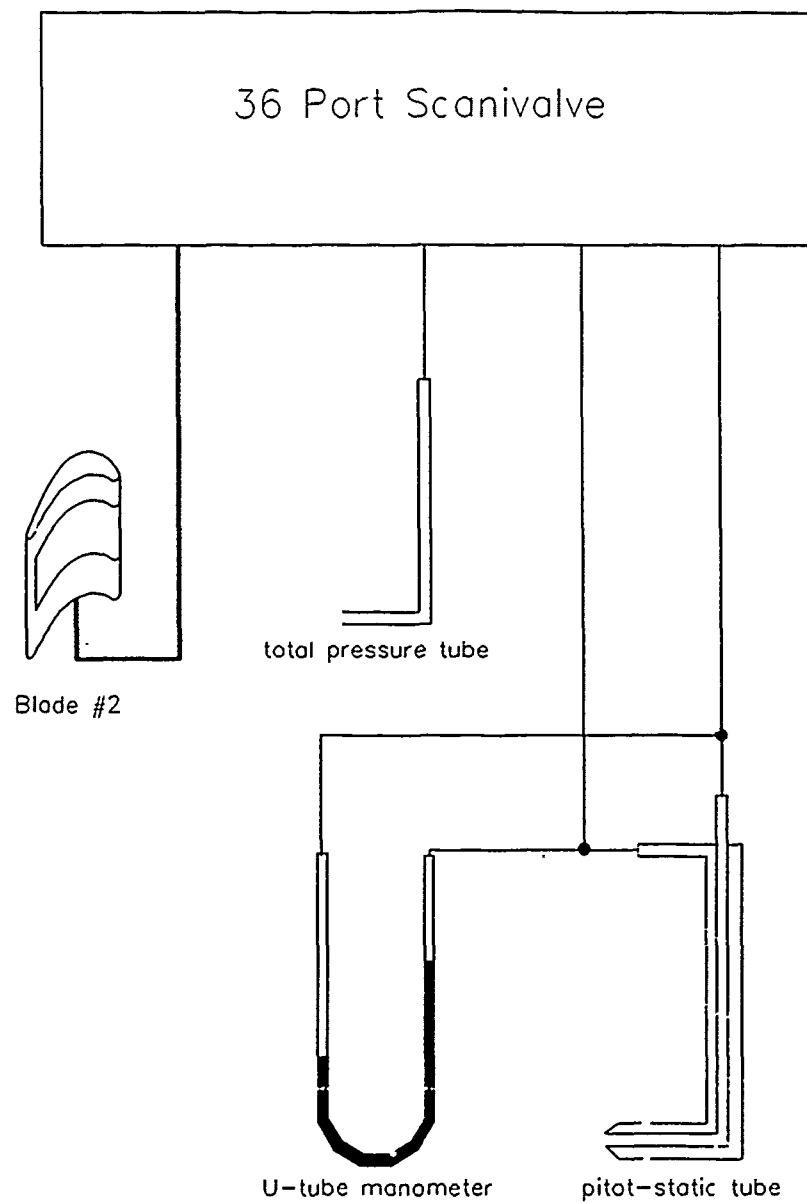
Figure 3.7 Pressure Measurement Schematic
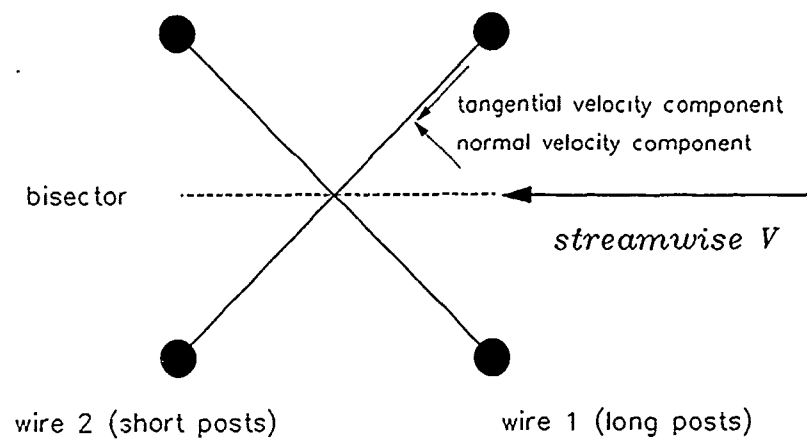
Figure 3.8 X-wire Configuration
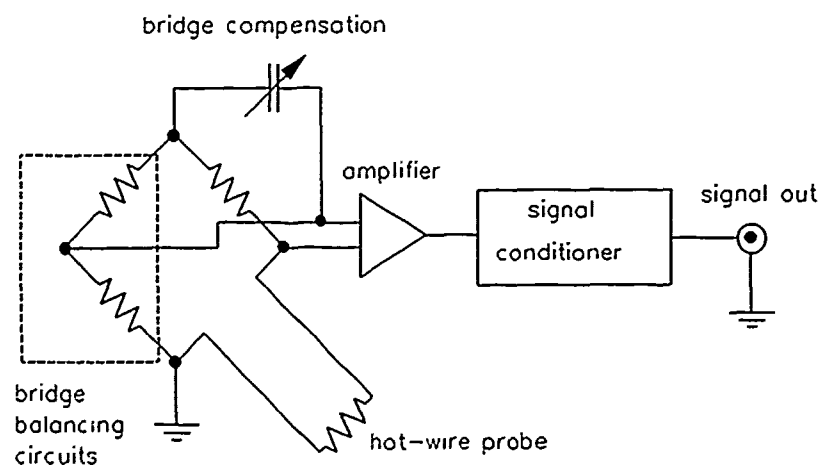
Figure 3.9 Simplified IFA-100 Schematic
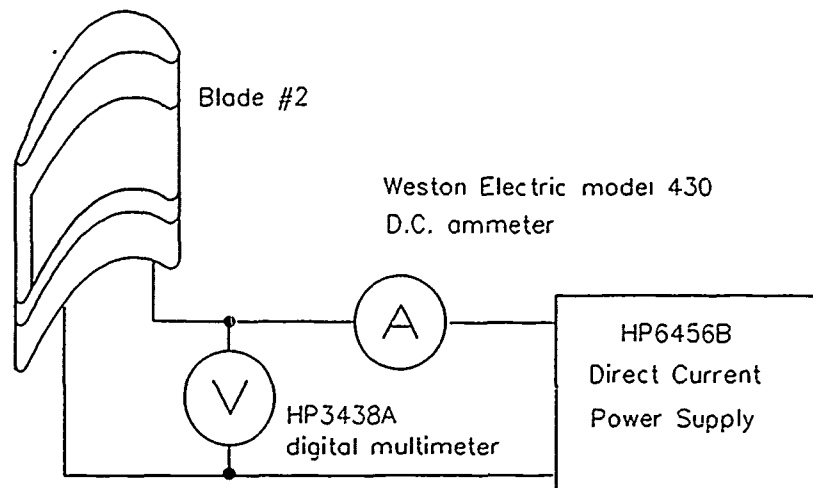
Figure 3.10 Instrumented Blade Power Schematic

GPIB	slot 0	slot 1	slot 2	slot 3	slot 4	slot 5	slot 6	slot 7	
	4	4	4	4	4		E	4	
	4	4	4	4	4		M	4	
	7	7	7	7	7		P	7	
	1	2	1	1	0		T	0	
	3	8	3	3	2		Y	1	
port	A	A	A	A	8			A	

44713A — 24 channel high–speed multiplexer
44728A — 8 channel relay actuator
44701A — integrating voltmeter
44702B — 13 bit high–speed voltmeter

Figure 3.11 Rear View of HP3852A
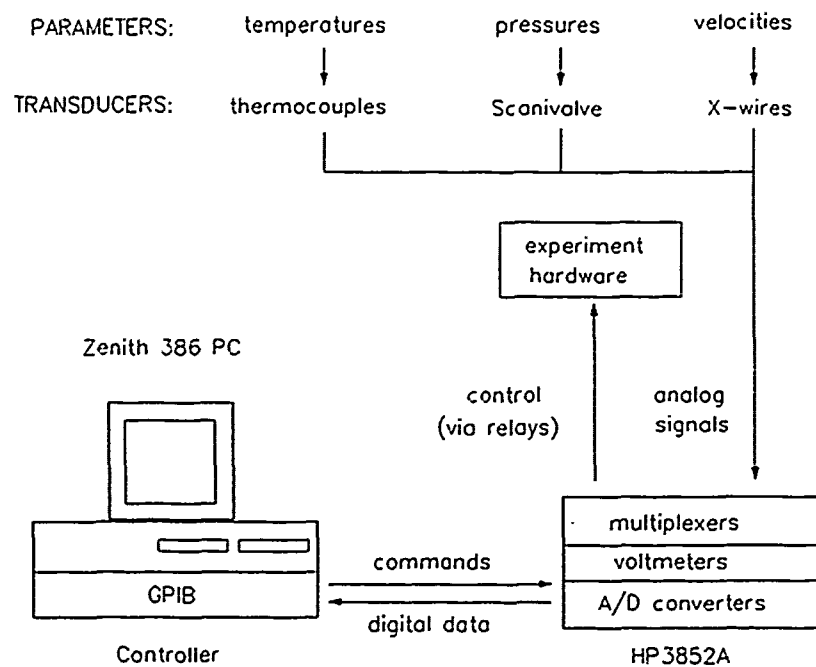
Figure 3.12 Data Acquisition System Flow Chart
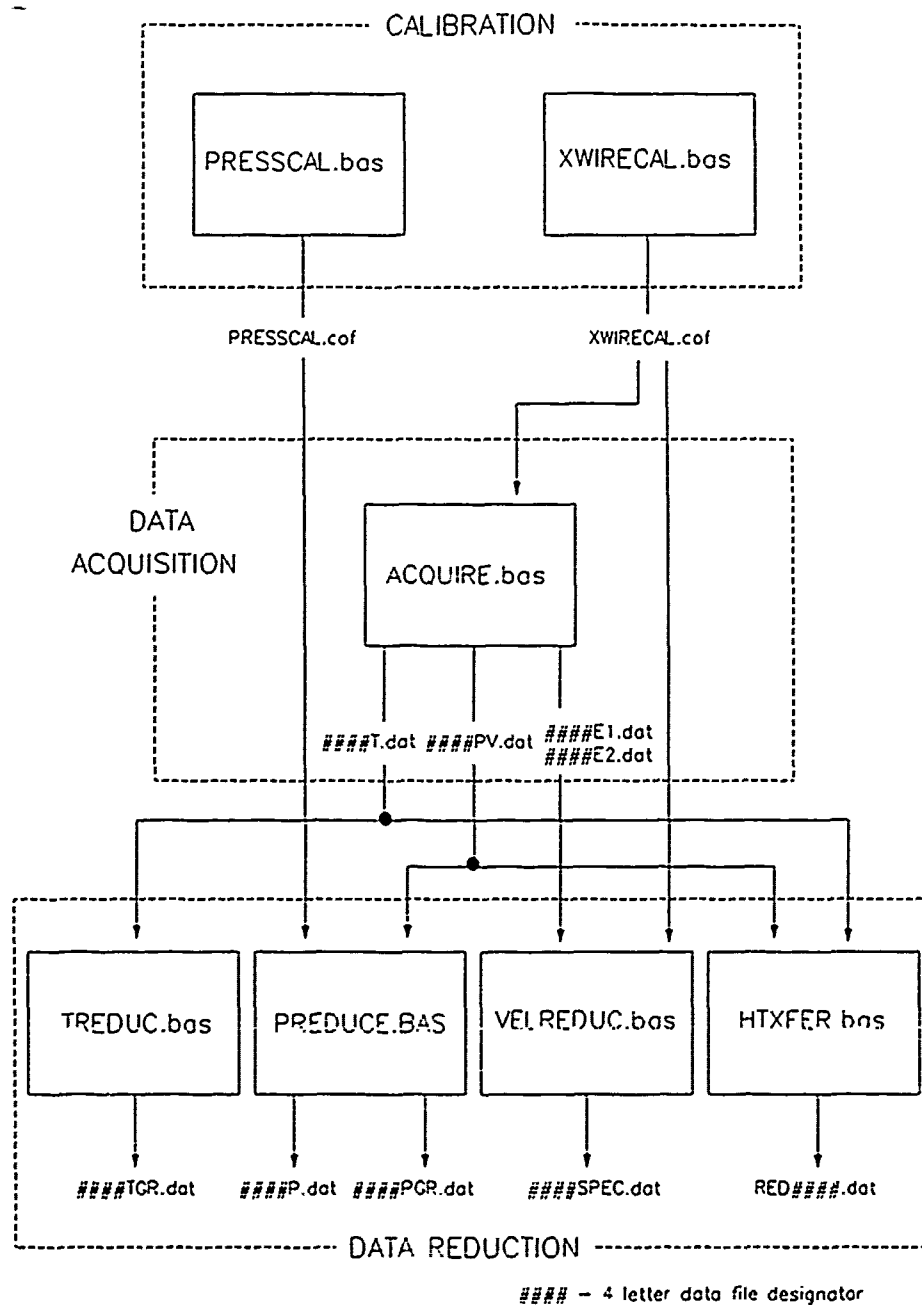
Figure 3.13 Software Flow Chart
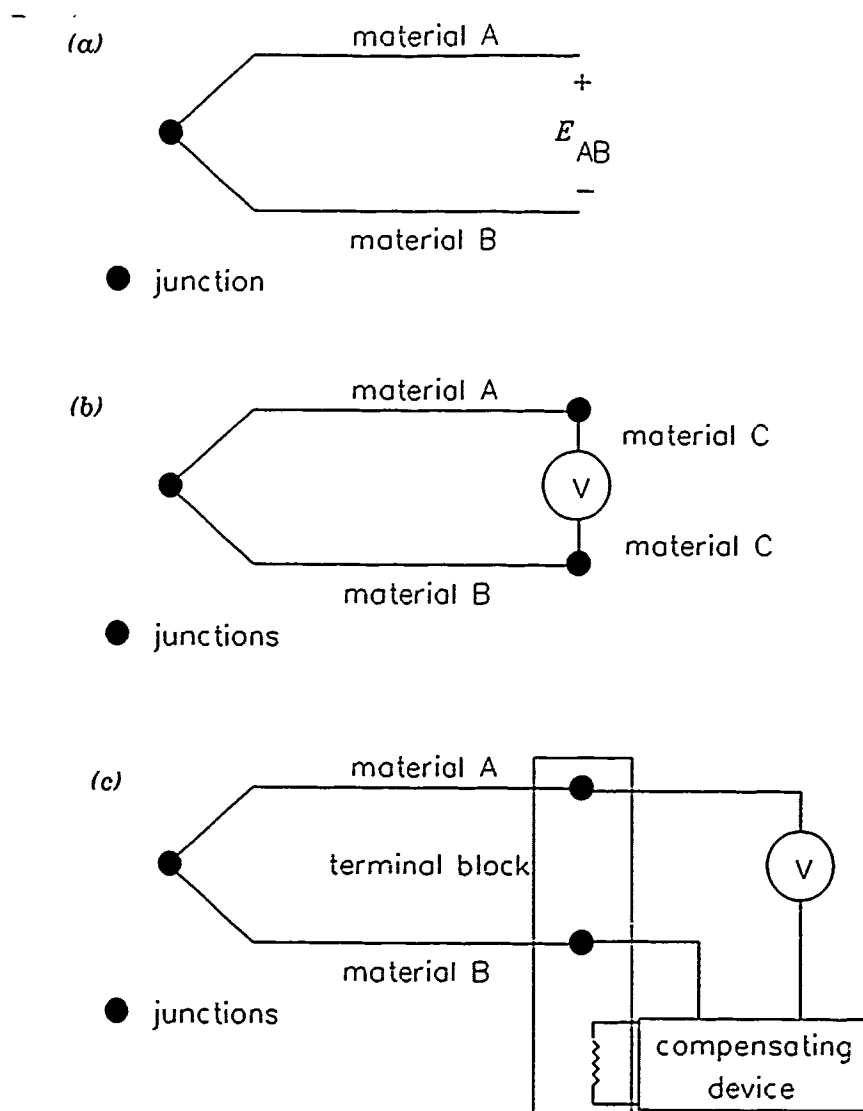
Figure 4.1 Thermocouple Schematics
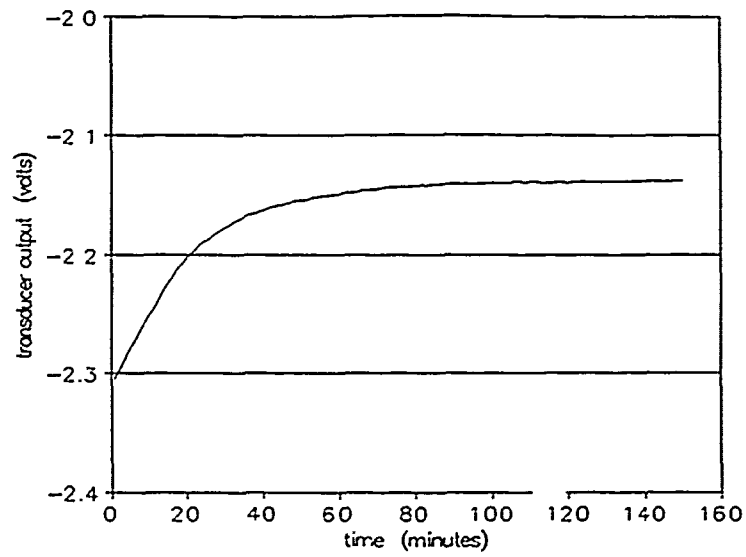
Figure 4.2 Data Acquisition System Warm-up Behavior
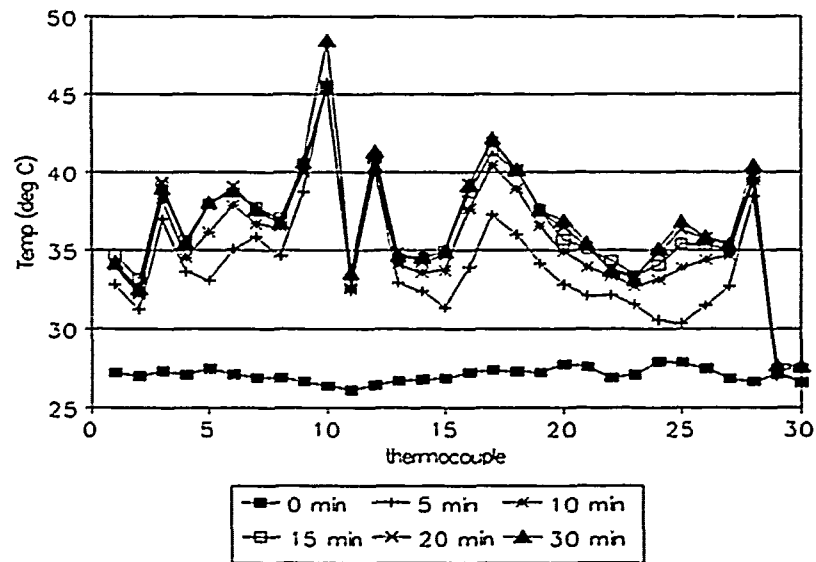
Figure 4.3 Turbine Blade Warm-up Behavior
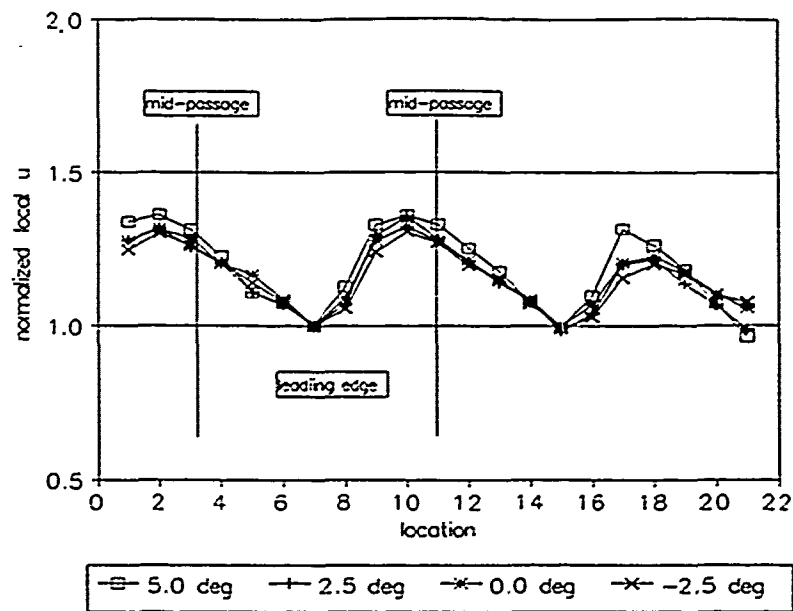
Figure 5.1a Low Turbulence Inlet Velocity Profile
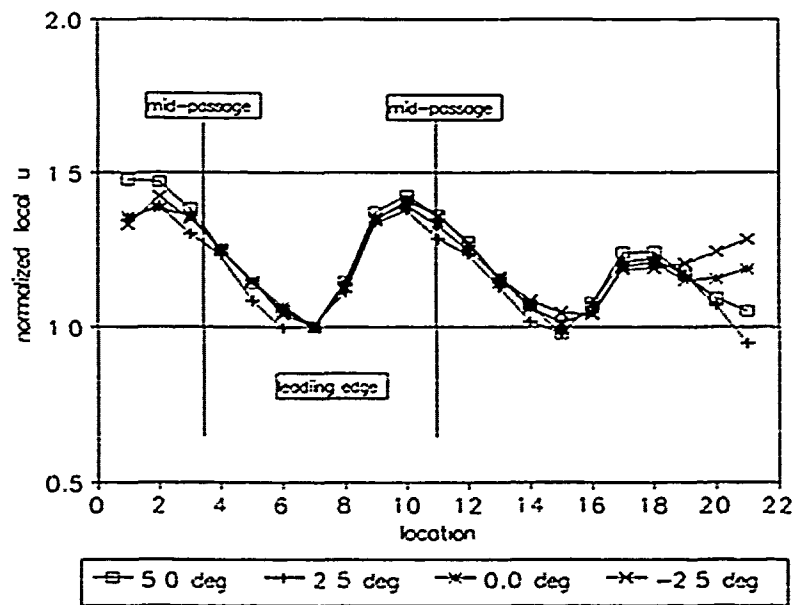
Figure 5.1b High Turbulence Inlet Velocity Profile
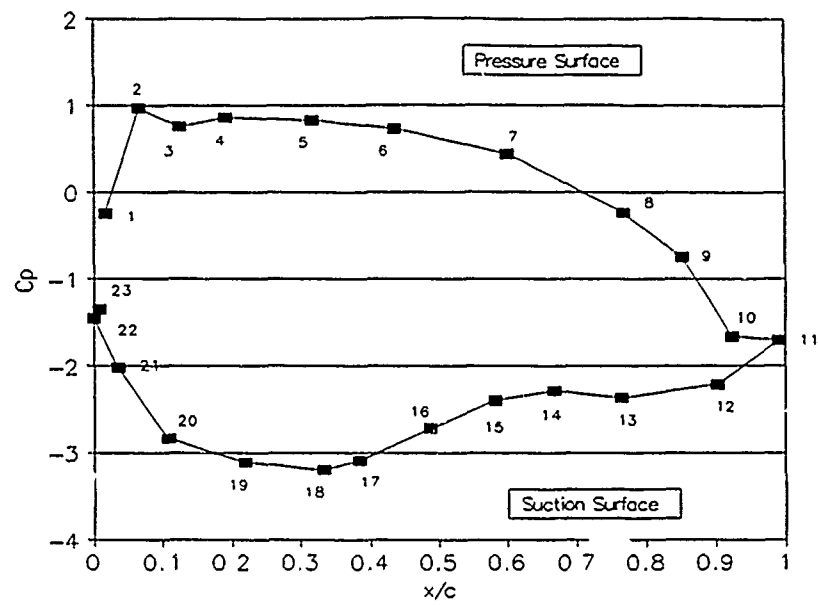
Figure 5.2 Typical Pressure Coefficient
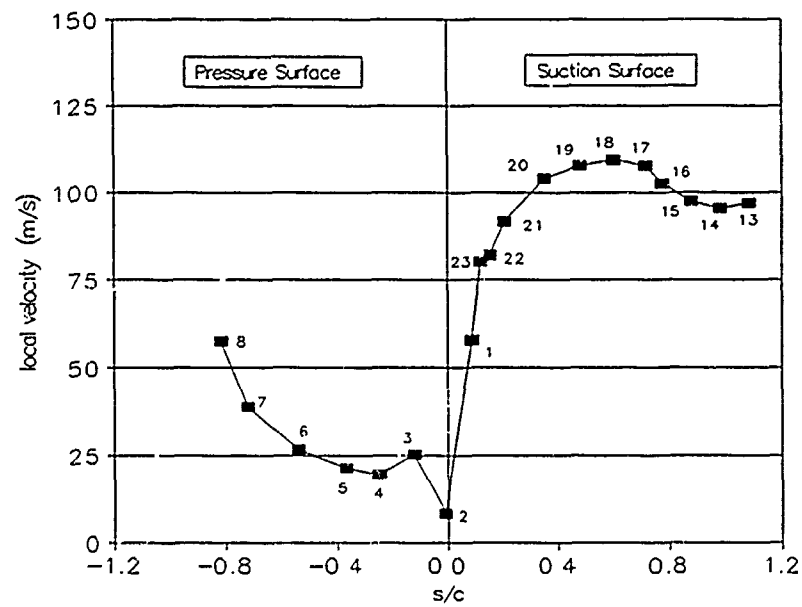
Figure 5.3 Typical Local Velocity
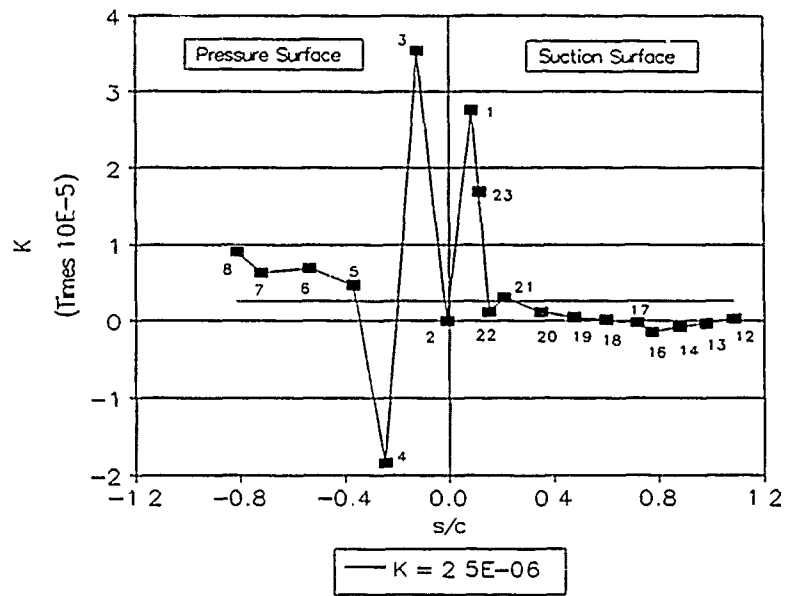
Figure 5.4 Typical Acceleration Parameter
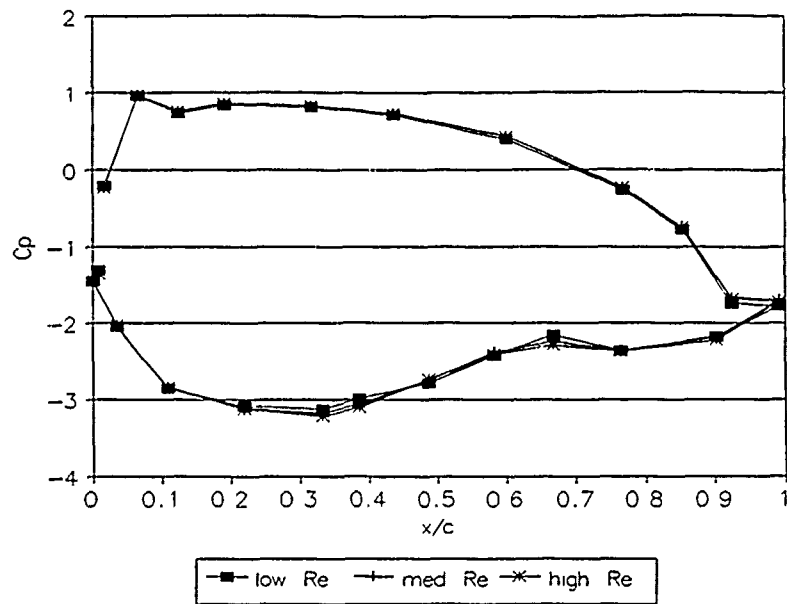
Figure 5.5a Variation in Cp with Re
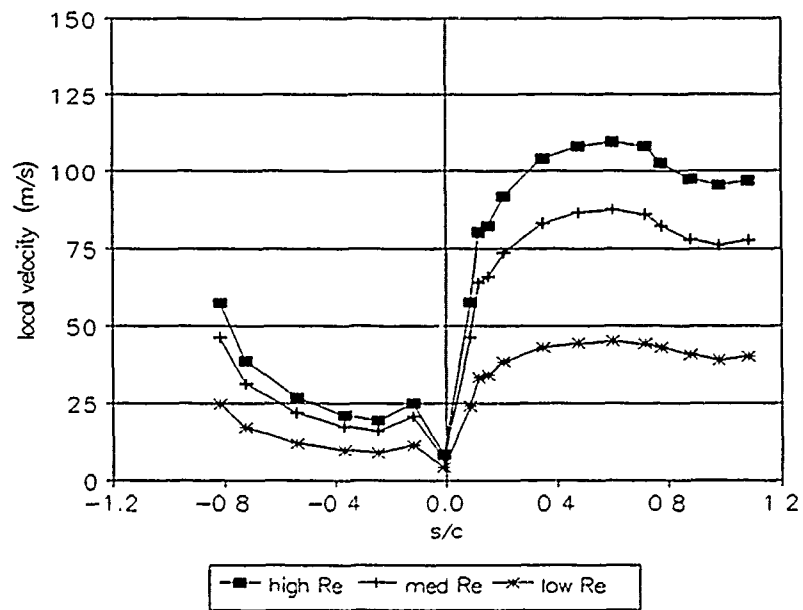
Figure 5.5b Variation in Local Velocity with Re
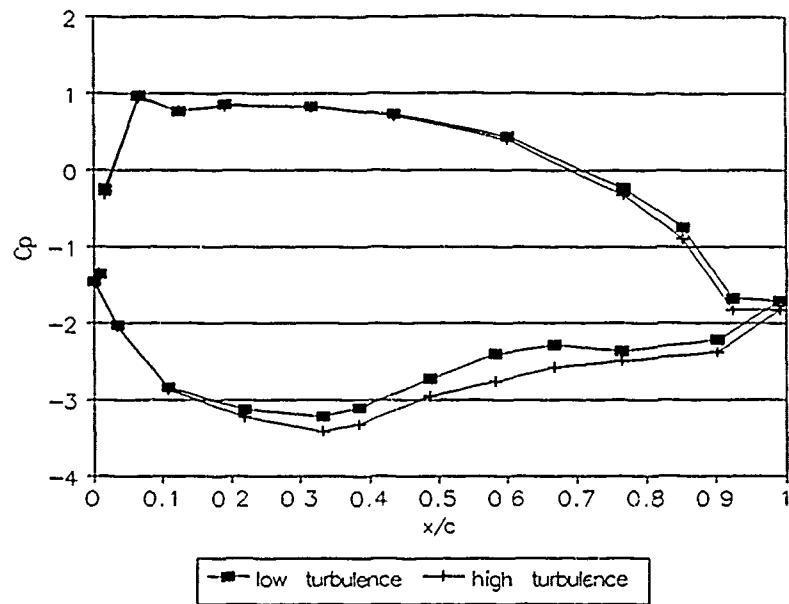
Figure 5.6a Typical Low/High Turbulence Cp
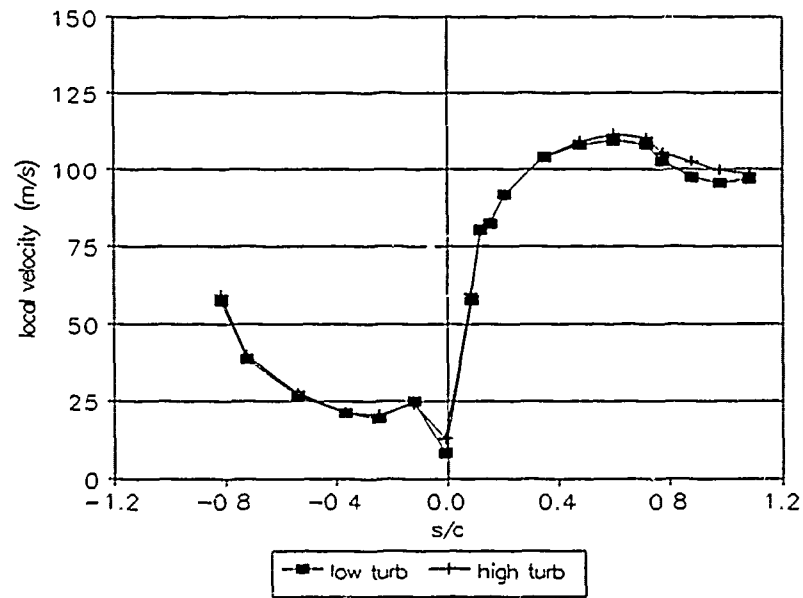
Figure 5.6b Low/High Turbulence Local Velocities
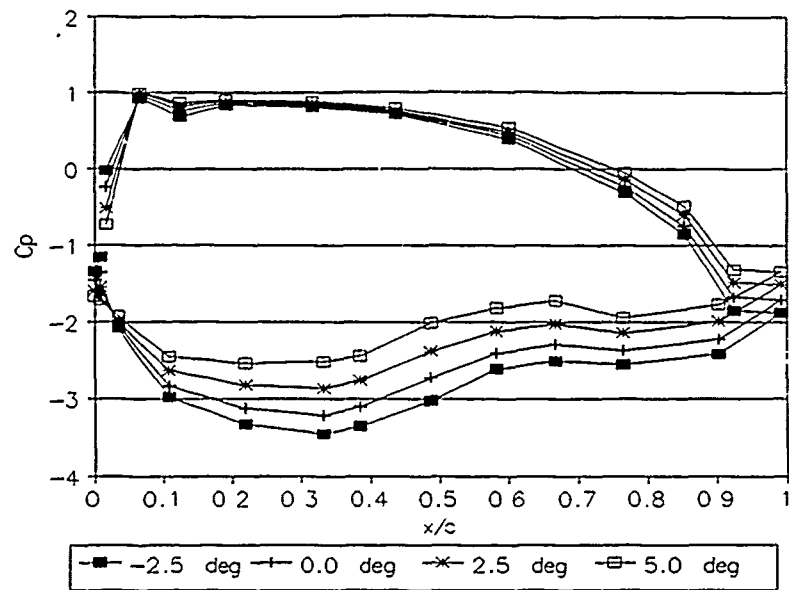
Figure 5.7a Variation in Cp with AOI, Low Tu
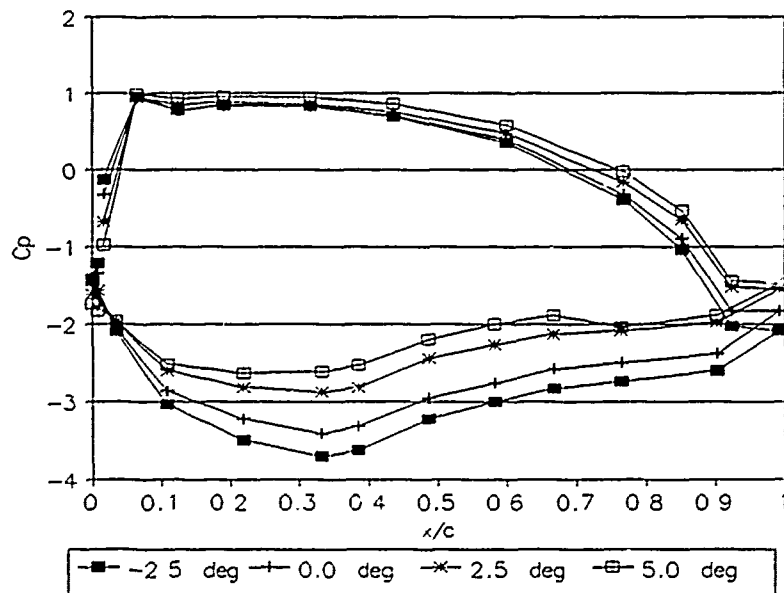
Figure 5.7b Variation in Cp with AOI, High Tu
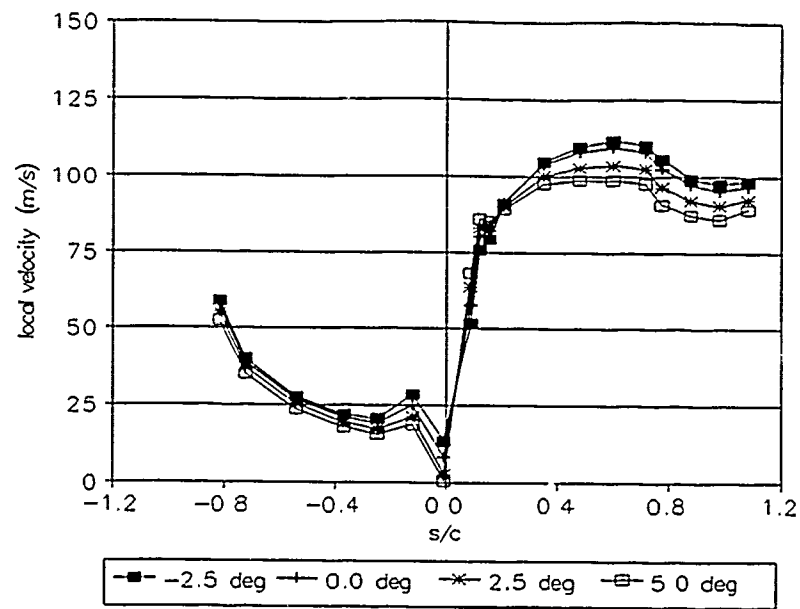
Figure 5.8 Variation in Local Velocity with AOI, Low Tu
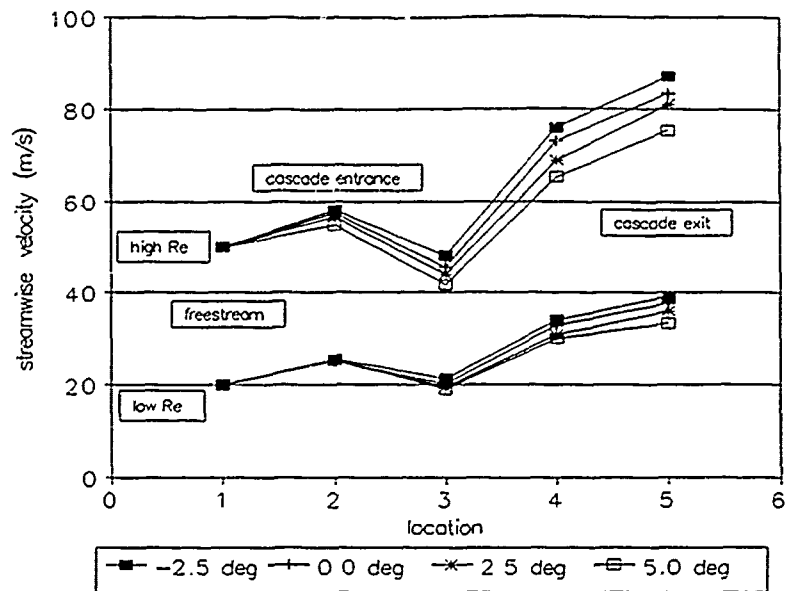
Figure 5.9a Cascade Passage Streamwise Velocity, Low Tu
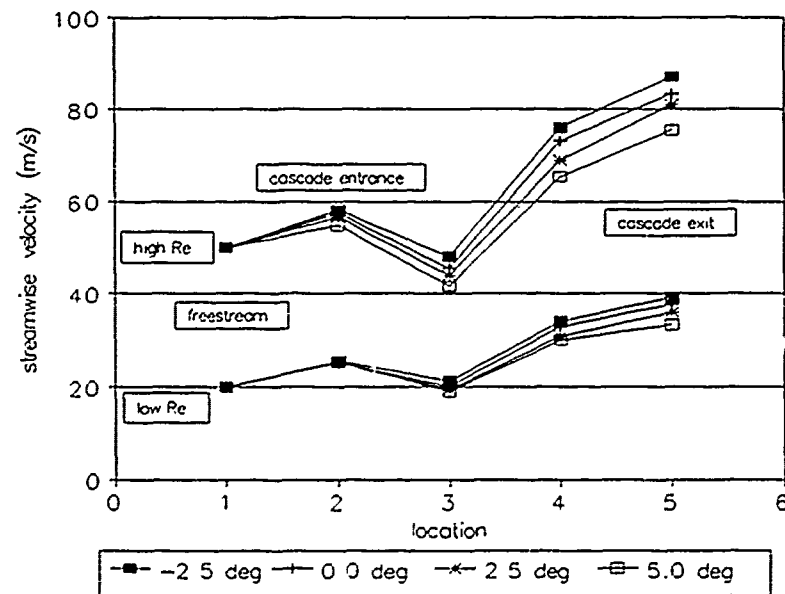
Figure 5.9b Cascade Passage Streamwise Velocity, High Tu
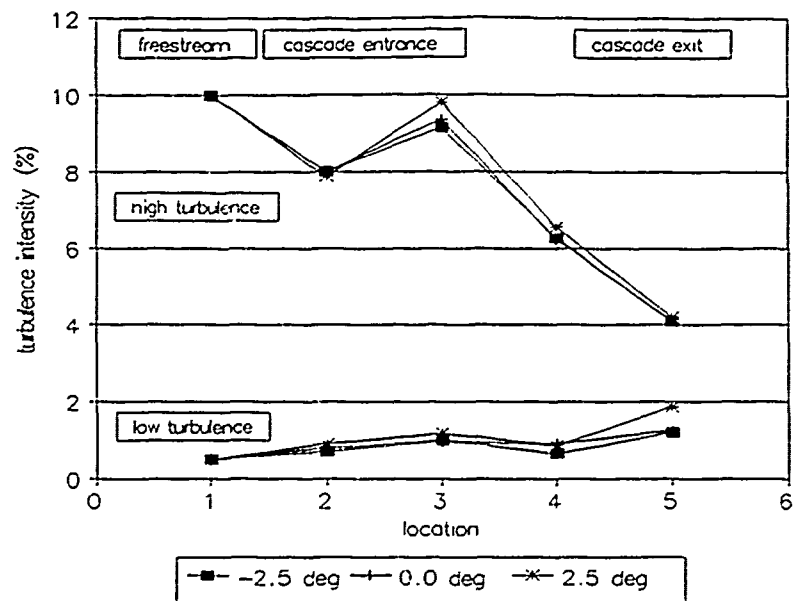
Figure 5.10a Cascade Passage Tu, Low Re
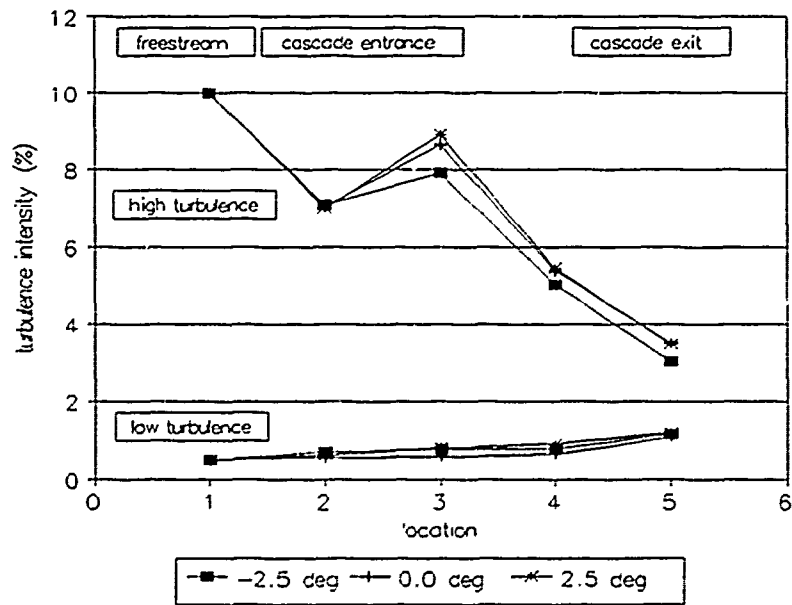
Figure 5.10b Cascade Passage Tu, High Re
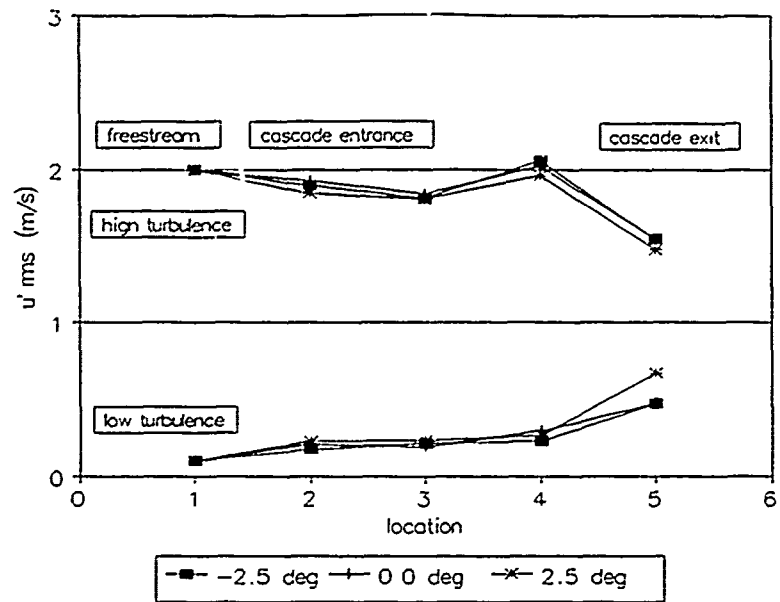
Figure 5.10c Cascade Passage RMS Velocity Fluctuation, Low Re
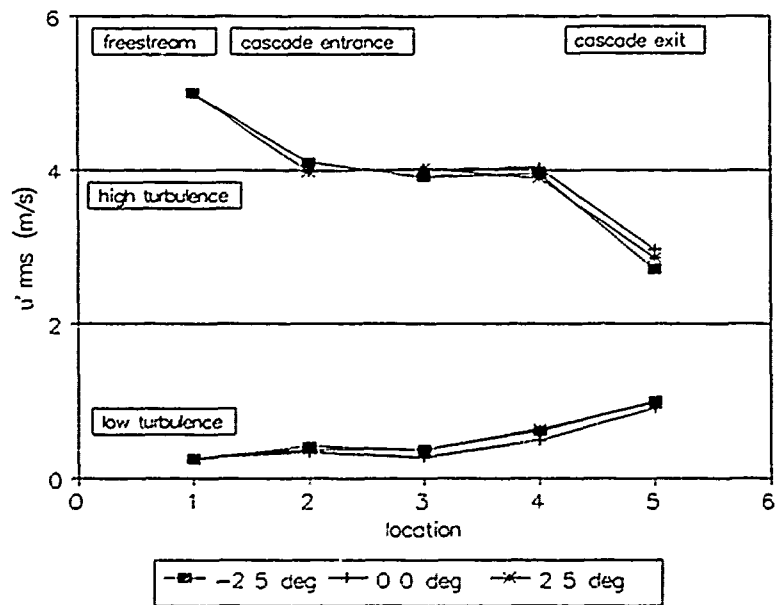
Figure 5.10d Cascade Passage RMS Velocity Fluctuation, High Re
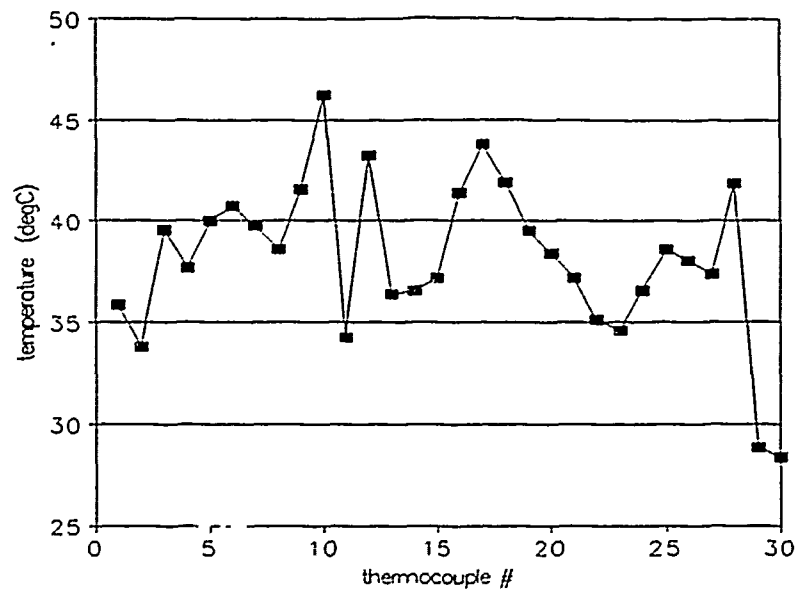
Figure 5.11 Typical Turbine Blade Temperature Scan
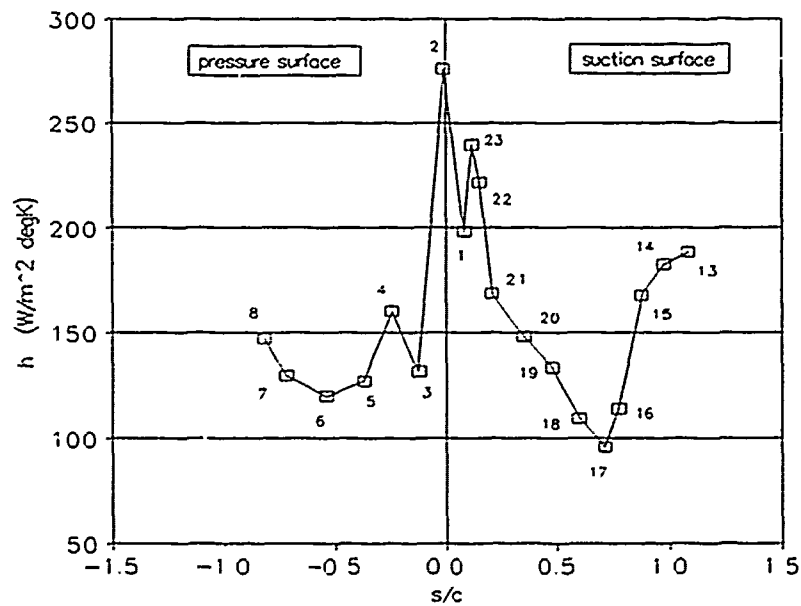
Figure 5.12 Typical Convective Heat Transfer Coefficient, Low Tu
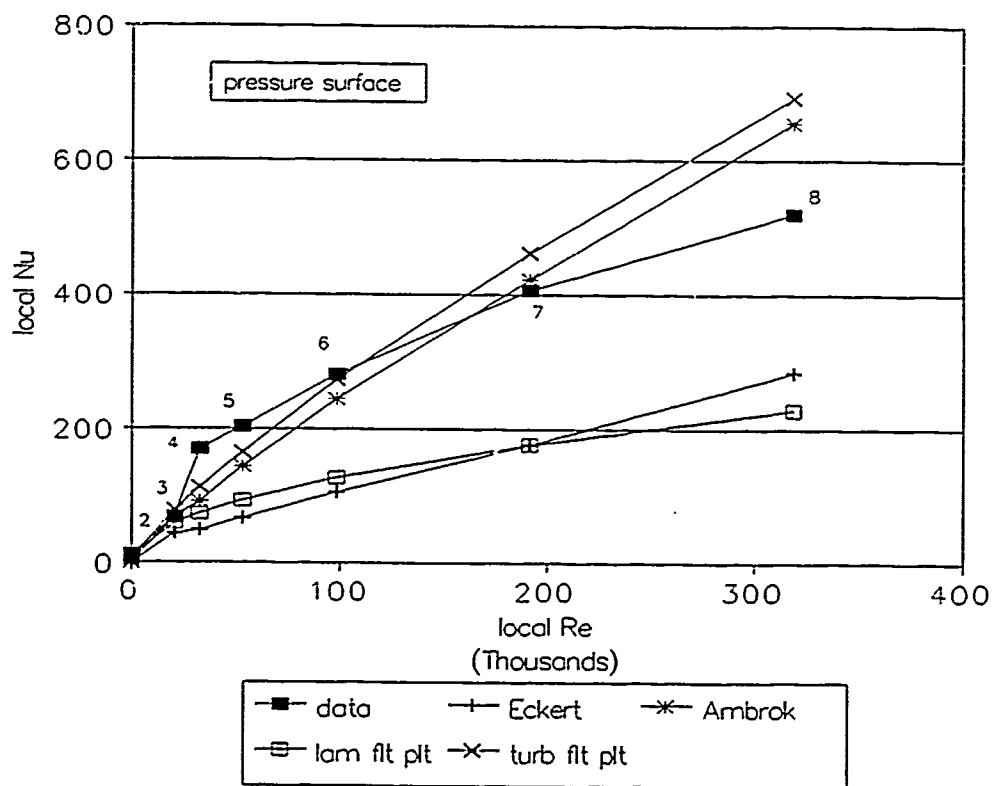
Figure 5.13 Experimental and Analytical Nu, Low Tu
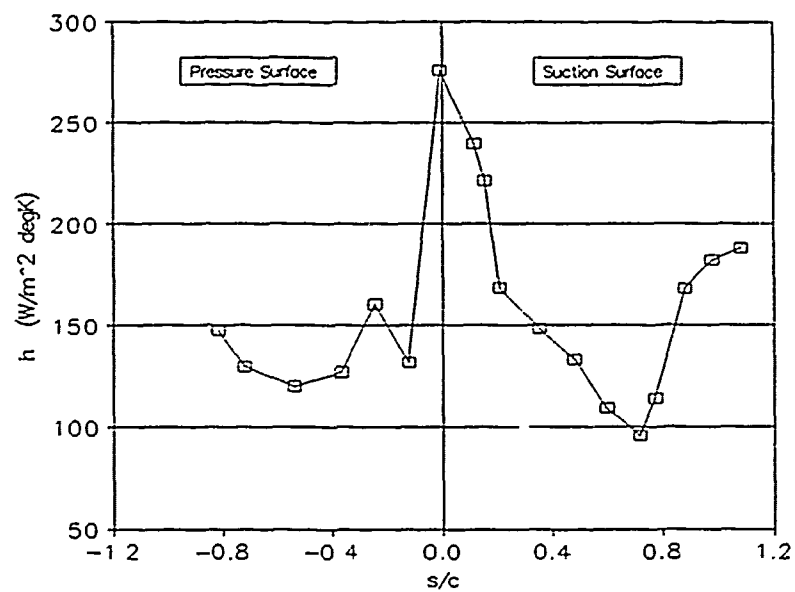
Figure 5.14 Corrected Heat Transfer Coefficients, Low Tu
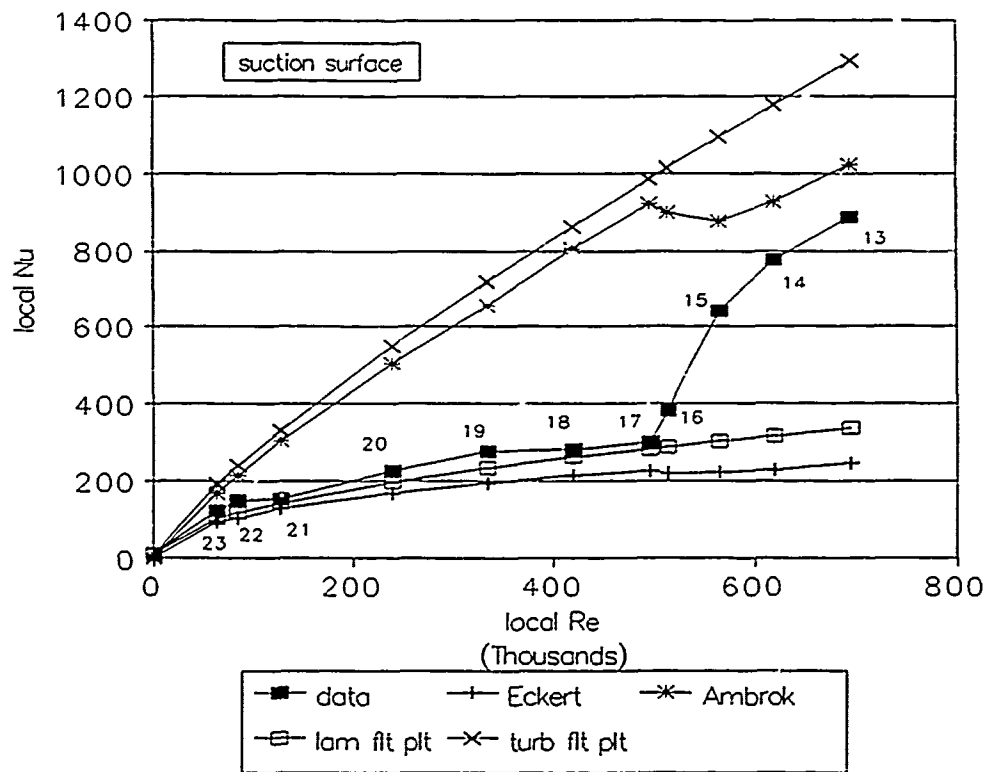
Figure 5.15 Experimental and Analytical Nu, Low Tu
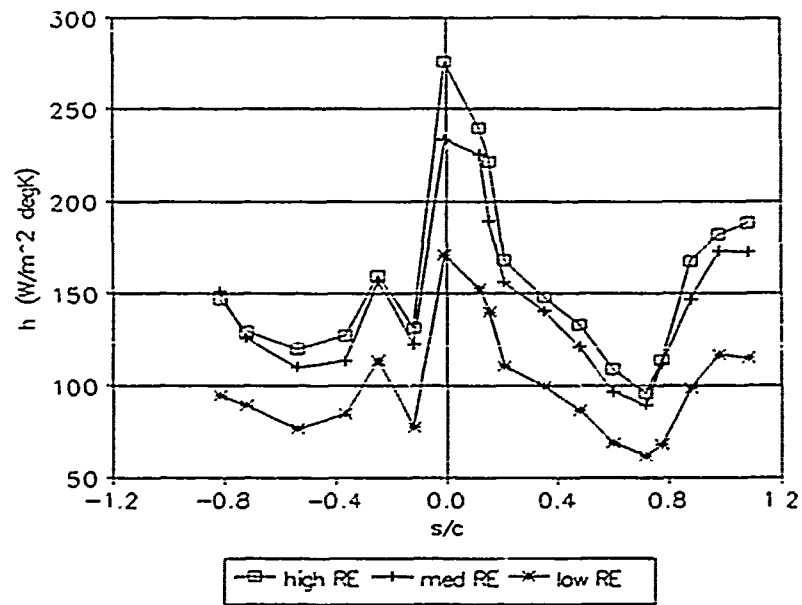
Figure 5.16 Variation in h with Re, Low Tu
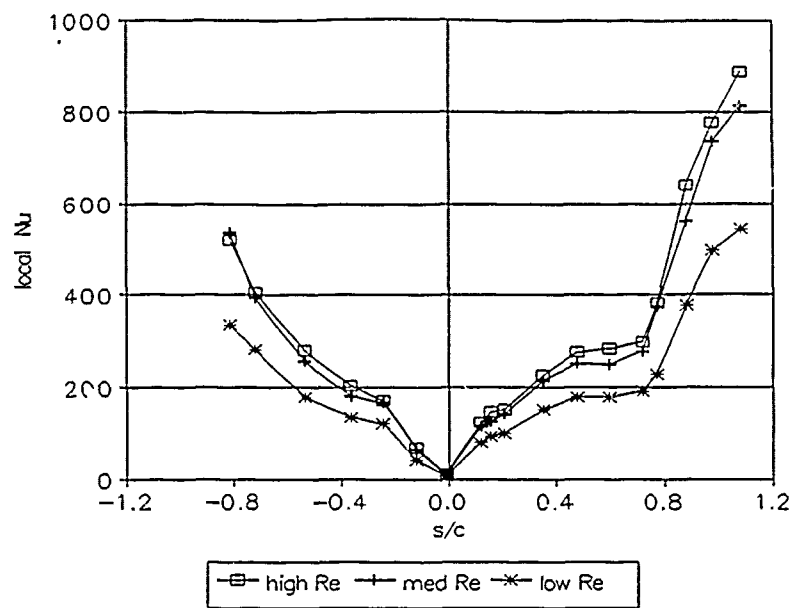
Figure 5.17a Variation in Local Nu with Re, Low Tu
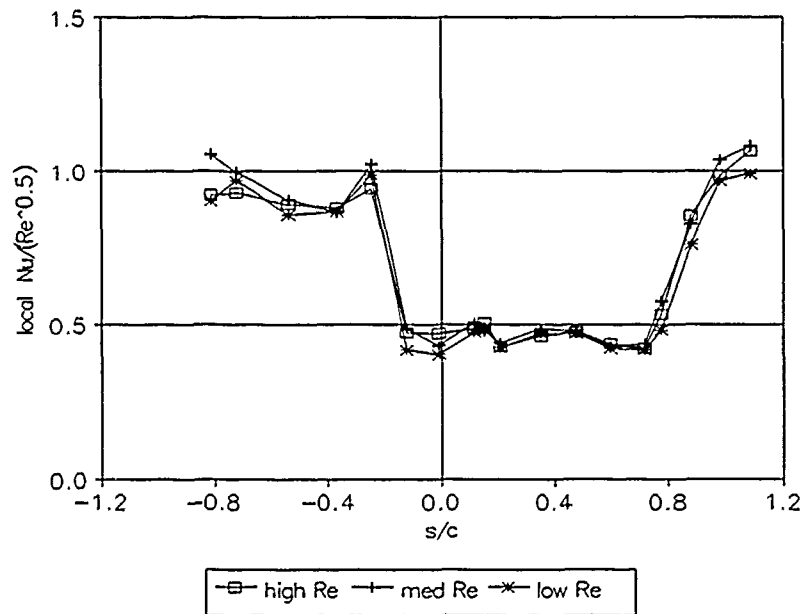
Figure 5.17b "Normalized" Local Nu, Low Tu
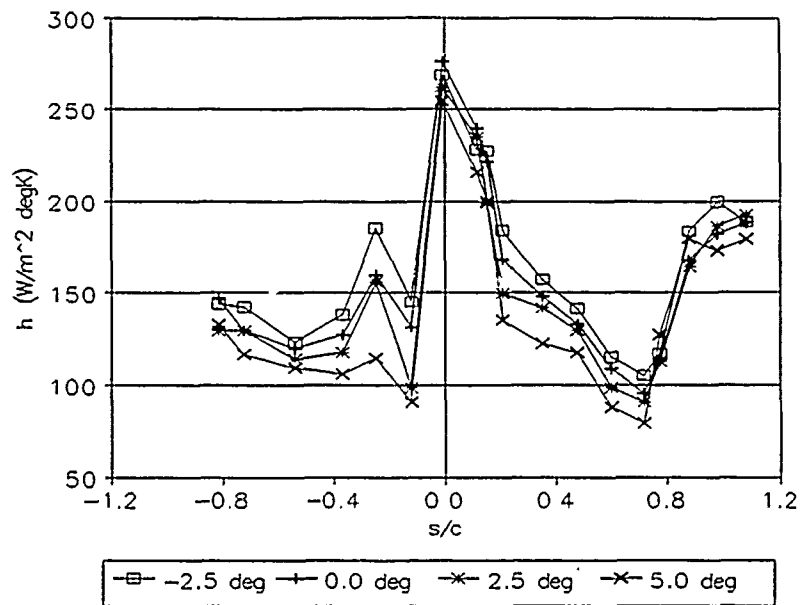
Figure 5.18a Variation in h with AOI, Low Tu
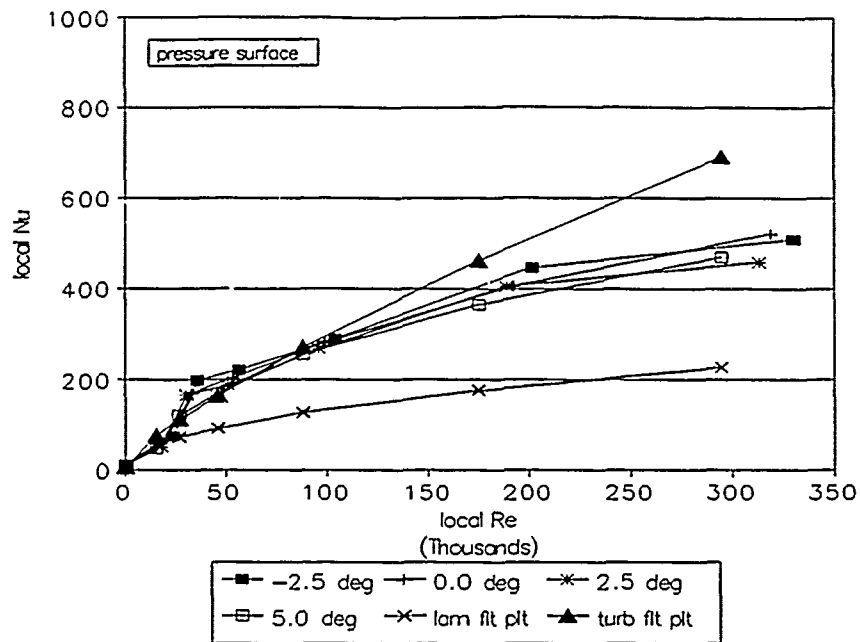
Figure 5.18b Experimental and Analytical Nu, Low Tu
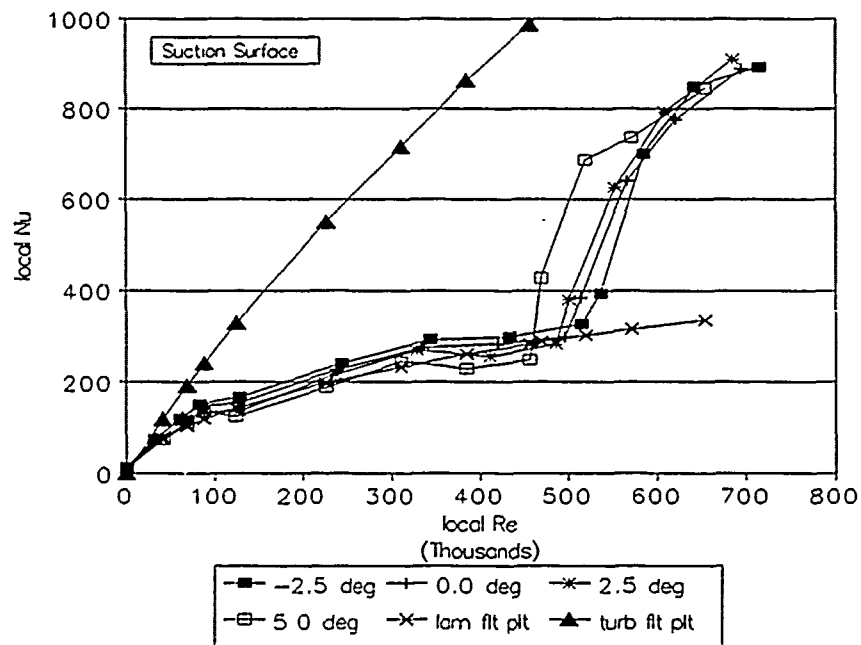
Figure 5.18c Experimental and Analytical Nu, Low Tu
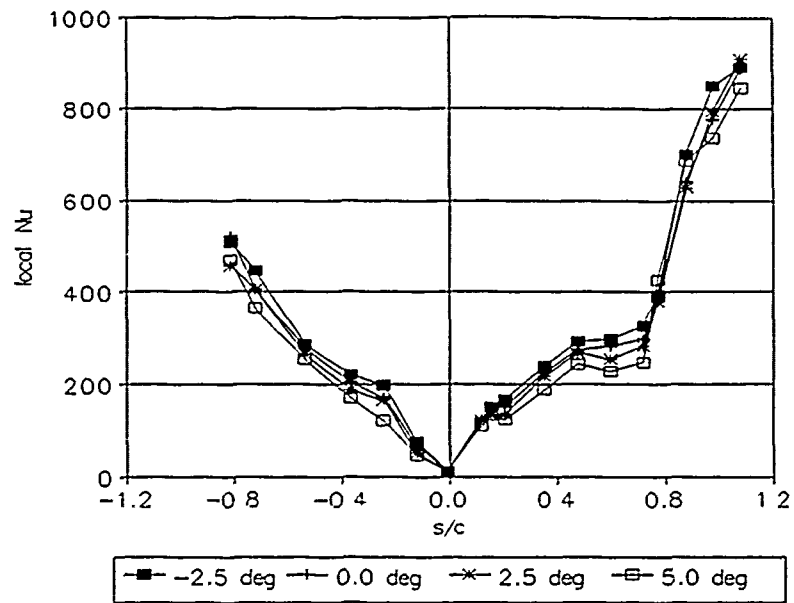
Figure 5.19a Variation in Local Nu with AOI, Low Tu
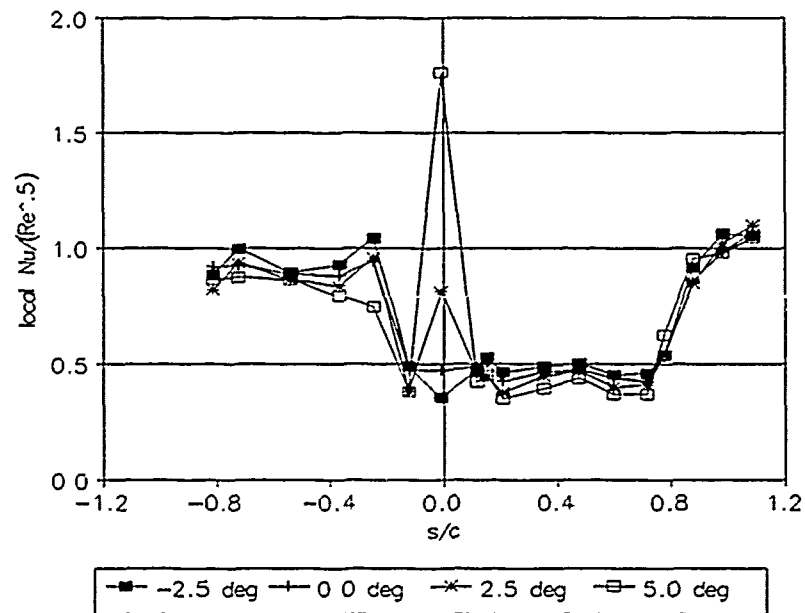
Figure 5.19b "Normalized" Local Nu, Low Tu
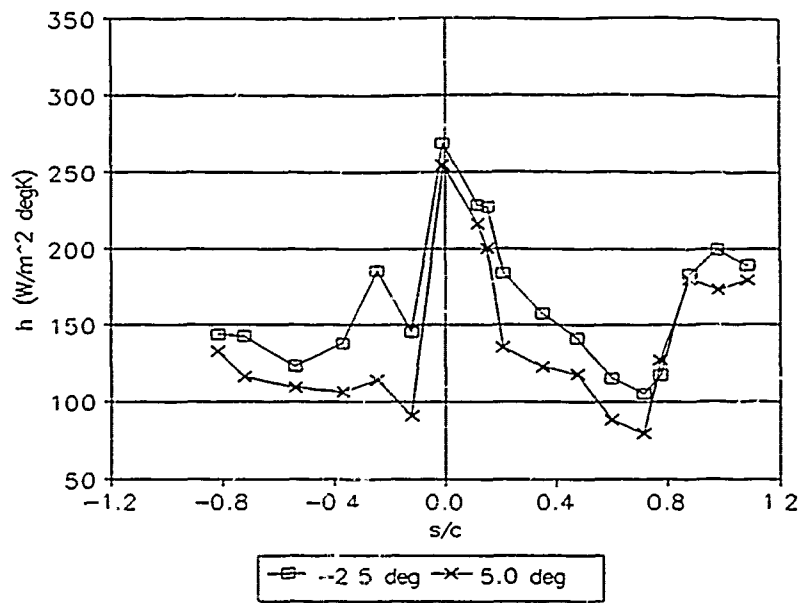
Figure 5.20 -2.5 deg and 5.0 deg Low Turbulence h
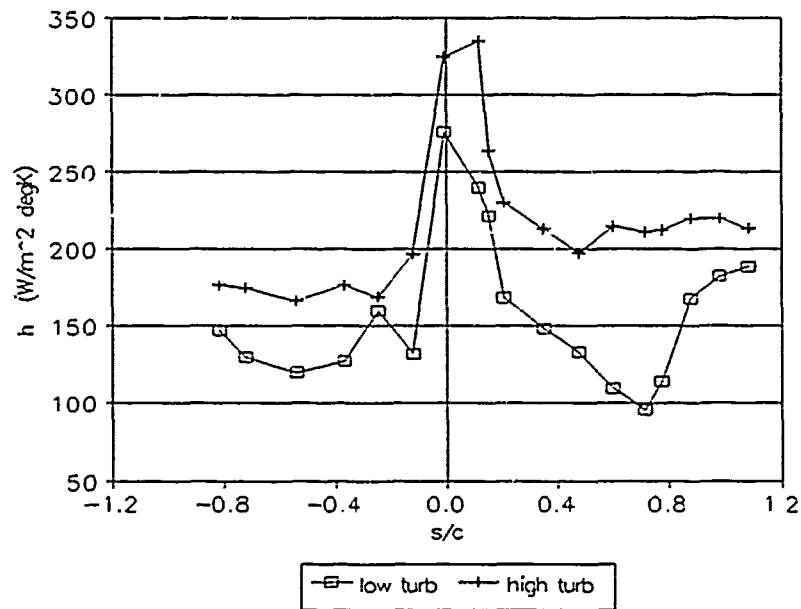
Figure 5.21 Typical Low/High Tu Heat Transfer Coefficients
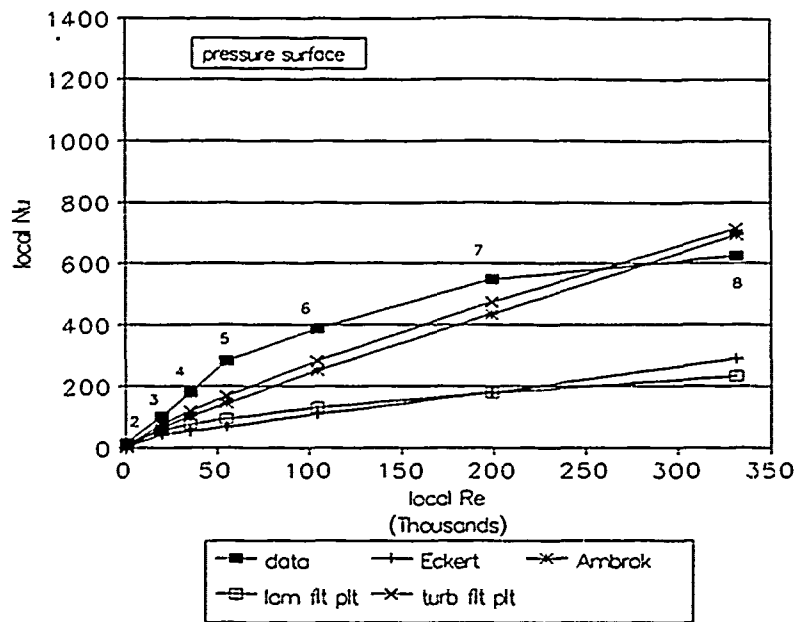
Figure 5.22a Experimental and Analytical Nu, High Tu
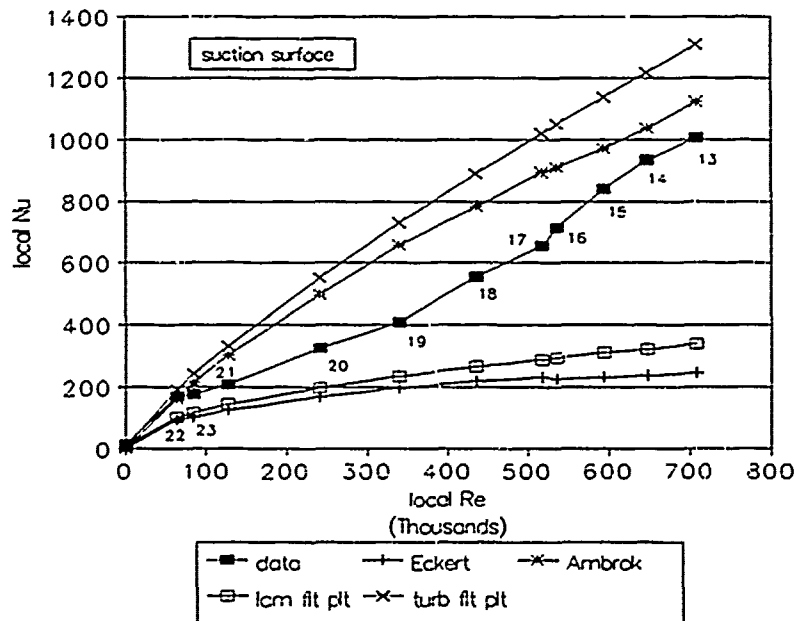
Figure 5.22b Experimental and Analytical Nu, High Tu
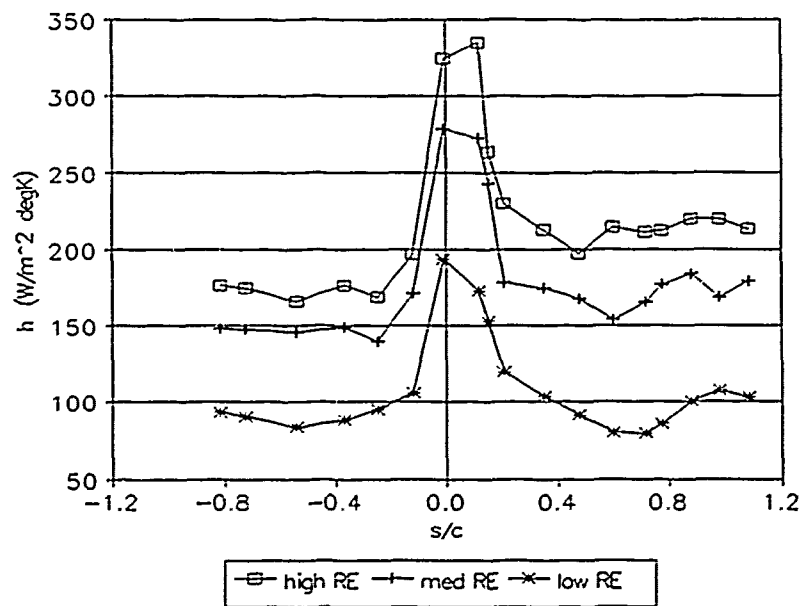
Figure 5.23 Variation in h with Re, High Tu
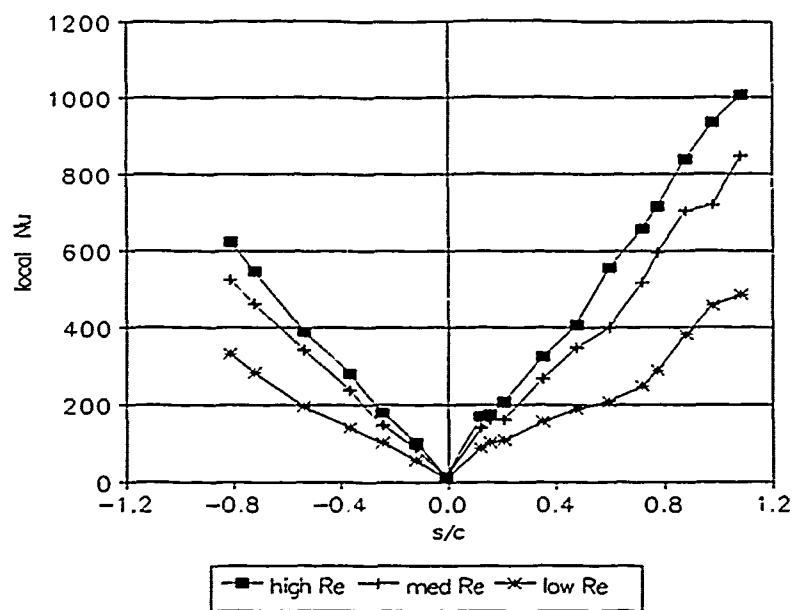
Figure 5.24a Variation in Local Nu with Re, High Tu
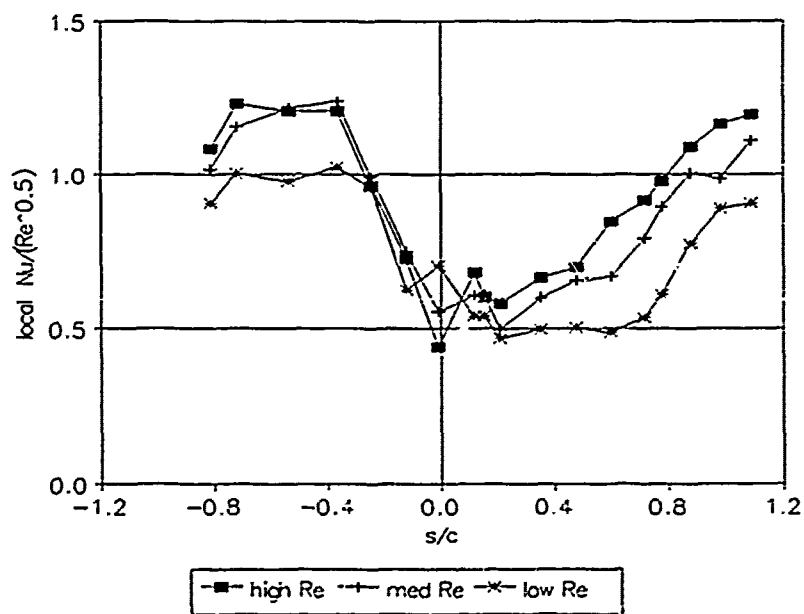
Figure 5.24b "Normalized" Local Nu, High Tu
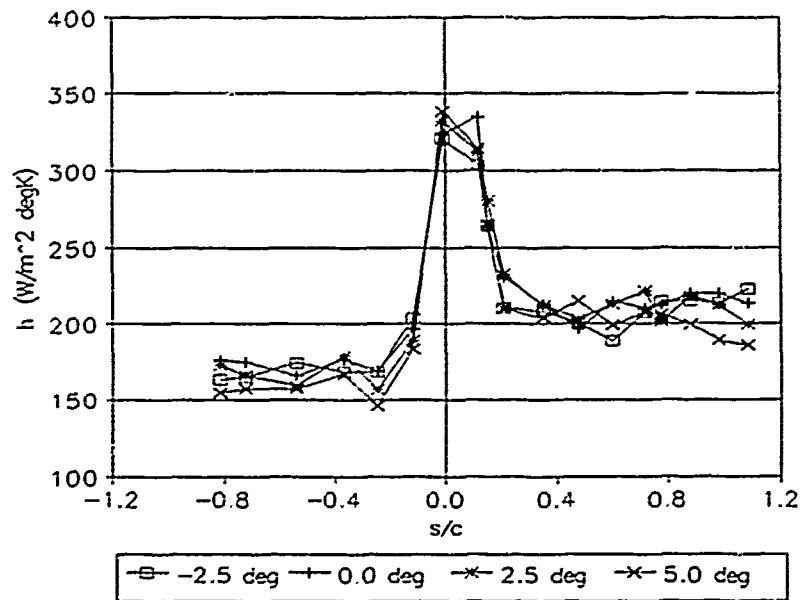
Figure 5.25a Variation in h with AOI, High Tu
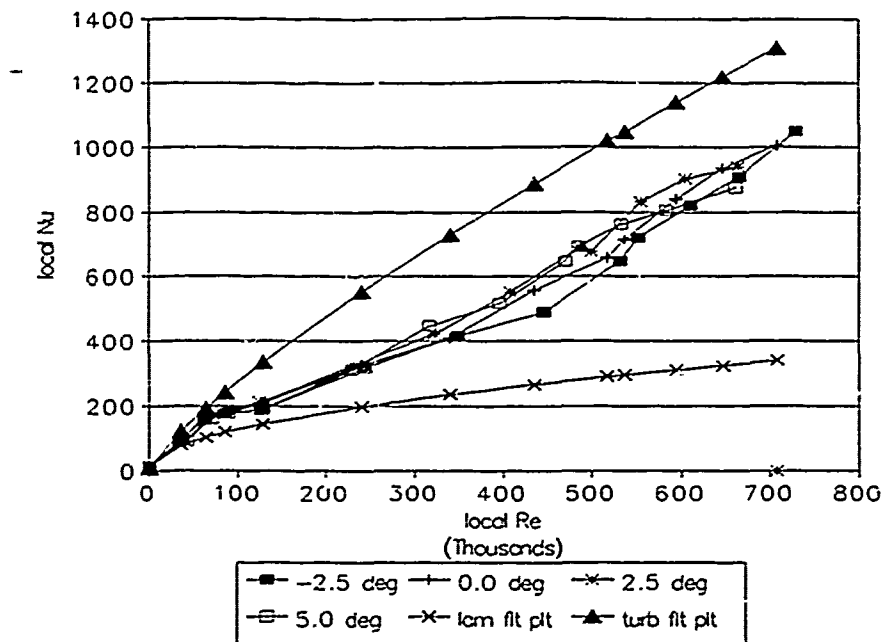
Figure 5.25b Experimental and Analytical Nu, High Tu
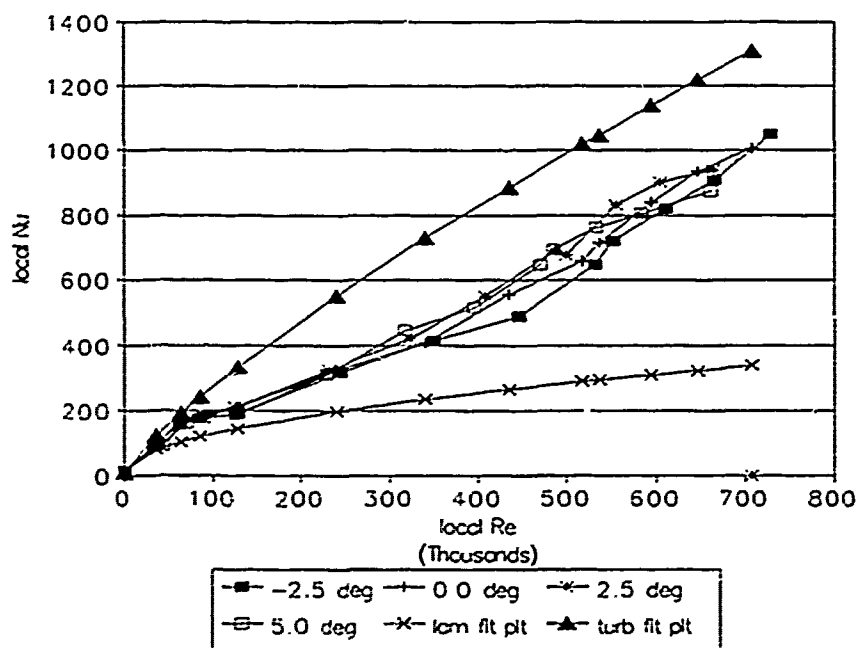
Figure 5.25c Experimental and Analytical Nu, High Tu
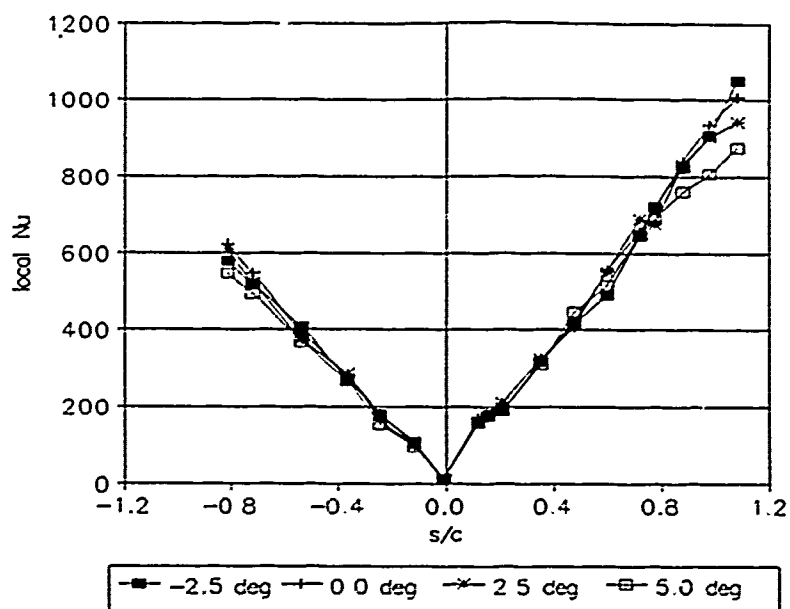
Figure 5.26a Variation in Local Nu with AOI, High Tu
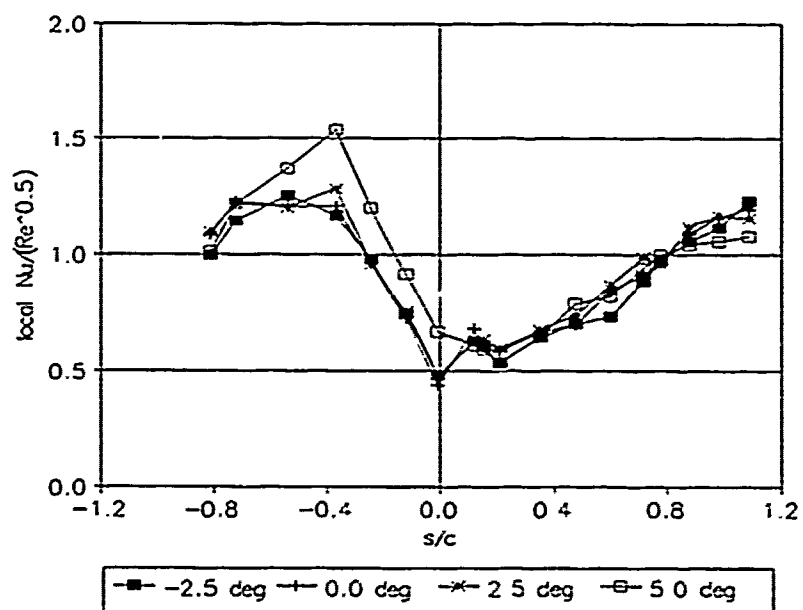
Figure 5.26b "Normalized" Local Nu, High Tu

Figure 5.27a Low/High Tu Local Nu, Pressure Surface

Figure 5.27b Low/High Turbulence Local Nu, Suction Surface
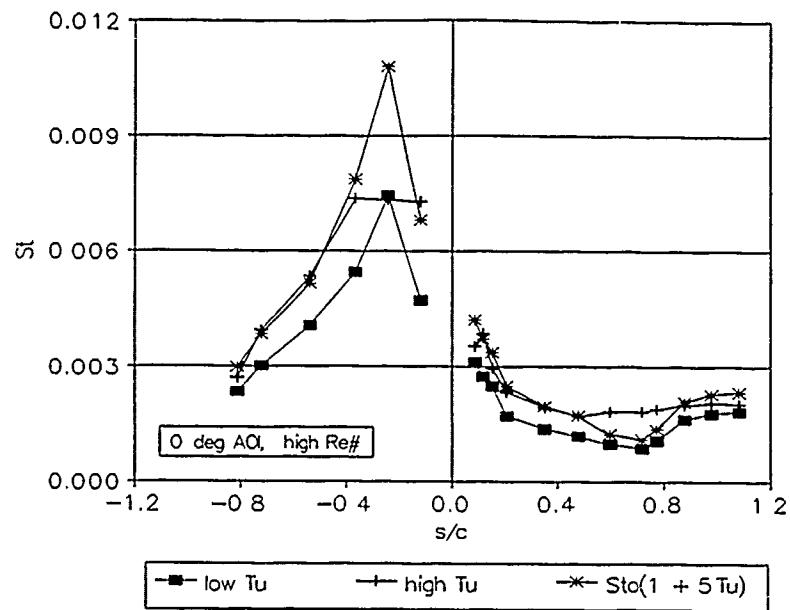
Figure 5.28a 0 deg AOI Stanton Numbers, High Re
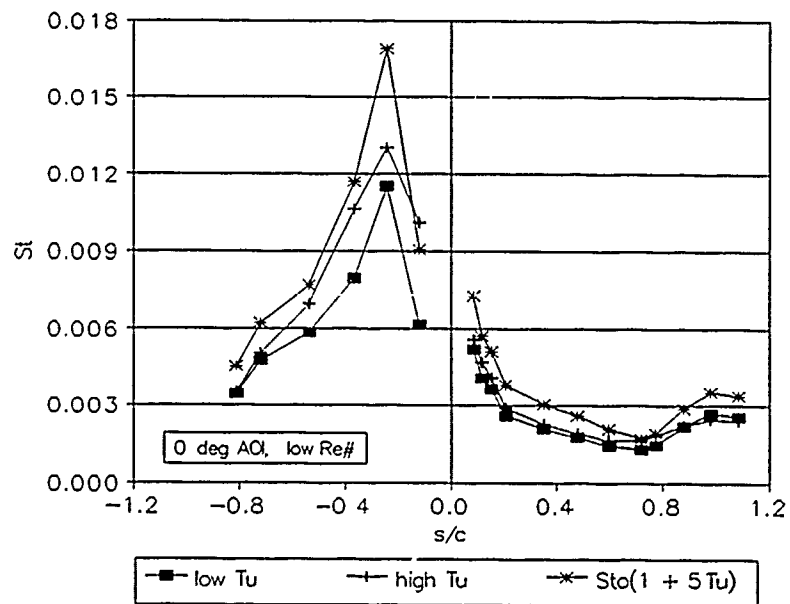
Figure 5.28b 0 deg AOI Stanton Numbers, Low Re
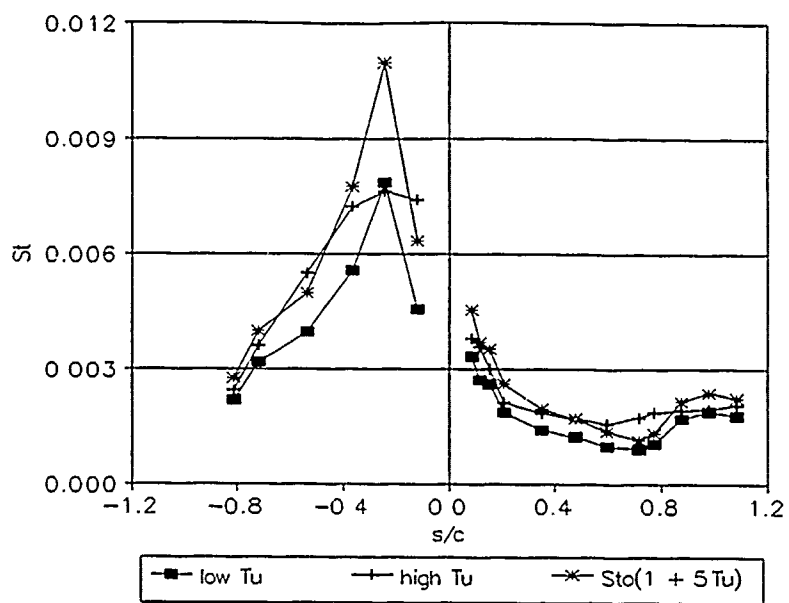
Figure 5.28c -2.5 deg AOI Stanton Numbers, High Re
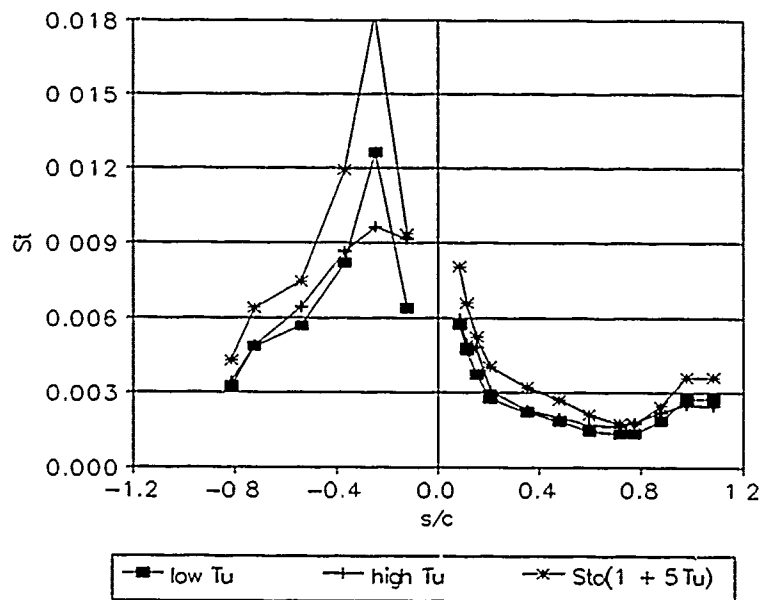
Figure 5.28d -2.5 deg AOI Stanton Numbers, Low Re

VIII -44
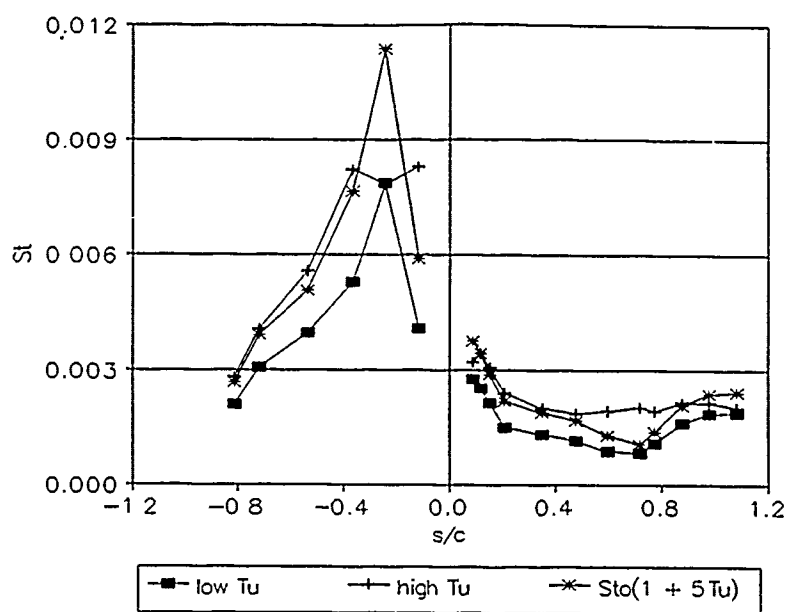
Figure 5.28e 2.5 deg AOI Stanton Numbers, High Re
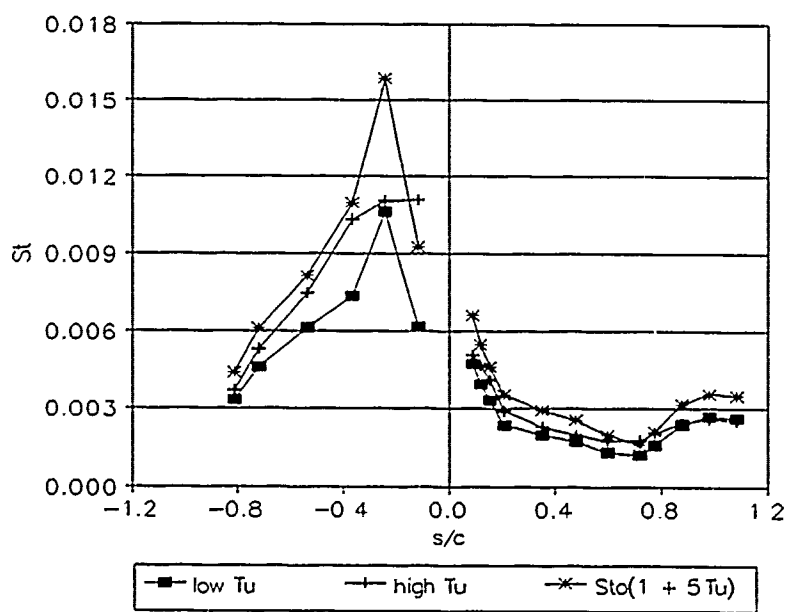
Figure 5.28f 2.5 deg AOI Stanton Numbers, Low Re
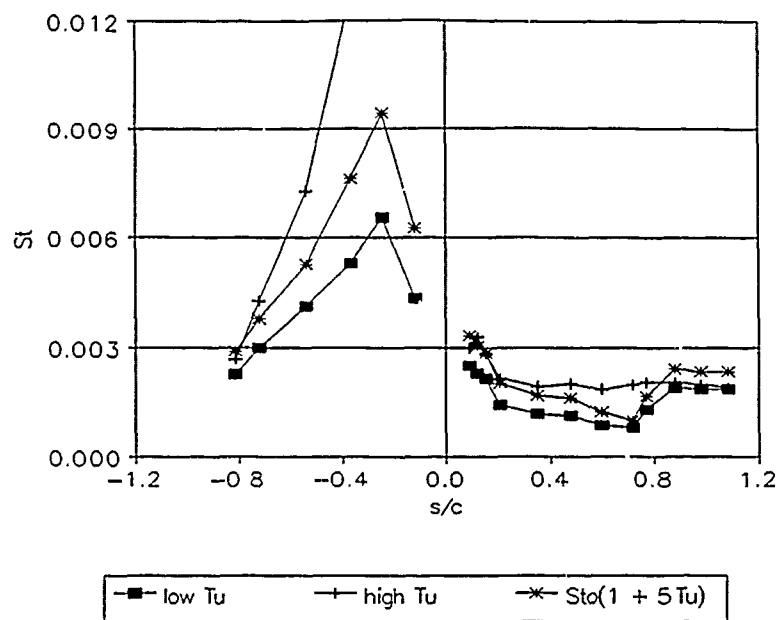
Figure 5.28g 5.0 deg AOI Stanton Numbers, High Re
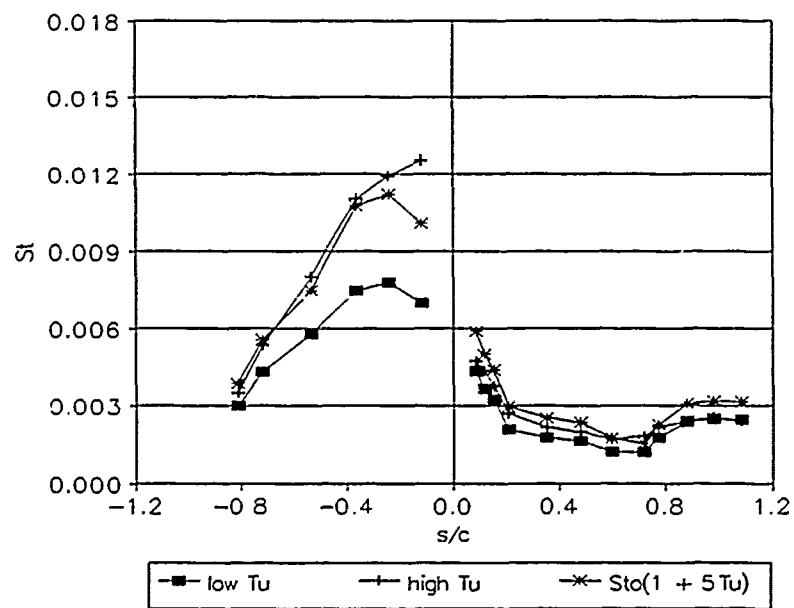
Figure 5.28h 5.0 deg AOI Stanton Numbers, Low Re

Appendix A: Turbulence Scales Calculations

1. Turbulence Space and Time Correlations

The statistical nature of turbulent flow lends itself to the existence of correlations, in both time and space, which may be used to describe the turbulent flow. These correlations can be used to determine the extent to which the "fluid motions have a certain connection with each other", often expressed in terms of the integral scale and the microscale.

Turbulent fluid motion is comprised of smaller and smaller eddies or cells. The size of the largest eddies, the integral scale, is a function of the flow passage geometry; the size of the smallest eddies, the microscale, is a function of the fluid viscosity. By applying correlation analysis to the turbulent flow velocity, relationships between the flow velocity at given points and times can be manipulated to yield the dimensions of integral scale and the microscale.

<u>Spatial Correlations</u> The spatial correlations, latitudinal and longitudinal, are illustrated in Figure A1. Latitudinal correlation is determined by comparing the fluid velocity at one point to the fluid velocity at a transversely located point at the same instant; longitudinal correlation is measured by comparing the fluid velocity at one point to the fluid velocity at a point downstream at the same instant. The normalized longitudinal correlation coefficient $f(x)$ and lateral correlation coefficient $g(y)$ are defined as

$$f(x) = \frac{\overline{u'(\zeta)u'(\zeta + x)}}{\overline{u'^2}} \qquad (A.1)$$

$$g(y) = \frac{\overline{u'(\zeta)u'(\zeta + y)}}{\overline{u'^2}} \qquad (A.2)$$

As mentioned, manipulation of the correlation yields the dimensions of the integral scale and the micro scale. It can be shown (Hinze, 1959) that about the origin, where the correlation is greatest, $f(x)$ [and $g(y)$] "approaches a parabolic function" with the curvature at the vertex representative of the rate of the local change in u'. Assuming that the smallest eddies in the flow are the cause of this change, a microscale λ_f can be defined such that

$$f(x) \approx 1 - \frac{x^2}{\lambda_f^2} \qquad (A.3)$$

and

$$\frac{1}{\lambda_f^2} = -\frac{1}{2}\left[\frac{\partial^2 f}{\partial x^2}\right]_{x=0} \qquad (A.4)$$

where $\frac{\partial^2 f}{\partial x^2}$ is obtained from the "osculating parabola" in Figure A3.

The integral scale Λ_f is defined as

$$\Lambda_f = \int_0^\infty f(x)dx \qquad (A.5)$$

Since the correlation decreases to zero as the distance increases, the above integral approaches the value of the correlation distance, which is comparable to the magnitude of the largest eddies.

Time Correlations The time correlation is measured by comparing the fluid velocity at one point with the fluid velocity at the same point but at different times, as illustrated in Figure A2. The nondimensional time correlation coefficient $R_E(\tau)$, also known as the Eulerian time-correlation coefficient, is defined as

$$R_E(t) = \frac{\overline{u'(\tau)u'(\tau-t)}}{\overline{u'^2}}$$ (A.6)

Unlike the spatial correlations, manipulation of $R_E(\tau)$ yields *time* scales. Since the same logic is applied to the definitions of both the spatial and time correlations, the scales are similarly defined. Whereas λ_f was a measure of the smallest eddies, the Eulerian micro time scale

$$\frac{1}{\tau_E^2} = -\frac{1}{2}\left[\frac{\partial^2 R_E}{\partial t^2}\right]_{t=0}$$ (A.7)

is a measure of smallest correlation times. Similarly, the Eulerian integral time scale,

$$T_f = \int_0^\infty R_E(t)\,dt$$ (A.8)

is a measure of the longest correlation times.

The spatial and time correlations are related by Taylor's hypothesis

$$\frac{\partial}{\partial t} = -\overline{U}\frac{\partial}{\partial x}$$ (A.9)

which is based on the assumption that "the fluctuations are too weak to induce any significant motion of their own, so that disturbances are convected along at the mean stream velocity" (Cebeci,). In cases where Taylor's hypothesis holds, it can be shown (Hinze, 1959) that

$$f(x) = R_E(t)$$ (A.10)

2. *Energy Relationships*

The turbulence may also be analyzed through the relationship between the frequencies and associated kinetic energies, or strengths, of the turbulent motions. The frequency/energy relationship has been defined as

$$\overline{u'^2} = \int_0^\infty E_{u'}(n)dn \qquad (A.11)$$

where $E_{u'}(n)$ is the "energy" and $E_{u'}(n)dn$ is the nth contribution to the average "kinetic energy", expressed as $\overline{u'^2}$.

There exists a logical relationship between the correlations and the energy distribution. If the micro correlations are a measure of the smallest disturbances, both in space and time, they must be associated with the high frequency energy contributions; by the same reasoning, the integral scales are associated with the low frequency energy contributions. Through Fourier analysis (Hinze, 1959), these relationships are

$$f(x) = \frac{1}{\overline{u'^2}} \int_0^\infty E_{u'}(n)\cos\frac{2\pi n x}{U}dn \qquad (A.12)$$

and

$$R_E(t) = \frac{1}{\overline{u'^2}} \int_0^\infty dn E_{u'}(n)\cos(2\pi n t)dn \qquad (A.13)$$

With the energy distribution $E_{u'}(n)$ a common factor in the equations above, the space and time scales can be expresses in terms of either the space correlation $f(x)$, the time correlation $R_E(t)$, or the energy distribution $E_{u'}(n)$. Manipulation of the definitions yields

$$\lim_{(n \to 0)} \frac{1}{\overline{u'^2}} E_{u'}(n) = 4\int_0^\infty R_E(t)dt = 4T_E \qquad (A.14)$$

$$\lim_{(n \to 0)} \frac{1}{\overline{u'^2}} E_{u'}(n) = \frac{4}{U}\int_0^\infty f(x)dx = \frac{4}{U}\Lambda_E \qquad (A.15)$$

and

A-4

$$\frac{1}{\tau_E^2} = -\frac{1}{2}\left[\frac{\partial^2 R_E}{\partial t^2}\right]_{t=0} = \frac{2\pi^2}{\overline{u'^2}}\int_0^\infty n^2 E_{u'}(n)\,dn \qquad (A.16)$$

$$\frac{1}{\lambda^2} = -\frac{1}{2}\left[\frac{\partial^2 f}{\partial x^2}\right]_{x=0} = \frac{2\pi^2}{\overline{U}^2\overline{u'^2}}\int_0^\infty n^2 E_{u'}(n)\,dn \qquad (A.17)$$

Further manipulation yields

$$\frac{1}{\lambda_f^2} = \frac{1}{2\overline{U}^2}\left[\frac{\partial^2 R_E}{\partial t^2}\right]_{t=0} \qquad (A.18)$$

and

$$\Lambda_f = \overline{U}\int_0^\infty F_E(t)\,dt \qquad (A.19)$$

Thus, both the micro and integral longitudinal scales can be determined from the Eulerian time correlation coefficient. This is very useful since it is relatively simple to obtain and manipulate the time correlation data.

3. *Turbulence Scales using the Eulerian Correlation Coefficients*

As mentioned, the time correlation is measured by comparing the fluid velocity at one point with the fluid velocity at the same point but at different times, such as with a single hot-wire anemometer sampling at a very high rate. The velocity $U(t)$ data is then statistically reduced to yield the mean velocity $\overline{U}$ and the instantaneous fluctuation $u'(t)$ such that

$$U(t) = \overline{U} + u'(t) \qquad (A.20)$$

The Eulerian time correlation coefficient is defined as

$$R_E(t) = \frac{\overline{u'(\tau)u'(\tau-t)}}{\overline{u'^2}} \qquad (A.21)$$

where the numerator may be calculated from

$$\frac{1}{T}\int_0^T u'(\tau)u'(\tau-t)d\tau \qquad (A.22)$$

The integral term is almost the *correlation integral*. By performing the following change of variables

$$\sigma = \tau \div t \qquad (A.23)$$

$$\tau = t + \sigma \qquad (A.24)$$

$$u'(\tau) = u'(t+\sigma) \qquad (A.25)$$

$$u'(\tau-t) = u'(\sigma) \qquad (A.26)$$

$$d\tau = d\sigma \qquad (A.27)$$

the integral term in the numerator reduces to

$$\int_0^T u'(\sigma)u'(t+\sigma)d\sigma \qquad (A.28)$$

which is the *autocorrelation function* for $u'(t)$. The autocorrelation function has the Fourier

$$H_{u'}(n)\cdot H_{u'}(n)^* \qquad (A.29)$$

where $H_{u'}(n) = Re(n) + iIm(n)$ is obtained from the Fourier transform of $u'(t)$

such that the inverse Fourier transform of $H_{u'}(n)\cdot H_{u'}(n)^*$ will yield the integral value.

In summary, the Eulerian time correlation coefficient $R_E(t)$ may be written

$$R_E(t) = \frac{\frac{1}{T}\int_0^T u'(\sigma)u'(t+\sigma)d\sigma}{\overline{u'^2}} \qquad (A.30)$$

For discrete data, such as that obtained with a hot-wire,

$$R_E(i) = \frac{\frac{1}{N}\sum_{j=1}^{N} u'(j)u'(j+i)}{\frac{1}{N}\sum_{j=1}^{N} u'^2} \qquad (A.31)$$

where

$$i, j = 1 .. N$$

and

$$n = i\Delta n \qquad (A.32)$$

$$n = \frac{f_{sample}}{N} \qquad (A.33)$$

$$t = i\Delta t \qquad (A.34)$$

$$\Delta t = \frac{1}{f_{sample}} \qquad (A.35)$$

To obtain the summation quantity in the numerator of equation A.31:

1   perform the discrete Fourier transform of $u'(t)$ to obtain
$H_{u'}(n) = Re(n) + iIm(n)$

2   form the product $H_{u'}(n) \cdot H_{u'}(n)^* = Re(n)^2 + Im(n)^2$

3   perform the inverse discrete Fourier transform of $H_{u'}(n) \cdot H_{u'}(n)^*$ to
obtain the summation quantity

With the discrete values of $R_E(t)$ determined, the microscale and integral scale can

be calculated. A program for calculating the scales based on this method,

TAYLOR.bas, is attached.

4. Turbulence Scales using the Energy Distribution

The magnitude of the scales may also be obtained through manipulations of the energy distribution relations above yielding

$$\frac{1}{\lambda_f^2} = \frac{2\pi^2}{\overline{U}^2 \overline{u'^2}} \int_0^\infty n^2 E_{u'}(n) dn \qquad (A.36)$$

and

$$\Lambda_f = \lim_{n \to 0} \frac{\overline{U}}{4\overline{u'^2}} E_{u'}(n) \qquad (A.37)$$

where $E_{u'}(n)$ is derived from the Fourier transform of u'. For discrete data, the definition of $E_{u'}(n)$ can be written

$$\frac{1}{N} \sum_{i=1}^N u'^2(i) = \sum_{n=1}^N E_{u'}(n) \Delta n \qquad (A.38)$$

Combining this with the discrete form of Parseval's theorem

$$\sum_{i=1}^N u'^2(i) = \frac{1}{N} \sum_{n=1}^N |H_{u'}(n)|^2 \qquad (A.39)$$

the energy distribution is obtained from the Fourier transform of u' as

$$E_{u'}(n) = \left[\frac{|H_{u'}(n)|}{N}\right]^2 \frac{1}{\Delta n} \qquad (A.40)$$

where

$$|H_{u'}(n)| = [Re^2(n) + Im^2(n)]^{\frac{1}{2}} \qquad (A.41)$$

5. Experimental Calculations

General. The concepts presented above were applied to turbulence data acquired in the TCTF during the heat transfer experiments. Although the turbulence scales were not required for any heat transfer analysis, the turbulence data was acquired for determining the turbulence intensities, discussed in Section VI.

Correlation Method Experimental Calculations. The turbulence scales were calculated from equations A.18 and A.19 where the discrete values of the correlation coefficient were computed using equations 3.31 - 3.35, incorporated in the QuickBASIC program TAYLOR.bas (attached).

Micro Scale. Using the discrete correlation coefficients computed by the TAYLOR.bas program, the equation of the "osculating parabola", required for the calculation of the micro scale, must be estimated. Suppose the osculating parabola has the form

$$f(t) = \alpha + bt + ct^2 \qquad (A.42)$$

Since

$$f(0) = 1 \qquad (A.43)$$

and

$$\frac{\partial f(t)}{\partial t}\Big|_{t=0} = b = 0 \qquad (A.44)$$

then

$$f(t) = 1 + 2ct^2 \qquad (A.45)$$

and

$$\frac{\partial^2 f(t)}{\partial t^2}\Big|_{t=0} = 2c \qquad\qquad (A.46)$$

Substituting equation A.46 into equation A.18

$$\lambda_f = \left[\frac{\overline{U}^2}{-c}\right]^{\frac{1}{2}} \qquad\qquad (A.47)$$

For the discrete $R_E(t)$, the value of c corresponds to the value of the correlation

coefficient at $t = \Delta t$ such that

$$c = \frac{R_E(\Delta t) - 1}{(\Delta t)^2} \qquad\qquad (A.48)$$

Figure A4 illustrates the discrete Eulerian time correlation coefficient $R_E(t)$ about

$t = 0$ for data acquired at 20000 Hz. The curve appears convex at $t = 0$ where it

should be concave; however, the equation for the osculating parabola can be

estimated using the method described above to obtain the value of c. As the data

acquisition rate is increased, the correlation coefficient curve more and more approxi-

mates a parabola about $t = 0$ yielding more and more accurate results. When the data

acquisition rate is increased to 50000 Hz, the maximum attainable for an X-wire in the

TCTF, a glimpse of concavity appears, as illustrated in Figure A5. By going to a 1-wire

anemometer system and maximizing the data acquisition rate at 100000 Hz, a clearly

well-behaved correlation coefficient curve appears, as illustrated in Figure A6. Since

these curves do not correspond to identical flow conditions, the microscale values

cannot be compared to each other; however, the microscale values obtained with the

correlation method can be compared to the values obtained with the energy method of

equations A.36 - A.41.

Integral Scale. Using the discrete correlation coefficients computed by TAYLOR:bas and the discrete form of equation A.19,

$$\Lambda_f = \overline{U} \sum_{i=1}^{N} R_E(i) \Delta t \qquad (A.48)$$

the value of the integral scale can theoretically be determined; however, a typical experimental correlation coefficient function is illustrated in Figure A7. The oscillating motion of the function is probably an artifact of "noise", either from the data acquisition equipment or the geometry of the TCTF. Summing over the entire function has yielded incorrect results; therefore, it was determined to sum the coefficients until the value of the coefficients became negative, illustrated in Figure A8. Although this method is not completely accurate, it approximates a "clean" correlation coefficient function. A clean correlation function will have negative values but will not oscillate.

Energy Method Experimental Calculations. The methods developed in equations A.38 through A.39 were incorporated into the QuickBASIC VELREDUC.bas program, listed in Appendix F. This program computes the discrete Energy values for discrete frequency values. A typical discrete Energy distribution is illustrated in Figure A9.

Micro Scale. The microscale calculation was straightforward, based on the discrete form of equation A.36

$$\lambda_f = \left[\frac{\overline{U}^2 \overline{u'^2}}{2\pi^2} \Delta n^3 \sum_{i=1}^{N} (i)^2 E(i) \right]^{\frac{1}{2}} \qquad (A.49)$$

Integral Scale. The integral scale calculation appears straightforward, based on the discrete Energy value obtained as n approaches 0 but not necessarily equal to 0. There are many methods, which all yield different answers, to obtain this value. The method that was decided upon was to take the average of values near the $n = 0$ point:

$$E(0) = \frac{1}{10} \sum_{i=1}^{10} E(i) \qquad (A.50)$$

Correlation Method vs Energy Method. The following comparisons are based on data acquired for different tunnel configurations; therefore, there is no relationship between each set of data, only between scales calculated by each method for each set of data.

From a typical data set of 16384 points acquired at 20000 Hz with an X-wire, the following numerical experimental results were obtained:

	correlation	energy
micro scale	3.772 mm	3.082 mm
integral scale	1.481 cm	1.010 cm

Although comparable, the results of the two methods do not verify the assumption of Taylor's hypothesis. As the data acquisition rate is increased to 50,000 Hz, the micro-scales, listed below, remain comparable but the integral scales agree less.

	correlation	energy
micro scale	2.509 mm	2.186 mm
integral scale	4.025 cm	3.254 cm

At the maximum data acquisition rate of 100000 Hz with the single hot-wire, the micro-scales computed by both methods are nearly equal; however, the integral scale still shows considerable disagreement.

	correlation	energy
micro scale	3.832 mm	3.788 mm
integral scale	4.794 cm	2.605 cm

The examples presented above are random samples of the data acquired for this experiment; some data sets showed better agreement while others showed worse. In general, the micro scales are in closer agreement than the integral scales, primarily due to the difficulties in calculating the integral scale, described above. As mentioned, there are many methods of determining Energy value as $n \to 0$, some of which yield more accurate results.

It is apparent that, as the data acquisition frequency is increased, the value of the microscale obtained with the correlation method approaches that obtained with Energy method; in other words, the Energy method yields a more accurate value regardless of the data acquisition frequency. Since it is desirable to acquire data at 20,000 Hz, twice the accepted highest fluctuation frequency of 10,000 Hz, the Energy method is preferred over the correlation method. In addition, for a given number of data points, a lower data acquisition frequency yields better resolution. The Energy method is also faster since it requires performing a Fourier transform only in the forward direction; no inverse Fourier transform is required as in the correlation method. For these reasons, the Energy method was used to analyze the turbulence scales in the TCTF.

Turbulence Scales in the TCTF. Figures A10 and A11 illustrate typical behaviors of the freestream turbulence scales for both low and high freestream turbulence at both low and high model Re. In general, there seems to be no discernable relation between

the AOI and the scale for both the microscale and the integral scale. One would expect some sort of relation for the high turbulence configuration since the effective spacing between the tubes in the fixed turbulence grid decreases as the AOI increases.

One obvious relation exists between the turbulence level and the scale, independent of AOI. The scales are larger for lower turbulence. This makes sense since, for a fixed velocity, the scales generally become larger as the distance from the turbulence source increases. For the low turbulence configuration, the turbulence source consists of the tunnel inlet and walls. When the grid is inserted, the scales decrease in size.

Another obvious relation exists between the freestream velocity and the scale. For the high turbulence configuration, both the micro and integral scale increase nearly linearly with the freestream velocity; however, for the low turbulence configuration, the increase appears more exponential than linear, probably due to the variation in the tunnel flow behavior as the tunnel velocity increases.

The streamwise scale behavior through a cascade passage is illustrated in Figures A12 through A16. The variation in the scales, particularly the microscale, mirrors the variation in streamwise velocity through the cascade passage, reillustrated in Figure A17. For the microscale, the overall trend is increasing scale corresponding to the increasing velocity through the cascade passage. In the high turbulence configuration, the variation is minimized and the relationship appears linear as observed for the freestream micro scale. The integral scale behavior deviates from the velocity trend as it decreases near the exit of the cascade at the point of maximum velocity; as with the microscale, the variation in scale is minimized for the high turbulence configuration.

6. Conclusion

Since it was not the intention of this experiment to fully analyze the scale behavior, no attempt was made to relate the scale behavior to the turbine blade heat transfer. The turbulence scale behavior described above applies only to the TCTF. Further studies involving controlled flow conditions are recommended. The variation in velocity, geometry, and turbulence level did not allow any the formation of absolute conclusions concerning relationships between the velocity, turbulence level, and turbulence scales.

The Eulerian time correlation approach to calculating the turbulence scales appears to be in agreement with the energy method, thereby "confirming" Taylor's hypothesis. The method appears to be more sensitive to the data acquisition rate and "noise" in the system; in addition, the Eulerian method is more computational intensive, requiring the calculation of both a forward and inverse Fourier transform. For these reasons, the energy method is preferred.
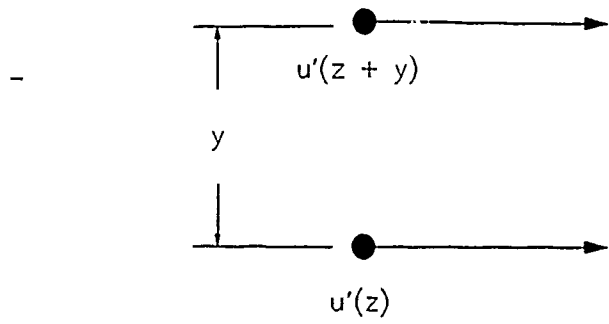
Latitudinal Correlation
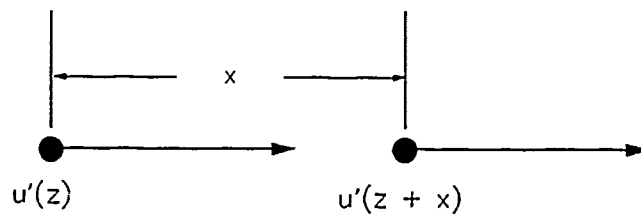
Longitudinal Correlation

Figure A1 Spatial Correlations
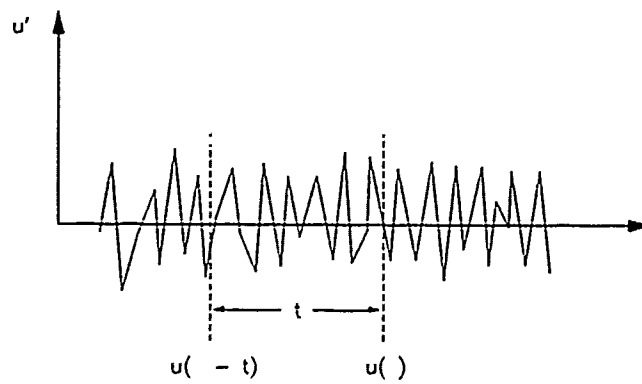
Figure A2 Time Correlation
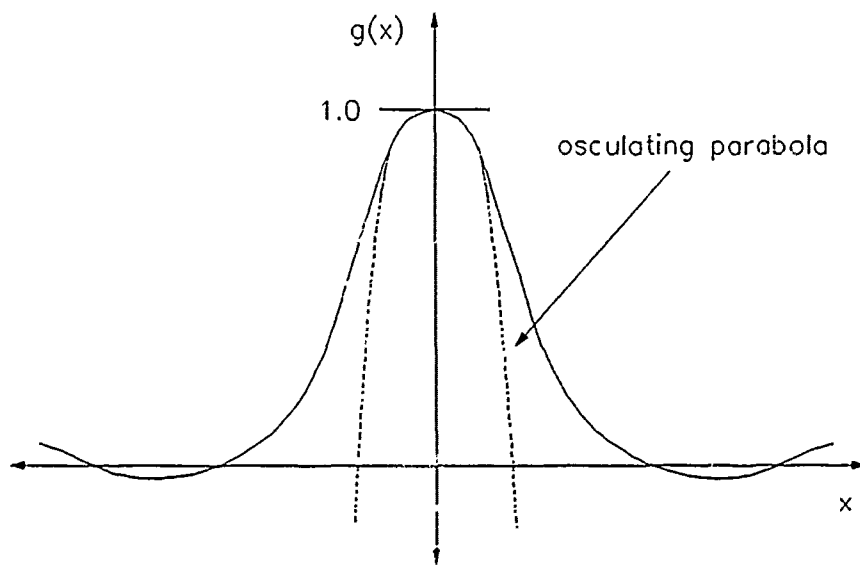
Figure A3 Osculating Parabola
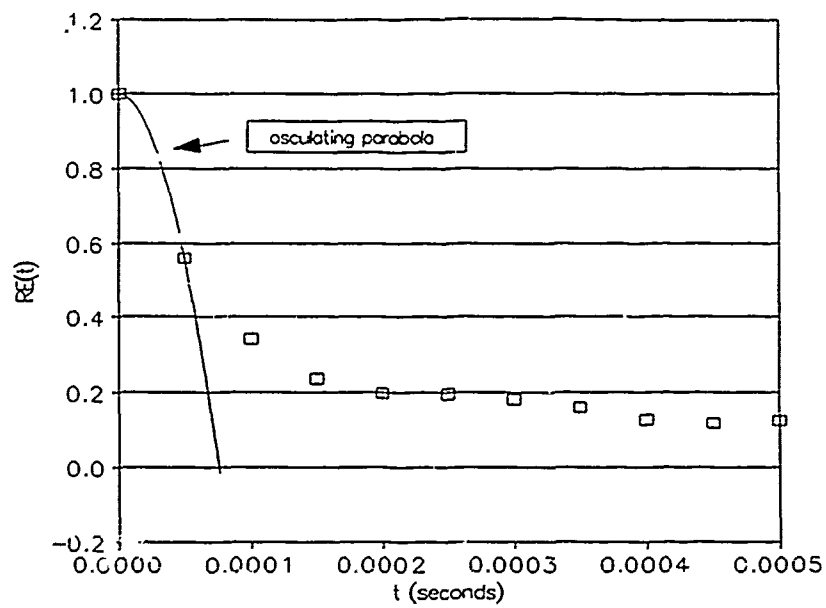
Figure A4 Eulerian Correlation for 20,000 'Iz
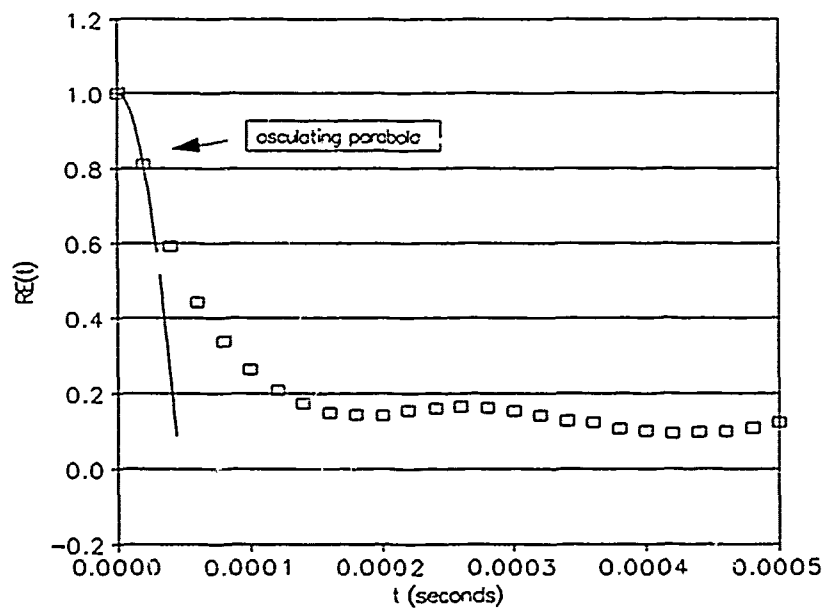
Figure A5 Eulerian Correlation for 50,000 Hz
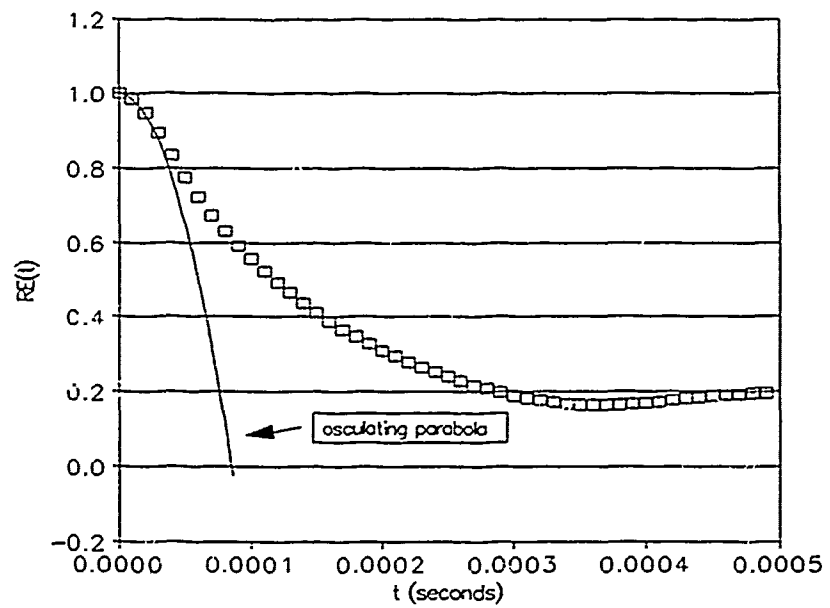
Figure A6 Eulerian Correlation for 100,000 Hz
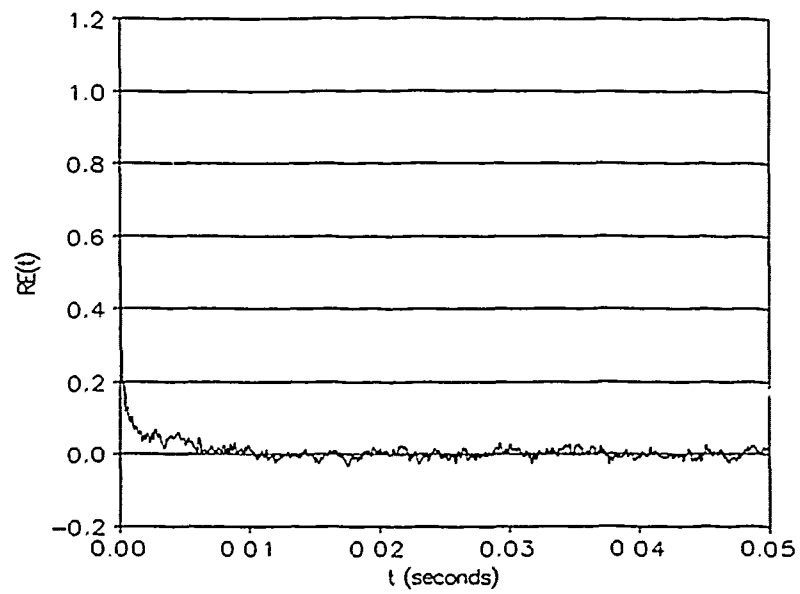
Figure A7 Typical Eulerian Correlation Function
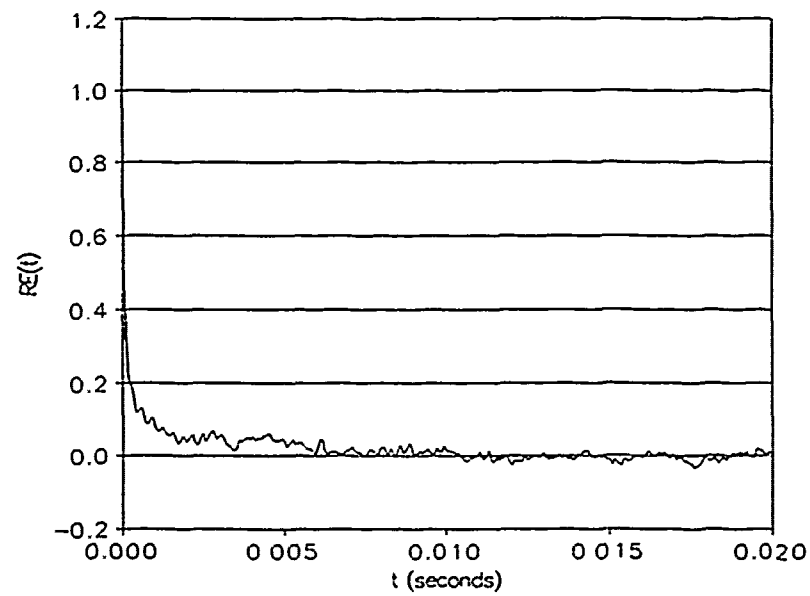
Figure A8 Point Where the Eulerian Correlation Crosses the X-Axix
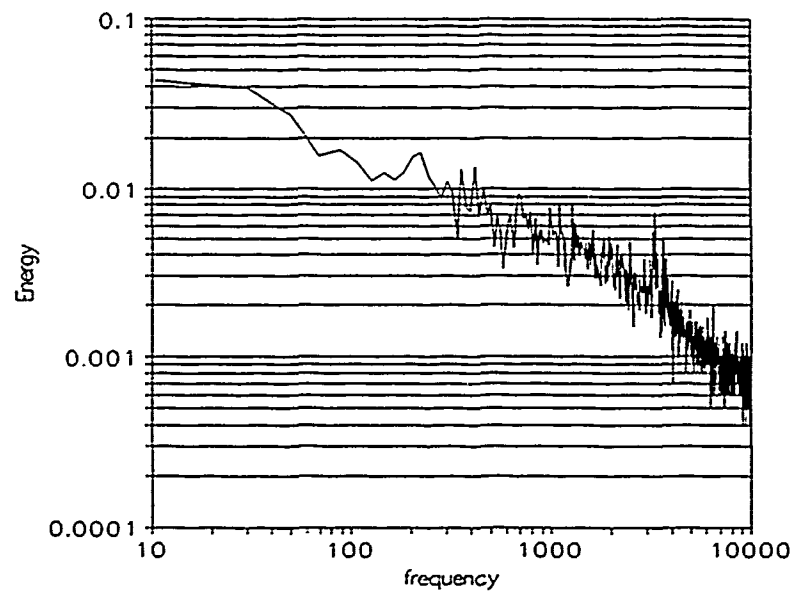
Figure A9 Typical Energy Distribution
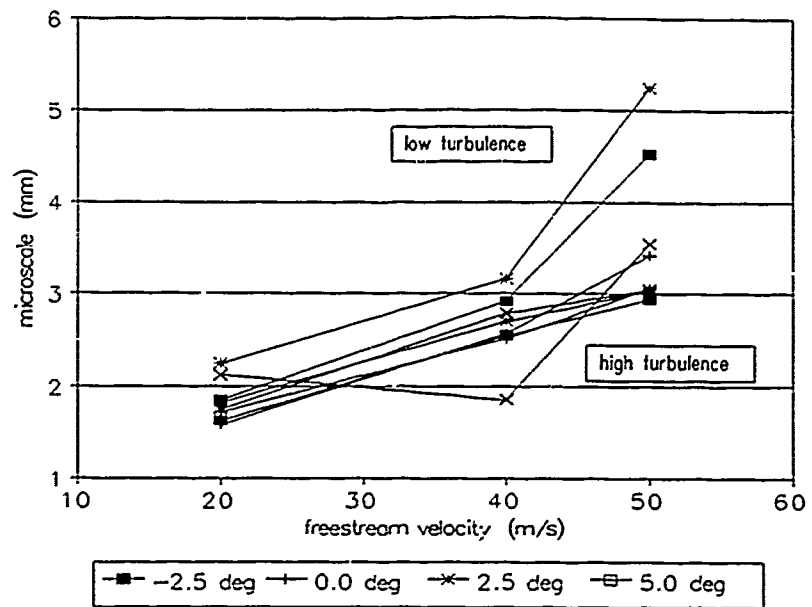
Figure A10 TCTF Freestream Microscale Behavior
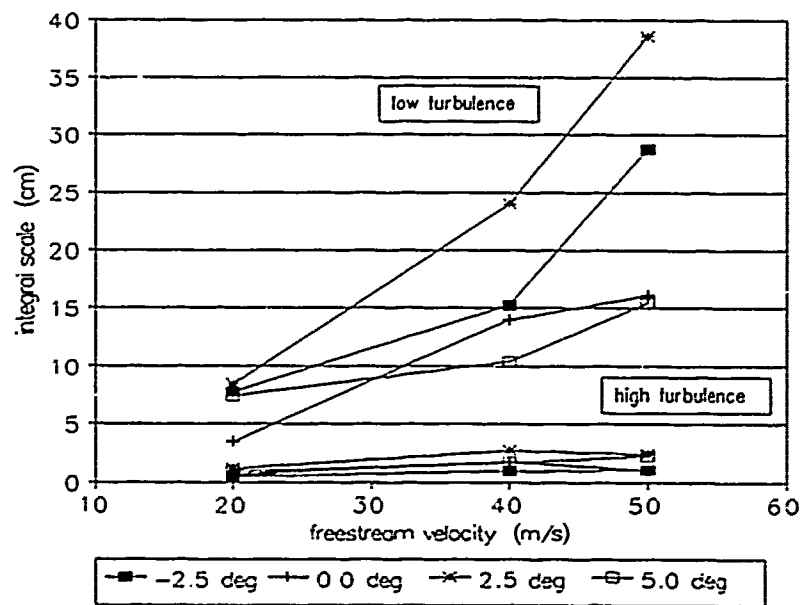
Figure A11 TCTF Freestream Integral Scale Behavior
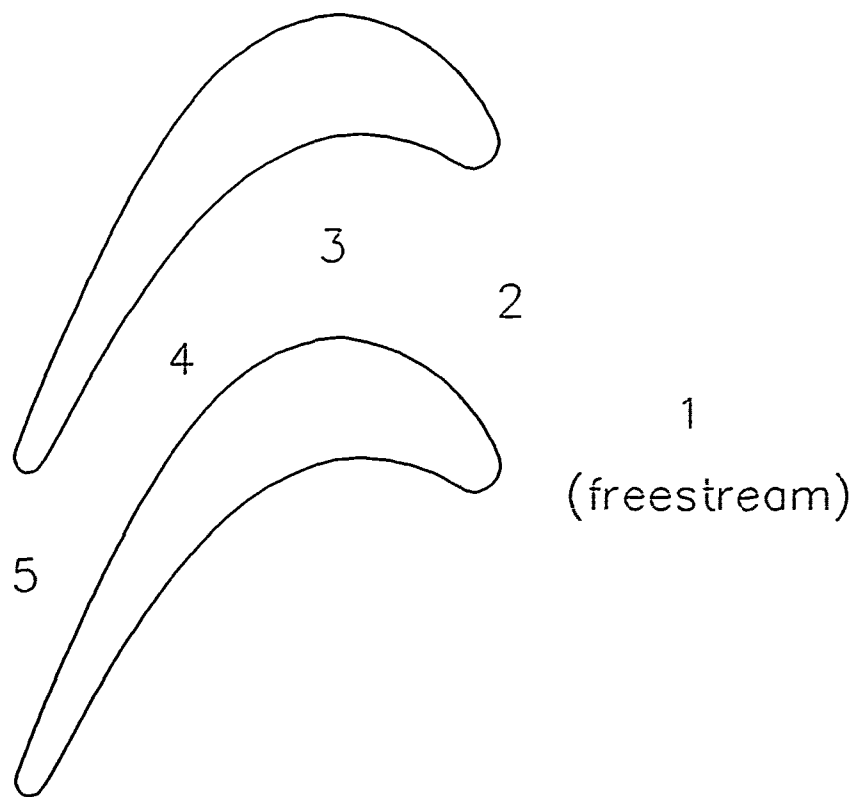
Figure A12 TCTF Cascade Passage Data Locations
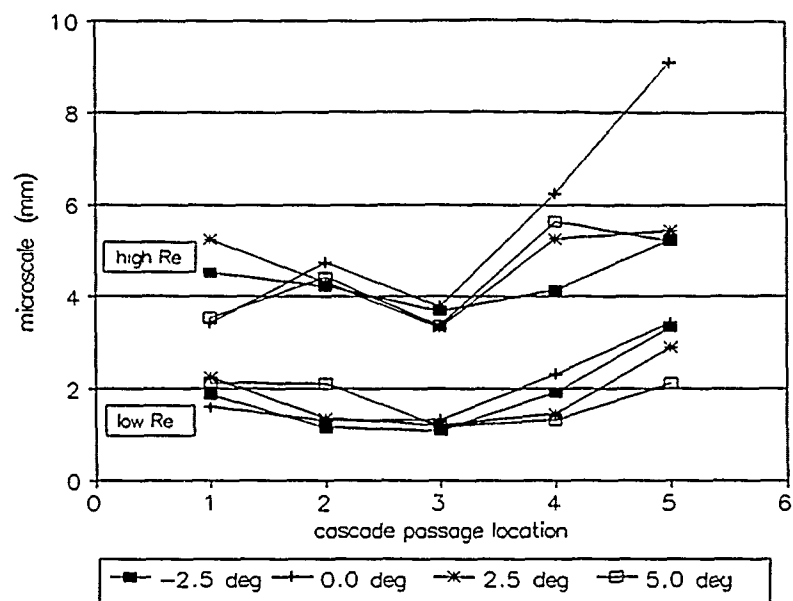
Figure A13 Low Turbulence Passage Microscale Behavior
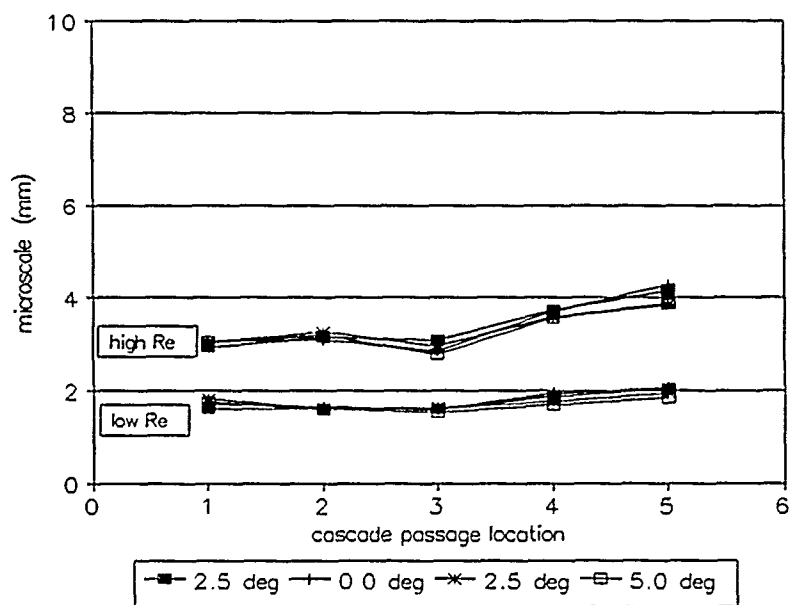
Figure A14 High Turbulence Passage Microscale Behavior

A-24
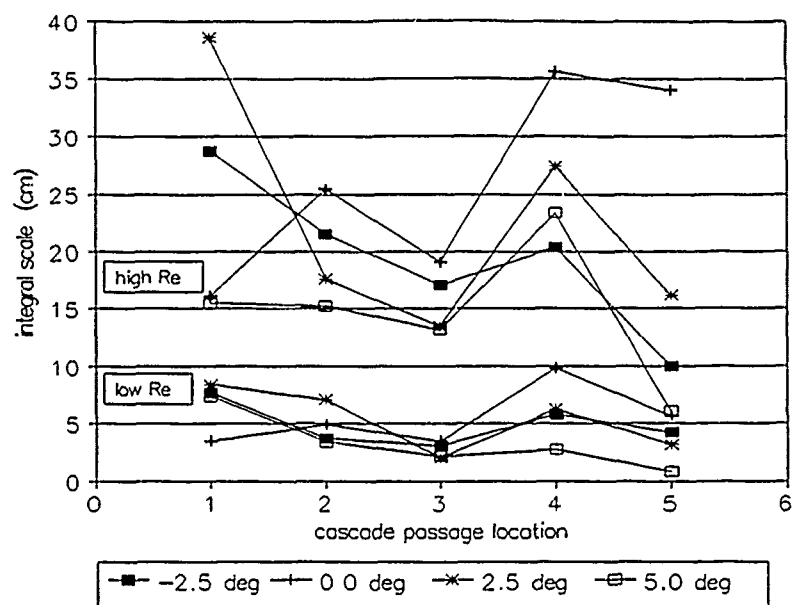
Figure A15 Low Turbulence Passage Integral Scale Behavior
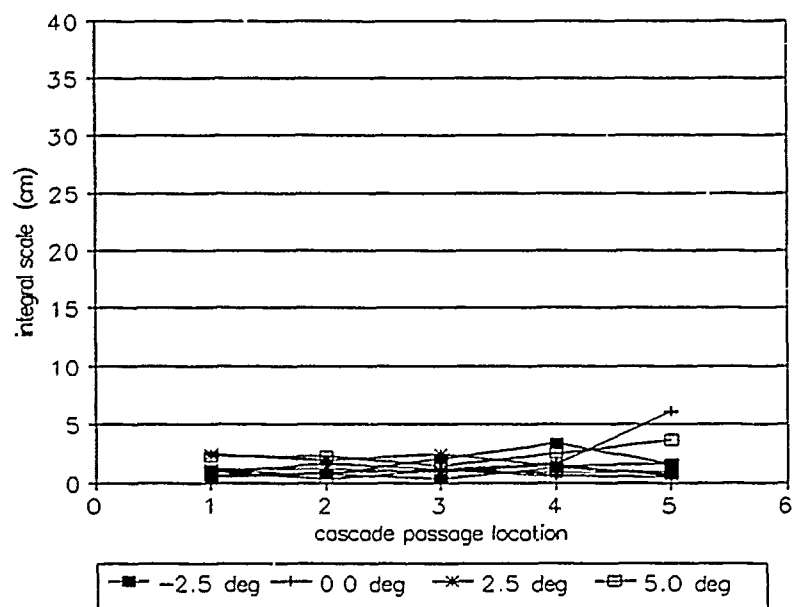
Figure A16 High Turbulence Passage Integral Scale Behavior

A-25

TAYLOR.BAS

This QUICKBASIC program calculates the micro and integral scale based on the correlation method described in Appendix A. Refer to Appendix F (Data Reduction Software) for complete subroutine listings.

```
DECLARE SUB STATS (NI, E1!(), E2!(), MEAN!(), STDDEV!())
DECLARE SUB REDUCE (E1(), E2(), N, infile1$, infile2$, calcoef$)
DECLARE SUB RealFT (dat(), N, ISIGN%)
DECLARE SUB Four1 (dat(), NN, ISIGN%)
DEFINT I-J
' see subprogram listings under VELREDUC.bas in Appendix F

' Main Program Block
'$DYNAMIC
DIM E1(16384), E2(16384), frequ(16384)
DIM MEAN(2), STDDEV(2), MICRO!(2), INTEGRAL!(2)

N = 16384                    'samples
fsample = 50000!              'hertz
dt = 1 / fsample              'seconds
df = fsample / N              'hertz

run$ = "hx14"

calcoef$ = "e:\steve\cal\044_84b.cof"
infile1$ = "a:\turb\" + run$ + "e1.dat"
infile2$ = "a:\turb\" + run$ + "e2.dat"
Refile$ = "e:\steve\scales\" + run$ + "nRE.dat"
' read in the x-wire voltages and converted to velocities

CALL REDUCE(E1(), E2(), N, infile1$, infile2$, calcoef$)
CALL STATS(N, E1(), E2(), MEAN(), STDDEV())

' obtain the FFT of u'(t) : H(f) stored in E1(i)

PRINT : PRINT "     performing FFT on u1"
halfn = N / 2

CALL RealFT(E1(), halfn, 1)

' calculate H(f) x H(f)*

PRINT : PRINT "     calculating H(f) X H(f)*"
E1(1) = E1(1) ^ 2
E1(2) = E1(2) ^ 2
FOR i = 3 TO N - 1 STEP 2
        E1(i) = E1(i) ^ 2 + E1(i + 1) ^ 2
        E1(i + 1) = 0!
NEXT i

' obtain the inverse FFT of H(f) x H(f)* to get the convolution u'(t)*u'(t)

PRINT : PRINT "     performing the inverse FFT on H(f) X H(f)*"
CALL RealFT(E1(), halfn, -1)

' divide the result of inverse FFT by n/2 factor (algorithm requirement)
FOR i = 1 TO N
        E1(i) = E1(i) / halfn
NEXT i

' calculate the correlation function by Taylor's Hypothesis
```

```
FOR i = 1 TO N
    E1 (i) = E1 (i) / (N * STDDEV(1) ^ 2)
NEXT i

' output the first 25 to a file for parabola fitting

OPEN Refile$ FOR OUTPUT AS #1
time = 0!
FOR i = 1 TO 25
    PRINT #1, time, E1 (i)
    time = time + dt
NEXT i
CLOSE #1
' calculate the turbulence scales
PRINT : PRINT '     calculating the integral scale'

i = 1
sum = 0
WHILE E1 (i) > 0
    sum = sum + E1 (i)
    i = i + 1
WEND
INTEGRAL!(1) = MEAN(1) * sum * dt

MICRO(1) = SQR((MEAN(1) ^ 2) / (-(E1 (2) - 1) / (dt ^ 2)))

PRINT USING 'micro = #.###### integral = #.######'; MICRO(1); INTEGRAL!(1)
END
```

X	Y		X	Y (cont)
-0.0023	0.2012		-3.7395	-2.0635
-0.0126	0.2516		-3.7282	-2.1139
-0.0352	0.3020		-3.6867	-2.1566
-0.0629	0.3523		-3.6388	-2.1697
-0.0956	0.4026		-3.5684	-2.1566
-0.1258	0.4530		-3.4954	-2.0660
-0.1598	0.5033		-3.4400	-1.9693
-0.2340	0.5953		-3.3771	-1.8647
-0.3309	0.7046		-3.3192	-1.7615
-0.4479	0.8053		-3.2664	-1.6715
-0.5914	0.9059		-3.1997	-1.5602
-0.7839	1.0066		-3.1431	-1.4633
-1.0481	1.0846		-3.0827	-1.3656
-1.2180	1.1085		-3.0173	-1.2608
-1.3891	1.0972		-2.9481	-1.1601
-1.5200	1.0659		-2.8814	-1.0594
-1.7011	1.0066		-2.8059	-0.9525
-1.8899	0.9059		-2.7405	-0.8622
-2.0384	0.8053		-2.6650	-0.7626
-2.1591	0.7046		-2.5769	-0.6543
-2.2598	0.6040		-2.4913	-0.5536
-2.3504	0.5033		-2.4007	-0.4505
-2.4309	0.4052		-2.3101	-0.3598
-2.5165	0.2968		-2.1994	-0.2553
-2.5870	0.2012		-2.0748	-0.1497
-2.6549	0.1007		-1.9415	-0.0478
-2.7254	-0.0025		-1.7804	0.0503
-2.7883	-0.0981		-1.5653	0.1510
-2.8487	-0.2051		-1.4243	0.2013
-2.9040	-0.3020		-1.2532	0.2391
-2.9644	-0.4026		-1.0620	0.2504
-3.0185	-0.5033		-0.8845	0.2340
-3.0701	-0.6040		-0.7197	0.2051
-3.1204	-0.6973		-0.5285	0.1460
-3.1745	-0.8053		-0.3322	0.0453
-3.2249	-0.9059		-0.2655	0.0101
-3.2727	-1.0066		-0.1988	0.0000
-3.3218	-1.1073		-0.1258	0.0214
-3.3728	-1.2101		-0.0755	0.0541
-3.4199	-1.3086		-0.0289	0.1057
-3.4627	-1.4025		-0.0025	0.1762
-3.5130	-1.5099		-0.0023	0.2013
-3.5558	-1.6079			
-3.6024	-1.7112			
-3.6439	-1.8009			
-3.6892	-1.9125			
-3.7307	-2.0132			

Appendix C: Thermocouple and Pressure Tap Locations

tap #	x/c	s (m)	s/c	surface
1	0.0174	0.0100	0.0875	suction
2	0.0652	0.0010	0.0087	leading edge
3	0.1243	0.0137	0.1199	pressure
4	0.1913	0.0280	0.2450	pressure
5	0.3157	0.0420	0.3675	pressure
6	0.4365	0.0615	0.5381	pressure
7	0.6000	0.0825	0.7218	pressure
8	0.7687	0.0930	0.8136	pressure
9	0.8522	0.1023	0.8950	pressure
10	0.9235	0.1085	0.9493	pressure
11	0.9913	0.1257	1.0997	trailing edge
12	0.9026	0.1363	1.1925	suction
13	0.7643	0.1240	1.0849	suction
14	0.6670	0.1120	0.9799	suction
15	0.5817	0.1005	0.8793	suction
16	0.4870	0.0885	0.7743	suction
17	0.3852	0.0820	0.7174	suction
18	0.3322	0.0683	0.5976	suction
19	0.2191	0.0545	0.4768	suction
20	0.1078	0.0402	0.3517	suction
21	0.0357	0.0238	0.2082	suction
22	0.0000	0.0175	0.1531	suction
23	0.0087	0.0135	0.1181	suction

Appendix D: Scanivalve Port Assignments

PORT	ASSIGNMENT
1	tap 1
2	tap 2
3	tap 3
4	tap 4
5	tap 5
6	tap 6
7	tap 7
8	tap 8
9	tap 9
10	tap 10
11	atmosphere
12	tap 11
13	tap 12
14	tap 13
15	tap 14
16	tap 15
17	tap 16
18	tap 17
19	tap 18
20	tap 19
21	tap 20
22	atmosphere
23	tap 21
24	tap 22
25	tap 23
26	pitot tube stagnation
27	atmosphere
28	pitot tube static

CHANNEL	ASSIGNMENT
000 - 006	not used
007	blade thermocouple 17
008	blade thermocouple 18
009	blade thermocouple 19
010	blade thermocouple 20
011	blade thermocouple 21
012	blade thermocouple 22
013	blade thermocouple 23
014	blade thermocouple 24
015	blade thermocouple 25
016	blade thermocouple 26
017	blade thermocouple 27
018	blade thermocouple 28
019	room temperature thermocouple
020	tunnel temperature thermocouple
021 - 023	not used
100	Scanivalve step control
101	Scanivalve home control
102 - 103	not used
104	blade surface power interrupt
105 - 107	not used
200	not used
201	blade thermocouple 1
202	blade thermocouple 2
203	blade thermocouple 3
204	blade thermocouple 4
205	blade thermocouple 5
206	blade thermocouple 6
207	blade thermocouple 7
208	blade thermocouple 8
209	blade thermocouple 9

CHANNEL	ASSIGNMENT
210	blade thermocouple 10
211	blade thermocouple 11
212	blade thermocouple 12
213	blade thermocouple 13
214	blade thermocouple 14
215	blade thermocouple 15
216	blade thermocouple 16
217 - 220	not used
221	Scanivalve pressure transducer
222 - 223	not used
300 - 320	not used
321	X-wire channel 1
322	X-wire channel 2
323	not used

Appendix F: Software

1. Calibration Software

PRESSCAL.BAS

```
'PRESSCAL.bas
' This program performs the calibration of the Scanivalve pressure
' transducer.  Before executing, prepare for the calibration by:
'
' 1.  set the Scanivalve on port 0;
' 2.  hook up a pressure/vacuum source and gage to port 0;
' 3.  do not overpressurize the gage (+/- 2 psi max);
' 4.  incrementally apply pressure/vacuum while acquiring data;
' 5.  when the calibration is complete, curve fit the data


DIM CAL(30) AS SINGLE
' initialize the screen and assign data file and directory

COLOR 7, 1
CLS
LOCATE 3, 1
PRINT ('                SCANIVALVE CALIBRATION PROGRAM')
VIEW PRINT 5 TO 24

INPUT 'Directory used to store the data file? (c:\steve\cal\) ', dir$
IF dir$ = '' THEN dir$ = 'c:\steve\cal\'
INPUT 'Name of file used to store data? (calib) ', flname$
IF flname$ = '' THEN flname$ = 'calib'
COLOR 1, 7
CLS 2
OPEN dir$ + flname$ + '.dat' FOR OUTPUT AS #1
' configure the HP3852 for reading the Scanivalve voltages

CALL IBFIND('HP3852', dvm%)
CALL IBWRT(dvm%, 'RST')
CALL IBWRT(dvm%, 'RST 600')
CALL IBWRT(dvm%, 'REAL C(49), L,H,M,S')
CALL IBWRT(dvm%, 'USE 600; NPLC 1')
' create the HP3852 measurement subroutine

CALL IBWRT(dvm%, 'SUB VOLTAGE')
CALL IBWRT(dvm%, 'AZERO ONCE,USE 600')
CALL IBWRT(dvm%, 'CONF DCV; NRDGS 50')
CALL IBWRT(dvm%, 'MEAS DCV, 221, USE 600, INTO C')
CALL IBWRT(dvm%, 'STAT L,H,M,S,C')
CALL IBWRT(dvm%, 'DISP M')
CALL IBWRT(dvm%, 'VREAD M')
CALL IBWRT(dvm%, 'SUBEND')
' begin the main program

I = 1
PRINT '<Press> any key to measure the pressure'
DO: LOOP WHILE INKEY$ = ''

DO
  PRINT '  MEASURING PRESSURE'

  ' measure the voltage, convert to kPa, and display to screen

  CALL IBWRT(dvm%, 'CALL VOLTAGE')
  rd$ = SPACE$(16)
  CALL ibrd(dvm%, rd$)
  vt! = VAL(rd$)
  PRINT USING 'Voltage output is ##.#### volts'; vt!
  INPUT 'Manometer height difference? ', dh!
  p! = dh! * .2483
  PRINT #1, USING '##.#### , ###.##### , ###.##########'; dh!; p!; vt!
  INPUT 'Continue? (y or n) ', ans$
```

```
    IF ans$ = 'n' OR ans$ = 'N' THEN
      EXIT DO
    END IF
      --
    PRINT : PRINT '<Press> any key to measure the pressure'
    DO: LOOP WHILE INKEY$ = ''
    I = I + 1
LOOP
' reset the HP3852

CALL IBWRT(dvm%, 'RST; CLR')
END
```

XWIRECAL.BAS

```basic
DECLARE SUB E1E2 (V(), E(), NPOINTS, SWITCH, filename$)
DECLARE SUB CONSTANTS (V(), E(), NPOINTS, SWITCH, filename$)
' XWIRECAL.bas
' This calibration program performs the hot-wire calibration by reading the
' voltage output by each wire and calculating the corresponding velocity
' based on the calibration tank pressure (by manual manometer input) and
' temperature (by automatic thermocouple input). Before executing, prepare
' for the calibration by:

' 1. attaching the tank Tcouple to Tcouple wire #29 (Channel 019 on the HP3852);
' 2. configuring the IFA100 for the xwire in use;
' 3. connecting the micromanometer to the calibration tank
DIM V(50), E(2, 50)

' initialize the screen

CLS
LOCATE 5, 7: PRINT '      X-wire calibration program for the HP 3852A'
PRINT
DO
  CLS : PRINT : PRINT '        MAIN MENU': PRINT
  PRINT STRING$(80, '_'): PRINT
  PRINT '1) obtain calibration voltages'
  PRINT '2) obtain calibration constants'
  PRINT '3) EXIT'
  PRINT : PRINT 'Type your selection (1, 2, or 3):'
  chs$ = INPUT$(1)
  ' Use SELECT CASE to process response.
  SELECT CASE chs$
      CASE '1': CALL E1E2(V(), E(), NPOINTS, SWITCH, filename$)
      CASE '2': CALL CONSTANTS(V(), E(), NPOINTS, SWITCH, filename$)
      CASE '3': EXIT DO
  END SELECT
LOOP

END
'
'
'
'

SUB CONSTANTS (V(), E(), NPOINTS, SWITCH, filename$)
' this subroutine calculates the X-wire calibration constants

CLS
DIM X(2, 50), Y(2, 50), a(2), B0(2), B1(2)
DIM ueff(2, 50)
DIM Eout(2, 50)
' if calibration data was just collected, go to line 20 and continue
IF SWITCH = 1 GOTO 20
LOCATE 1, 7: INPUT 'enter the calibration data filename'; filename$

' read in previously collected data from a data file

OPEN 'e:\steve\cal\' + filename$ + '.dat' FOR INPUT AS #1
i = 0
WHILE NOT EOF(1)
      i = i + 1
      INPUT #1, dummy, V(i), E(1, i), E(2, i)
WEND
CLOSE #1
NPOINTS = i
20    OPEN 'e:\steve\cal\' + filename$ + '.cal' FOR OUTPUT AS #2
CLS : LOCATE 1, 7: PRINT USING 'there are ## data points'; NPOINTS
PRINT

' remove the IFA gain and offset

gain = 10!: offset = 1!
FOR i = 1 TO NPOINTS
      temp1 = E(1, i): temp2 = E(2, i)
      E(1, i) = E(1, i) / gain + offset
      E(2, i) = E(2, i) / gain + offset
```

```basic
        LOCATE i + 1, 7
        PRINT USING "##.## ##.### ##.### ##.### ##.###"; V(i); temp1; E(1, i); temp2; E(2, i)
        PRINT #2, USING "##.## ##.### ##.### ##.### ##.###"; V(i); temp1; E(1, i); temp2; E(2, i)
NEXT i
INPUT "press ENTER to continue"; ans$

PI = 3.1416
mu = (PI / 2!) 'radians
a(1) = mu / 2!
a(2) = a(1)

' calculate the XWIRE effective velocities
c1 = (COS(a(1)) ^ 2) + ((.15 * SIN(a(1))) ^ 2)
c2 = (COS(a(2)) ^ 2) + ((.15 * SIN(a(2))) ^ 2)
PRINT c1, c2
FOR i = 1 TO NPOINTS
        ueff(1, i) = c1 * V(i) ^ 2
        ueff(2, i) = c2 * V(i) ^ 2
        ueff(1, i) = SQR(ueff(1, i))
        ueff(2, i) = SQR(ueff(2, i))
        PRINT ueff(1, i), ueff(2, i)
        PRINT #2, ueff(1, i), ueff(2, i):
NEXT i
INPUT ; "hit enter key to continue", ans$
' fit the data to a straight line using King's Law
FOR j = 1 TO 2
FOR i = 1 TO NPOINTS
        Y(j, i) = E(j, i) ^ 2
        X(j, i) = ueff(j, i) ^ .45
NEXT i
SUMX = 0!
SUMY = 0!
SUMXX = 0!
SUMXY = 0!
FOR i = 1 TO NPOINTS
        SUMX = SUMX + X(j, i)
        SUMY = SUMY + Y(j, i)
        SUMXX = SUMXX + X(j, i) ^ 2
        SUMXY = SUMXY + X(j, i) * Y(j, i)
NEXT i
B1(j) = NPOINTS * SUMXY - SUMX * SUMY
B1(j) = B1(j) / (NPOINTS * SUMXX - SUMX ^ 2)
B0(j) = (SUMY - SUMX * B1(j)) / NPOINTS

' print the calibration data to files

PRINT USING "B0 = +##.####, B1 = +##.####"; B0(j); B1(j)
PRINT #2, USING "B0 = +##.####, B1 = +##.####"; B0(j); B1(j)
NEXT j

INPUT ; "hit ENTER to continue", ans$
PRINT
PRINT "  vel      E1exp      E1fit      E2exp      E2fit"
PRINT

FOR j = 1 TO 2
FOR i = 1 TO NPOINTS
        Eout(j, i) = B0(j) + B1(j) * ueff(j, i) ^ .45
        Eout(j, i) = SQR(Eout(j, i))
NEXT i
NEXT j
FOR i = 1 TO NPOINTS
        PRINT V(i), E(1, i), Eout(1, i), E(2, i), Eout(2, i)
        PRINT #2, V(i), E(1, i), Eout(1, i), E(2, i), Eout(2, i)
NEXT i
' display results to screen using the BASIC graphics
INPUT ; "continue (Y/N) :", ans$
CLS
SCREEN 9
Xmin = 0: Xmax = 639
Ymin = 0: Ymax = 319
LINE (Xmin, Ymin)-(Xmax, Ymax), 5, BF
```

```
Emax = 1.2 * E(1, NPOINTS)
Umax = 1.2 * ueff(1, NPOINTS)
FOR j = 1 TO 2  .
x1 = 0: y1 = 0
x1 = 639 * ueff(j, 1) / Umax
y1 = (1! - Eout(j, 1) / Emax) * 319
FOR i = 2 TO NPOINTS
    x2 = 639 * ueff(j, i) / Umax
    y2 = (1! - Eout(j, i) / Emax) * 319
    LINE (x1, y1)-(x2, y2)
    x1 = x2: y1 = y2
NEXT i
nbox = 2

FOR i = 1 TO NPOINTS
    x2 = 639 * ueff(j, i) / Umax
    y2 = (1! - E(j, i) / Emax) * 319
    x1 = x2 - nbox: x2 = x2 + nbox
    y1 = y2 - nbox: y2 = y2 + nbox
    LINE (x1, y1)-(x2, y2), 2, BF
NEXT i
NEXT j
INPUT "press ENTER to continue"; ans$

SCREEN 0: CLS

' output the calibration constants to the data file

OPEN "e:\steve\cal\" + filename$ + ".cof" FOR OUTPUT AS #1
FOR i = 1 TO 2
    PRINT #1, B0(i), B1(i)
NEXT i
CLOSE #1
CLOSE #2
END SUB
'
'
'
'

SUB E1E2 (V(), E(), NPOINTS, SWITCH, filename$)
' This subroutine performs the voltage scan on the hot wire for
' conversion to velocities. Two channels are scanned consecutively
' with the HP44702B and the FET Multiplexer. The FET is connected
' internally to the HP44702B via a ribbon cable.
CLS
DEFINT I-M

' initialize the HP3852

CALL IBFIND("hp3852", dvm%)
CALL IBWRT(dvm%, "RST; CLR")
rd$ = SPACE$(16)
' measure the calibration tank temperature

LOCATE 7, 7: PRINT "measuring calibration tank air temperature"
CALL IBWRT(dvm%, "USE 600;RST 600;REAL TT; AZERO ONCE")
CALL IBWRT(dvm%, "CONFMEAS TEMPJ, 019, INTO TT")
CALL IBWRT(dvm%, "VREAD TT")
CALL IBWRT(dvm%, "disp on")
CALL IBRD(dvm%, rd$)
TTC = VAL(rd$)
TTF = TTC * (9! / 5!) + 32!
LOCATE 9, 7
PRINT USING "the tank temp. is ##.## degC or ##.## degF"; TTC; TTF
' input the probe and file information

LOCATE 11, 7: INPUT "enter the probe serial #"; sn$
LOCATE 13, 7: INPUT "enter the filename for data output"; filename$
calfile$ = "c:\steve\cal\" + filename$ + ".dat"
LOCATE 15, 7: PRINT USING "the calibration data for probe & is in &"; sn$; calfile$
OPEN calfile$ FOR OUTPUT AS #1
LOCATE 19, 7: INPUT "press ENTER to continue"; ans$
CLS
' compute current air density, rho!
```

```
rholowl = 1.3947: drho! = .4666: Tlow! = 23.15: dTemp! = 100!
rho! = rholowl - drho! * (TT + Tlow!) / dTemp!
' main program
    ‾
NPOINTS = 0
10    PRINT 'Press any key to begin scan '
DO: LOOP WHILE INKEY$ = ''

NPOINTS = NPOINTS + 1
PRINT '  Scanning hot wire voltages.'
' proceed with channel 1 and channel 2 voltage scan.
nminus1$ = 'REAL WAVE(1999), CHAN1(999), CHAN2(999)'
nscans$ = 'PRESCAN 1000; POSTSCAN 0'
nsamples$ = 'XRDGS 400, 2000 INTO WAVE'
CLS : LOCATE 7, 7: PRINT 'voltage scan in progress'
' read hotwires
CALL IBWRT(dvm%, 'RST; CLR; RST 400')
CALL IBWRT(dvm%, 'DISP OFF')
CALL IBWRT(dvm%, 'USE 400')
CALL IBWRT(dvm%, nminus1$)
CALL IBWRT(dvm%, 'REAL L1,L2,H1,H2,AV1,AV2,S1,S2')

' configure the HP44702B for high-speed scanning.
CALL IBWRT(dvm%, 'SCANMODE ON;CONF DCV;ARMODE BEFORE')
CALL IBWRT(dvm%, 'TERM RIBBON;range 9;RDGSMODE COMPLETE')
CALL IBWRT(dvm%, nscans$)

' set the time (in seconds) between samples

sper$ = 'SPER 0.001'
CALL IBWRT(dvm%, sper$)
CALL IBWRT(dvm%, 'STTRIG INT')

' scan the X-wires
CALL IBWRT(dvm%, 'CLWRITE SENSE,321-322;ASCAN ON;AZERO ONCE;SCTRIG INT')
CALL IBWRT(dvm%, nsamples$)

' dump the scanned voltages from the voltmeter buffer to the HP3852 mainframe

CALL IBWRT(dvm%, 'SUB SEPARAT')   'Separate the readings into 2 arrays
CALL IBWRT(dvm%, 'INTEGER I,J')
CALL IBWRT(dvm%, 'J = 0')
CALL IBWRT(dvm%, 'FOR I = 0 TO 1999 STEP 2')
CALL IBWRT(dvm%, 'CHAN1(J) = WAVE(I)')
CALL IBWRT(dvm%, 'CHAN2(J) = WAVE(I+1)')
CALL IBWRT(dvm%, 'J = J+1')
CALL IBWRT(dvm%, 'NEXT I')
CALL IBWRT(dvm%, 'SUBEND')
CALL IBWRT(dvm%, 'CALL SEPARAT')
CALL IBWRT(dvm%, 'stat L1,H1,AV1,S1,CHAN1')
CALL IBWRT(dvm%, 'stat L2,H2,AV2,S2,CHAN2')
rd$ = SPACE$(16)
CALL IBWRT(dvm%, 'vread AV1')
CALL IBRD(dvm%, rd$)
E(1, NPOINTS) = VAL(rd$)
CALL IBWRT(dvm%, 'vread AV2')
CALL IBRD(dvm%, rd$)
E(2, NPOINTS) = VAL(rd$)
CALL IBWRT(dvm%, 'SCTRIG HOLD')
CALL IBWRT(dvm%, 'DISP ON; RST; CLR')
' Compute approximate velocity at orifice
PRINT , INPUT 'input current tank pressure (in H2O)'; Ptank!
V(NPOINTS) = SQR(Ptank! * 248.7 * 2! / rho!)
PRINT : PRINT 'current air speed is: ', V(NPOINTS), ' m/sec'
PRINT : PRINT Ptank, V(NPOINTS), E(1, NPOINTS), E(2, NPOINTS)
PRINT #1, Ptank!, V(NPOINTS), E(1, NPOINTS), E(2, NPOINTS)
PRINT : INPUT 'quit?  (y or n) ', q$
IF q$ <> 'y' THEN GOTO 10

CLOSE #1
SWITCH = 1

END SUB
```

2. Data Acquisition Software

ACQUIRE.BAS - main program

```
' ACQUIRE.BAS

' This QuickBASIC program performs automated data acquisition for the
' Turbine Cascade Test Facility in Bldg 19 through the HP3852A.
' To execute, at the c:\steve prompt enter QB/L QBIB4 /AH.
' This will access the GPIB library and allow large data matrix
' manipulation for turbulence data acquisition.
' user written subroutines
DECLARE SUB TEMPACQ (dvm%, file$)
DECLARE SUB PRESSACQ (dvm%, Ttunnel, file$)
DECLARE SUB VELACQ (dvm%, file$)
DECLARE SUB PLOTT (xdat() AS SINGLE, ydat() AS SINGLE, xmin!, xmax!, ymin!, ymax!, xlab$, ylab$, pltlab$,
ntot%)
DECLARE SUB TEMPS (dvm%, Troom, Ttunnel)
DECLARE SUB VSET (dvm%, Ttunnel)
DECLARE SUB TSET (dvm%)
' read in the thermocouple and pressure port chord locations for plotting purposes

DIM chord(24) AS SINGLE  'chord locations are common
OPEN "c:\steve\dat\chord.dat" FOR INPUT AS #1
FOR i = 1 TO 23
INPUT #1, chord(i)
NEXT i
CLOSE #1

' initialize the HP3852 data acquisition unit

CALL IBFIND("hp3852", dvm%)
CALL IBWRT(dvm%, "RST; CLR")
' initialize the screen
CLS : COLOR 3, 0: LOCATE 2, 12
PRINT "          HP3852 Controller Program"
LOCATE 4, 12
PRINT " Lt Galassi 6/89, Capt Acree 7/90, Capt Meschwitz 7/91"
LOCATE 6, 12
PRINT "This program controls the HP3852 Data Acquisition System"
LOCATE 12, 1
CALL TEMPS(dvm%, Troom, Ttunnel)
PRINT

' input the data run filename

INPUT "Run Designation for all data files ? (enter run #):", file$
' routine Branching for the MAIN MENU
DO
    CLS : PRINT : PRINT "        MAIN MENU": PRINT
    PRINT STRING$(80, "_"): PRINT
    PRINT "1) Temperature Run"
    PRINT "2) Pressure Run"
    PRINT "3) Turbulence Run"
    PRINT "4) Position X-wire"
    PRINT "5) Monitor Blade Temperature"
    PRINT "6) Change File Designator"
    PRINT "7) EXIT"
    PRINT : PRINT USING "the current file designator is &"; file$
    PRINT : CALL TEMPS(dvm%, Troom, Ttunnel)
    PRINT : PRINT "Type your selection (1-7):"
    chs$ = INPUT$(1)

    ' Use SELECT CASE to process response.
    SELECT CASE chs$
    CASE "1": CALL TEMPACQ(dvm%, file$)
    CASE "2": CALL PRESSACQ(dvm%, Ttunnel, file$)
    CASE "3": CALL VELACQ(dvm%, file$)
    CASE "4": CALL VSET(dvm%, Ttunnel)
    CASE "5": CALL TSET(dvm%)
    CASE "6": CLS : INPUT "New file designation:", file$:
    CASE "7": CLS : EXIT DO
```

```
    CASE ELSE
     END SELECT
LOOP
    –
END
```

Subroutine PLOTT

```
SUB PLOTT (xdat() AS SINGLE, ydat() AS SINGLE, xmin!, xmax!, ymin!, ymax!, xlab$, ylab$, pltlab$, ntot%)
' this section of the code creates a plot of ydat vs xdat
CLS
SCREEN 9  'Hi-res graphics mode
VIEW (120, 10)-(570, 290), , 1
WINDOW (xmin!, ymin!)-(xmax!, ymax!)
style% = &HFF00
LOCATE 23, 42: PRINT pltlab$
LOCATE 1, 9: PRINT ymax!: LOCATE 10, 7: PRINT ylab$: LOCATE 21, 9: PRINT ymin!
LOCATE 22, 14: PRINT xmin!: LOCATE 22, 43: PRINT xlab$: LOCATE 22, 71: PRINT xmax!
VIEW PRINT 24 TO 25:
PRINT SPC(14); , "press any key to return to Main Menu"
CLS
LINE (1, 0)-(0, 0), , , style%
FOR i = 1 TO ntot%
   X = xdat(i)
   Y = ydat(i)
   LINE -(X, Y)
NEXT i
DO: LOOP WHILE INKEY$ = ""

CLS
SCREEN 0: COLOR 3, 0
END SUB
```

Subroutine PRESSACQ

```
SUB PRESSACQ (dvm%, Ttunnel, file$)

' This subroutine performs a pressure scan on the turbine blade
'  using the HP3852A data acquisition system  and low speed voltmeter.
' The voltmeter takes and averages 50 readings per port.

DIM pscan(28), ydat!(28), xdat!(28)
SHARED chord() AS SINGLE
DEFINT I-M

' initialize the screen

CLS
LOCATE 8, 7: PRINT 'BLADE PRESSURE SURVEY (approx 115 sec. duration)'
' set up the HP44701 for voltage measurements
CALL IBWRT(dvm%, 'RST 600')
CALL IBWRT(dvm%, 'REAL PSCAN(28),C(49),L,H,M,S')
' perform the actual pressure scan
CALL IBWRT(dvm%, 'USE 600;AZERO ONCE; NPLC 16')
CALL IBWRT(dvm%, 'CLOSE 101')              'call homes the scanivalve
CALL IBWRT(dvm%, 'OPEN 101;CONF DCV')
CALL IBWRT(dvm%, 'NRDGS 50')
CALL IBWRT(dvm%, 'MEAS DCV, 221,INTO C')    'read atmospheric pressure
CALL IBWRT(dvm%, 'STAT L,H,M,S,C')
CALL IBWRT(dvm%, 'PSCAN(0) = M')
CALL IBWRT(dvm%, 'DISP PSCAN(0)')
CALL IBWRT(dvm%, 'SUB LOOP')                'HP 3852A subroutine
CALL IBWRT(dvm%, 'INTEGER I')
CALL IBWRT(dvm%, 'FOR I = 1 TO 28')
CALL IBWRT(dvm%, 'CLOSE 100')
CALL IBWRT(dvm%, 'OPEN 100 ;CONF DCV; NRDGS 50')
CALL IBWRT(dvm%, 'MEAS DCV, 221, USE 600, INTO C')
CALL IBWRT(dvm%, 'STAT L,H,M,S,C')
CALL IBWRT(dvm%, 'PSCAN(I) = M')
CALL IBWRT(dvm%, 'DISP PSCAN(I)')
CALL IBWRT(dvm%, 'NEXT I')
CALL IBWRT(dvm%, 'SUBEND')
CALL IBWRT(dvm%, 'CALL LOOP')
SLEEP 120                        'allow 120 seconds for scan
CALL IBWRT(dvm%, 'VREAD PSCAN')

' write pressure voltage readings onto the data file on the hard disk
outfile$ = 'c:\steve\pressure\' + file$ + 'pv.dat'
CALL IBRDF(dvm%, outfile$)
CALL IBWRT(dvm%, 'RST; CLR')

' write the tunnel temperature to the pressure data file
OPEN outfile$ FOR APPEND AS #1
PRINT #1, Ttunnel
CLOSE #1
' read in the file for display

OPEN outfile$ FOR INPUT AS #1
FOR i = 0 TO 28
   INPUT #1, pscan(i)
NEXT i
CLOSE #1

' calculate the tunnel q
q = pscan(26) - pscan(28)
' perform shift on PSCAN() to collapse the vector.
' this technique is recommended by the Scanivalve manufacturer to help
'  identify step motor miscues.
'  array locations are assigned as follows:
' 0,11,22,29-36 - Atmospheric pressure
' 1-10,12-21,23-25 - Blade static pressures
' 26 -Pitot head press.
' 28- Pitot static press.
```

```
FOR i = 11 TO 20
    pscan(i) = pscan(i + 1)
NEXT i


FOR i = 21 TO 23
    pscan(i) = pscan(i + 2)
NEXT i

' this section drives the plotter.
ntot% = 23    'This no. corresponds to the total no. of pressure ports
ylab$ = 'Cp'
xlab$ = 'x/c'
pltlab$ = 'Cp on the turbine blade'
xmin! = 0!
xmax! = 1!
ymin! = -5
ymax! = 5
FOR i = 1 TO ntot%
    ydat!(i) = (pscan(i) - pscan(28)) / q
    xdat!(i) = chord(i)
NEXT i
CALL PLOTT(xdat!(), ydat!(), xmin!, xmax!, ymin!, ymax!, xlab$, ylab$, pltlab$, ntot%)
END SUB
```

Subroutine TEMPACQ

```
DEFSNG I-M
SUB TEMPACQ (dvm%, file$)
' This subroutine performs the temperature scan on the turbine blade
'  and stores the data in c:\steve\temp\file$.dat. The HP3852 is used to
'  acquire data through the HP 44713A FET Multiplexers.
' The program momentarily interrupts the power to the turbine blade
'  with relay channel 104 so as not to overload the thermocouples
SHARED chord() AS SINGLE
DIM temp(30), xdat(30), ydat(30)
DEFINT I-M
' read the blade temperatures, and Ttunnel and Troom.
' the first 16 Tcouples (wire #s 1-16) are on slot 2 (Channels 201-216),
'  and the next 14 (wire #s 17-30) are on slot 0 (Channels 007-020).
CLS

' configure the HP3852 and measure the temperatures

LOCATE 7, 7: PRINT 'measuring temperatures'
CALL IBWRT(dvm%, 'RST 600; USE 600')
CALL IBWRT(dvm%, 'AZERO ONCE')
CALL IBWRT(dvm%, 'REAL A(29)')
CALL IBWRT(dvm%, 'DISP OFF')
CALL IBWRT(dvm%, 'CONF TEMPJ')
CALL IBWRT(dvm%, 'CLOSE 104')                          'blade current off
CALL IBWRT(dvm%, 'MEAS TEMPJ, 201-216, 007 - 020, INTO A')
CALL IBWRT(dvm%, 'OPEN 104')                           'blade current on
CALL IBWRT(dvm%, 'VREAD A')

' transfer the readings to the PC for temporary storage

LOCATE 9, 7: PRINT 'transferring data to PC hard disk storage'
CALL IBRDF(dvm%, 'c:\steve\temp\bladetem.dat')
CALL IBWRT(dvm%, 'DISP ON; RST; CLR')

' create permanent storage and display readings to the screen

LOCATE 11, 7
PRINT 'creating permanent storage'
OPEN 'c:\steve\temp\bladetem.dat' FOR INPUT AS #1
OPEN 'c:\steve\temp\' + file$ + 'T.dat' FOR OUTPUT AS #2
LOCATE 13, 7: PRINT '  TC#      Temp'
LOCATE 14, 7: PRINT '         (degC)'
FOR i = 1 TO 30
    INPUT #1, temp(i)
    PRINT #2, temp(i)
NEXT i
CLOSE #1
CLOSE #2

FOR i = 1 TO 30 STEP 2
    PRINT USING ' ## ###.###     ## ##.###'; i; temp(i); i + 1; temp(i + 1)
NEXT i
INPUT '    press ENTER to continue'; rtn$

' create a file for 'GRAPHER'
OPEN 'c:\steve\plt\' + file$ + 'TGR.dat' FOR OUTPUT AS #1
FOR i = 1 TO 23
    PRINT #1, USING '#.####### ##.#####'; chord(i); temp(i)
NEXT i
CLOSE #1
' plot the temperature readings
ntot1% = 8    'This no. is the total no. of pressure side thermocouples
ntot2% = 12   'This no. is to the total no. of suction side thermocouples
ylab$ = 'Temp. (C)': xlab$ = 'x/c'
pltlab$ = 'Temp. on turbine blade '
xmin! = 0!: xmax! = 1!: ymin! = 20: ymax! = 65
FOR i = 1 TO ntot1%
    ydat(i) = temp(i)
    xdat(i) = chord(i)
NEXT i
```

```
FOR i = ntot1% + 1 TO ntot2%
    xdat(i) = chord(i)
    ydat(i) = 0
NEXT i
FOR i = ntot2% + 1 TO ntot1% + ntot2% + 3
    ydat(i) = temp(i - 4)
    xdat(i) = chord(i)
NEXT i
ntot% = ntot1% + ntot2% + 3
CALL PLOTT(xdat!(), ydat!(), xmin!, xmax!, ymin!, ymax!, xlab$, ylab$, pltlab$, ntot%)
END SUB
```

Subroutine TEMPS

```
DEFSNG I-M
SUB TEMPS (dvm%, Troom, Ttunnel)
' This subprogram configures the HP3852 to read the room temperature
'  on Channel 012 (wire 29) and the tunnel temperature on Channel 020 (wire 30)
CALL IBWRT(dvm%, 'USE 600;RST 600;REAL Troom, Ttunnel;AZERO ONCE')
' read the room temperature

CALL IBWRT(dvm%, 'CONFMEAS TEMPJ, 019, INTO Troom')
CALL IBWRT(dvm%, 'DISP Troom')
CALL IBWRT(dvm%, 'VREAD Troom')
rd$ = SPACE$(16)
CALL IBRD(dvm%, rd$)
Troom = VAL(rd$)        'convert the string value into a number

' read the tunnel temperature
CALL IBWRT(dvm%, 'CONFMEAS TEMPJ, 020, INTO Ttunnel')
CALL IBWRT(dvm%, 'DISP Ttunnel')
CALL IBWRT(dvm%, 'VREAD Ttunnel')
rd$ = SPACE$(16)
CALL IBRD(dvm%, rd$)
Ttunnel = VAL(rd$)      'convert the string value into a number

PRINT USING "the room temp is:   ##.## degF (##.## degC)"; (Troom * 9! / 5!) + 32!; Troom
PRINT USING "the tunnel temp is: ##.## degF (##.## degC)"; (Ttunnel * 9! / 5!) + 32!; Ttunnel
CALL IBWRT(dvm%, 'RST; CLR')
END SUB
```

Subroutine VSET

```
    SUB TSET (dvm%)
    ' This subprogram screen displays, in bar graph form, the room temperature
    '  and the 5 internal blade temperatures

    DIM temp(6)

    CLS
    temp0$ = SPACE$(16)
    temp1$ = SPACE$(16)
    temp2$ = SPACE$(16)
    temp3$ = SPACE$(16)
    temp4$ = SPACE$(16)
    temp5$ = SPACE$(16)
    ' set the screen graphics

    SCREEN 9

    ymin = 0!: ymax = 100!
    LINE (0, 0)-(639, 319), 3, BF
    FOR i = 0 TO 10
    Y = (1 - i / 10) * 319
    LINE (0, Y)-(639, Y)
    NEXT i

    ' outline the T = 60 degC line
    yset = 60!
    ytol = .5
    y0 = yset - ytol
    y1 = yset + ytol
    y0 = (1! - (y0 - ymin) / (ymax - ymin)) * 319
    y1 = (1! - (y1 - ymin) / (ymax - ymin)) * 319
    LINE (0, y0)-(639, y1), 6, BF
    yset = (1 - (yset - ymin) / (ymax - ymin)) * 319
    LINE (0, yset)-(639, yset)
    ' initialize the HP

    CALL IBWRT(dvm%, "RST 600; USE 600")
    CALL IBWRT(dvm%, "AZERO ONCE")
    CALL IBWRT(dvm%, "DISP OFF")
    DO
     ' take the temperature measurements

     CALL IBWRT(dvm%, "REAL A(5)")
     CALL IBWRT(dvm%, "CONFMEAS TEMPJ, 020, 014 - 018, USE 600 INTO A")

     ' transfer the measurements to the PC

     CALL IBWRT(dvm%, "VREAD A(0)")
     CALL IBRD(dvm%, temp0$)
     temp(1) = VAL(temp0$)
     CALL IBWRT(dvm%, "VREAD A(1)")
     CALL IBRD(dvm%, temp1$)
     temp(2) = VAL(temp1$)
     CALL IBWRT(dvm%, "VREAD A(2)")
     CALL IBRD(dvm%, temp2$)
     temp(3) = VAL(temp2$)
     CALL IBWRT(dvm%, "VREAD A(3)")
     CALL IBRD(dvm%, temp3$)
     temp(4) = VAL(temp3$)
     CALL IBWRT(dvm%, "VREAD A(4)")
     CALL IBRD(dvm%, temp4$)
     temp(5) = VAL(temp4$)
     CALL IBWRT(dvm%, "VREAD A(5)")
     CALL IBRD(dvm%, temp5$)
     temp(6) = VAL(temp5$)

     ' plot the measurements on the PC graphics screen

     nplot = 6
     ymin = 0!: ymax = 100!
     xmax = nplot
```

```
nbox = 20
y0 = 0
FOR i = 1 TO nplot
  y1 = (1 - temp(i) / ymax) * 319
  x1 = ((i) / (xmax + 1)) * 639
  x0 = x1 - nbox: x1 = x1 + nbox
  LINE (x0, y0)-(x1, y1), 3, BF
NEXT i
y0 = 319
FOR i = 1 TO nplot
  y1 = (1 - temp(i) / ymax) * 319
  x1 = ((i) / (xmax + 1)) * 639
  x0 = x1 - nbox: x1 = x1 + nbox
  LINE (x0, y0)-(x1, y1), 5, BF
NEXT i

LOOP UNTIL INKEY$ <> ""

SCREEN 0: COLOR 3, 0
CALL IBWRT(dvm%, "CLR; RST")
END SUB
```

Subroutine VELACQ

```
SUB VELACQ (dvm%, file$)
    DIM E1(16384), E2(16384)
    ' This subroutine performs the voltage scan on the hot wire for
    ' conversion to velocities. Two channels are scanned consecutively
    ' with the HP44702B and the FET Multiplexer. The FET is connected
    ' internally to the HP44702B (high speed voltmeter) via a ribbon cable.
    CLS
    DEFINT I-M

    ' set the number of scans per channel
    nscans = 16384
    N = nscans
    nsamples = 2 * nscans
    nminus1 = nsamples - 1
    nscans$ = STR$(nscans)
    nsamples$ = STR$(nsamples)
    nminus1$ = STR$(nminus1)
    nminus1$ = 'REAL WAVE(' + nminus1$ + '), OUT(8191)'
    nscans$ = 'PRESCAN ' + nscans$ + '; POSTSCAN 0'
    nsamples$ = 'XRDGS 400, ' + nsamples$ + ' INTO WAVE'
    CLS : LOCATE 2, 7: PRINT '          Turbulence scan in progress'

    ' configure the HP3852

    CALL IBWRT(dvm%, 'CLR; RST')
    CALL IBWRT(dvm%, 'RST 400; USE 400')
    CALL IBWRT(dvm%, nminus1$)
    CALL IBWRT(dvm%, 'DISP OFF')
    CALL IBWRT(dvm%, 'SCANMODE ON; CONF DCV; ARMODE BEFORE')
    CALL IBWRT(dvm%, 'TERM RIBBON; range 9; RDGSMODE COMPLETE')
    CALL IBWRT(dvm%, nscans$)
    CALL IBWRT(dvm%, 'STTRIG INT')
    ' set the sample period = 1 / fsample
    period = .00005
    period$ = STR$(period)
    sper$ = 'SPER ' + period$
    CALL IBWRT(dvm%, sper$)
    ' trigger the scans
    LOCATE 4, 7: PRINT 'Acquiring Data'
    CALL IBWRT(dvm%, 'CLWRITE SENSE,321-322; ASCAN ON; AZERO ONCE; SCTRIG INT')

    ' transfer the data from the 44702B VM to the hard disk via HP mainframe

    FOR i = 0 TO 3
        LOCATE 6, 7: PRINT USING 'transfering #### data points to PC file FREQ#.dat'; N / 2; i
        CALL IBWRT(dvm%, 'XRDGS 400, 8192 INTO OUT')
        CALL IBWRT(dvm%, 'VREAD OUT')
        filename$ = 'c:\steve\dat\FREQ' + LTRIM$(STR$(i)) + '.DAT'
        CALL IBRDF(dvm%, filename$)
    NEXT i
    CALL IBWRT(dvm%, 'DISP ON;RST; CLR')
    ' read in hot wire data from temporary storage

    k = 0

    FOR j = 0 TO 3
        infile$ = 'c:\steve\dat\freq' + LTRIM$(STR$(j)) + '.DAT'
        LOCATE 8, 7: PRINT USING 'reading in raw X-wire data from &'; infile$
        OPEN infile$ FOR INPUT AS #1
        FOR i = 1 TO N / 4
    k = k + 1
    INPUT #1, E1(k), E2(k)
        NEXT i
        CLOSE #1
    NEXT j
    ' write anemometer voltages to hard disk in binary files
```

```basic
e1file$ = "c:\steve\dat\" + file$ + "e1.dat"
e2file$ = "c:\steve\dat\" + file$ + "e2.dat"
LOCATE 10, 7: PRINT "writing data in binary files"
LOCATE 12, 7: PRINT USING "writing files & and &"; e1file$; e2file$
OPEN e1file$ FOR BINARY AS #1
OPEN e2file$ FOR BINARY AS #2

' remove the IFA gain and offset
gain = 10!: offset = 1!
FOR i = 1 TO N
    E1(i) = E1(i) / gain + offset
    E2(i) = E2(i) / gain + offset
    PUT #1, , E1(i)
    PUT #2, , E2(i)
NEXT i
CLOSE #1
CLOSE #2
' print the first 5 and last 5 entries for E1 and E2
CLS
LOCATE 3, 7: PRINT "    E1          E2": PRINT
FOR i = 1 TO 5
    PRINT USING "##### ##.####  ##### ##.####"; i; E1(i); i; E2(i)
NEXT i
FOR i = N - 4 TO N
    PRINT USING "##### ##.####  ##### ##.####"; i; E1(i); i; E2(i)
NEXT i
LOCATE 20, 7: INPUT "press ENTER to return to the Main Menu"; ans$
END SUB
```

F-18

Subroutine VSET

```
DEFSNG I-M
      SUB VSET (dvm%, Ttunnel)
      ' This program displays the sum of the X-wire voltages and the U and V
      ' components of velocity.  Maximizing the sum of the voltages or zeroing
      ' the V component of the velocity ensures that the bisector is aligned
      ' with the mean velocity vector.
      DIM B0(2), B1(2)

      ' initialize the screen

      COLOR 3, 0
      CLS
      LOCATE 3, 20: PRINT "X-WIRE ALIGNMENT PROGRAM"
      PRINT : PRINT "The X-WIRE bisector is aligned with the mean velocity"
      PRINT "vector when the sum of the x-wire voltages (below) is maximized"
      VIEW PRINT 8 TO 24

      ' read in the hot-wire calibration constants

      OPEN "c:\steve\cal\xwirecal.cof" FOR INPUT AS #1
      FOR j = 1 TO 2
         INPUT #1, B0(j), B1(j)
      NEXT j

      ' compute current air density, rho!
      rholow! = 1.3947: drho! = .4666: Tlow! = 23.15: dTemp! = 100!
      rho! = rholow! - drho! * (Ttunnel + Tlow!) / dTemp!

      ' initialize the HP3852

      CALL IBWRT(dvm%, "RST; CLR")
      CALL IBWRT(dvm%, "DISP OFF")

      DO

         ' take the x-wire voltage readings (100 readings per channel)

         CALL IBWRT(dvm%, "RST 400")
         CALL IBWRT(dvm%, "USE 400")
         CALL IBWRT(dvm%, "REAL WAVE(199), CHAN1(99), CHAN2(99)")
         CALL IBWRT(dvm%, "REAL L1,L2,H1,H2,AV1,AV2,S1,S2")
         CALL IBWRT(dvm%, "SCANMODE ON;CONF DCV;ARMODE BEFORE")
         CALL IBWRT(dvm%, "TERM RIBBON;RANGE 9;RDGSMODE COMPLETE")
         CALL IBWRT(dvm%, "PRESCAN 100; POSTSCAN 0")
         CALL IBWRT(dvm%, "SPER 0.001")
         CALL IBWRT(dvm%, "STTRIG INT")
         CALL IBWRT(dvm%, "CLWRITE SENSE,321-322;ASCAN ON;AZERO ONCE;SCTRIG INT")
         CALL IBWRT(dvm%, "XRDGS 400, 200 INTO WAVE")

         ' separate the WAVE array into 2 arrays

         CALL IBWRT(dvm%, "SUB SEPARAT")
         CALL IBWRT(dvm%, "INTEGER I,J")
         CALL IBWRT(dvm%, "J = 0")
         CALL IBWRT(dvm%, "FOR I = 0 TO 199 STEP 2")
         CALL IBWRT(dvm%, "CHAN1(J) = WAVE(I)")
         CALL IBWRT(dvm%, "CHAN2(J) = WAVE(I+1)")
         CALL IBWRT(dvm%, "J = J+1")
         CALL IBWRT(dvm%, "NEXT I")
         CALL IBWRT(dvm%, "SUBEND")
         CALL IBWRT(dvm%, "CALL SEPARAT")

         ' take the mean of the 100 readings

         CALL IBWRT(dvm%, "stat L1,H1,AV1,S1,CHAN1")
         CALL IBWRT(dvm%, "stat L2,H2,AV2,S2,CHAN2")
         rd$ = SPACE$(16)
         CALL IBWRT(dvm%, "vread AV1")
         CALL IBRD(dvm%, rd$)
         E1 = VAL(rd$)
```

F-19

```
CALL IBWRT(dvm%, 'vread AV2')
CALL IBRD(dvm%, rd$)
E2 = VAL(rd$)

CALL IBWRT(dvm%, 'SCTRIG HOLD')
CALL IBWRT(dvm%, 'RST; CLR')

' remove the IFA100 gain and offset

gain = 10!: offset = 1!
tempE1 = E1
tempE2 = E2
E1 = E1 / gain + offset
E2 = E2 / gain + offset
' calculate wire effective velocities
E1 = ((E1 ^ 2 - B0(1)) / B1(1)) ^ 2.22
E2 = ((E2 ^ 2 - B0(2)) / B1(2)) ^ 2.22
' calculate velocities in wire coordinates, then lab coordinates
k = .15
PI = 3.1416
mu = PI / 4
XX = (E1 ^ 2 - (k * E2) ^ 2) / (1! - k ^ 4)
IF XX < 0! THEN XX = X ^ 2
X = SQR(XX)
YY = (E2 ^ 2 - (k * E1) ^ 2) / (1! - k ^ 4)
IF YY < 0! THEN YY = Y ^ 2
Y = SQR(YY)
U = COS(mu) * X + SIN(mu) * Y
V = -SIN(mu) * X + COS(mu) * Y

 PRINT USING 'E1 + E2 = ##.####  U = +##.###  V = +##.###'; (E1 + E2); U; V

LOOP UNTIL INKEY$ <> ''

CALL IBWRT(dvm%, 'DISP ON; RST; CLR')
VIEW PRINT: CLS
END SUB
```

3. Data Reduction Software

PREDUCE.BAS

```
' PREDUCE.BAS

' This program reads in the pressure voltage readings from the data files
' created by ACQUIRE.BAS and converts them into pressure values using the
' calibration constants stored in PCOEFF.DAT.  This program also creates
' a data file for GRAPHER.
DIM pvolts(28), pressure(28), chord(23), Cp(23)
' initialize screen and input the pressure data file to be reduced

CLS
LOCATE 1, 7: PRINT 'PRESSURE DATA REDUCTION PROGRAM'
LOCATE 3, 7:
INPUT 'Enter the 4 letter file designator'; file$

' read in the pressure calibration coefficients
LOCATE 5, 7: PRINT 'reading in the pressure calibration coefficients'
OPEN 'e:\steve\cal\PCOEFF.dat' FOR INPUT AS #1
INPUT #1, m, b
PRINT USING 'the calibration curve is P = ##.####V + ##.#####'; m; b
CLOSE #1
INPUT '     press ENTER to continue'; ans$
' read in the pressure voltage readings
PRINT
PRINT USING 'reading in the voltage readings from &pv.dat'; file$
PRINT
OPEN 'e:\steve\htxfer\pressure\' + file$ + 'pv.dat' FOR INPUT AS #1
FOR i = 0 TO 28
    INPUT #1, pvolts(i)
    PRINT USING 'port ##  voltage = ###.###### volts'; i; pvolts(i)
NEXT i
INPUT #1, Ttunnel
PRINT : PRINT USING 'Ttunnel = ###.#### degC'; Ttunnel
CLOSE #1
INPUT '     press ENTER to continue'; ans$
' convert the voltage readings into kPa pressures
PRINT : PRINT 'converting the voltages to pressures'
PRINT
FOR i = 0 TO 28
    pressure(i) = (m * pvolts(i)) + b
    PRINT USING '   port ##    P = ###.##### Kpa'; i; pressure(i)
NEXT i
INPUT '     press ENTER to continue'; ans$
' write the pressures to a data file for permanent storage
PRINT : PRINT 'writing the pressures to &p.dat'
OPEN 'e:\steve\htxfer\pressure\' + file$ + 'p.dat' FOR OUTPUT AS #1
PRINT #1, USING '     the calibration for this data is P(kPa) = ##.#####V(volts) + ##.#####)'; m; b
FOR i = 0 TO 28
    PRINT #1, USING '   ##   ##.#######   ##.######'; i; pvolts(i); pressure(i)
NEXT i

' calculate the tunnel q, deltah, and velocity
q = pressure(26) - pressure(28)
rho = (101.3 + pressure(28)) / (.28708 * (Ttunnel + 273.15))
deltah = q * 1000! / 249!
vel! = SQR(2000! * q / rho)

' print the velocity information to a file

PRINT #1, "
PRINT
PRINT #1, USING '    the tunnel q is    ###.####### kPa'; q
PRINT USING '    the tunnel q is    ###.####### kPa'; q
PRINT #1, USING '    the tunnel deltah is   ###.####### in H2O'; deltah
PRINT USING '    the tunnel deltah is  ###.####### in H2O'; deltah
PRINT #1, USING '    the tunnel velocity is ###.####### m/s'; vel!
PRINT USING '    the tunnel velocity is ###.####### m/s'; vel!
CLOSE #1
INPUT '     press ENTER to continue'; ans$
```

```
' "collapse the vector" by eliminating atmospheric pressure readings
PRINT
FOR i = 1 TO 10
    PRINT USING '     tap ##    P = ###.#### Kpa'; i; pressure(i)
NEXT i
FOR i = 11 TO 20
    pressure(i) = pressure(i + 1)
    PRINT USING '     tap ##    P = ###.#### Kpa'; i; pressure(i)
NEXT i
FOR i = 21 TO 23
    pressure(i) = pressure(i + 2)
    PRINT USING '     tap ##    P = ###.#### Kpa'; i; pressure(i)
NEXT i
INPUT '      press ENTER to continue'; ans$
' calculate the blade surface pressure coefficients (Cp)
PRINT : PRINT 'calculating Cps'
FOR i = 1 TO 23
    Cp(i) = (pressure(i) - pressure(28)) / q
    PRINT USING 'tap ##  Cp = ###.#####'; i; Cp(i)
NEXT i
' writing the chord locations and the Cps to the GRAPHER file
LOCATE 15, 7: PRINT 'writing the chord locations and Cps to &pgr.dat'; file$
OPEN 'e:\steve\chord.dat' FOR INPUT AS #1
OPEN 'e:\steve\htxfer\pressure\' + file$ + 'pgr.dat' FOR OUTPUT AS #2
FOR i = 1 TO 23
    INPUT #1, chord(i)
    PRINT #2, USING '#.########  ,  ###.########'; chord(i); Cp(i)
NEXT i
CLOSE #1
CLOSE #2
END
```

TREDUCE.BAS

```
' TREDUCE.BAS

' This program reads in the temperature readings from the data files
'  created by ACQUIRE.BAS and converts them into chord representative values
DIM temp(30), chord(23)
' initialize the screen

CLS
LOCATE 1, 7: PRINT 'TEMPERATURE DATA REDUCTION PROGRAM'
LOCATE 3, 7:
10    INPUT 'Enter the 4 letter file designator'; file$

' read in the temperature readings
PRINT
PRINT USING 'reading in the temperature readings from &&t.dat'; file$
PRINT
OPEN 'e:\steve\htxfer\temp\' + file$ + 't.dat' FOR INPUT AS #1
FOR i = 1 TO 30
   INPUT #1, temp(i)
   PRINT USING 'tc ##  temp = ###.###### degC'; i; temp(i)
NEXT i
CLOSE #1
INPUT '    press ENTER to continue'; ans$
' writing the chord locations and the temperatures to the GRAPHER file
LOCATE 15, 7: PRINT 'writing the chord locations and temps to &pgr.dat'; file$
OPEN 'e:\steve\chord.dat' FOR INPUT AS #1
OPEN 'e:\steve\htxfer\temp\' + file$ + 'tgr.dat' FOR OUTPUT AS #2
FOR i = 1 TO 23
   INPUT #1, chord(i)
   PRINT #2, USING '#.########  ,  ###.########'; chord(i); temp(i)
NEXT i
CLOSE #1
CLOSE #2
GOTO 10
END
```

HTXFER.BAS

HTXFER.BAS

'This program calculates the blade heat transfer

```basic
DECLARE SUB PREDUCE (file$, Uinf, Cp(), pressure(), q)

DIM visc(23) AS SINGLE
DIM Tscan(30) AS SINGLE
DIM deltal(23) AS SINGLE
DIM deltaT(23) AS SINGLE
DIM resistivity(23) AS SINGLE
DIM Cp(23) AS SINGLE
DIM pressure(28) AS SINGLE
DIM rho(23) AS SINGLE
DIM mu(23) AS SINGLE
DIM vel(23) AS SINGLE
DIM Re(23) AS SINGLE
DIM s(23) AS SINGLE
DIM h(23) AS SINGLE
DIM Nu(23) AS SINGLE
DIM Nutheorl(23) AS SINGLE
DIM Nutheort(23) AS SINGLE
DIM St(23) AS SINGLE
DIM Sttheorl(23) AS SINGLE
DIM Sttheort(23) AS SINGLE
DIM chord(23) AS SINGLE
DIM K(23) AS SINGLE
DIM fltpltl(23) AS SINGLE
DIM fltpltt(23) AS SINGLE


DEFINT I-J
' read in thermocouple distances along the blade surface S() for local calculations
    OPEN 'e:\steve\dat\SNEW.dat' FOR INPUT AS #1
    FOR i = 1 TO 23: INPUT #1, s(i): NEXT i
    CLOSE #1

' read in the chord positions of the thermocouples and pressure taps

    OPEN 'e:\steve\dat\chord.dat' FOR INPUT AS #1
    FOR i = 1 TO 23: INPUT #1, chord(i): NEXT i
    CLOSE #1
' read in the deltal distances between the surface thermocouples and the
' internal thermocouples for the conduction calculations
    OPEN 'e:\steve\dat\DELTAL.DAT' FOR INPUT AS #1
    FOR i = 1 TO 23
        INPUT #1, deltal(i)
    NEXT i
    CLOSE #1

' main loop

    FOR alpha = 1 TO 4
    FOR test = 1 TO 6
    file$ = 'hx' + LTRIM$(STR$(alpha)) + LTRIM$(STR$(test))
    CLS : PRINT USING 'processing data file &'; file$
' read the blade temperatures and current from storage
    OPEN 'e:\steve\htxfer\temp\' + file$ + 't.dat' FOR INPUT AS #1
    FOR i = 1 TO 30
        INPUT #1, Tscan(i)
    NEXT i
    INPUT #1, Curr!
    CLOSE #1

    Tinf! = Tscan(30)       'Use tunnel temperature as Tfreestream
' print the blade temperatures and power to the screen
    PRINT USING 'tunnel temp = ###.### degC'; Tinf!
    PRINT : PRINT '  i      degC      i      degC'
    FOR i = 1 TO 15
        PRINT USING '  ##    ###.###    ##    ###.###'; i; Tscan(i); i + 15; Tscan(i + 15)
    NEXT i
    PRINT : PRINT USING 'the blade current is ##.## amps'; Curr!
'    INPUT 'press enter to continue'; ans$
```

```
' read in the Pressure Coefficients on the blade to be used in computation of

    CALL PREDUCE(file$, Vinf!, Cp(), pressure(), q)
' Construct deltaT(i), the internal temp differences

    FOR i = 1 TO 3
            deltaT(i) = Tscan(i) - Tscan(24)
    NEXT i

    FOR i = 22 TO 23
            deltaT(i) = Tscan(i) - Tscan(24)
    NEXT i

    deltaT(4) = Tscan(4) - Tscan(25)
    deltaT(5) = Tscan(5) - Tscan(26)
    deltaT(6) = Tscan(6) - (Tscan(25) + Tscan(26) + Tscan(15)) / 3!
    deltaT(7) = Tscan(7) - Tscan(27)
    deltaT(8) = Tscan(8) - Tscan(28)
    deltaT(9) = Tscan(9) - Tscan(12)
    deltaT(10) = Tscan(10) - Tscan(12)
    deltaT(11) = Tscan(11) - Tscan(28)
    deltaT(12) = Tscan(12) - Tscan(9)
    deltaT(13) = Tscan(13) - Tscan(28)
    deltaT(14) = Tscan(14) - (Tscan(27) + Tscan(28) + Tscan(7)) / 3!
    deltaT(15) = Tscan(15) - Tscan(27)
    deltaT(16) = Tscan(16) - (Tscan(26) + Tscan(27) + Tscan(6)) / 3!
    deltaT(17) = Tscan(17) - Tscan(26)
    deltaT(18) = Tscan(18) - Tscan(26)
    deltaT(19) = Tscan(19) - .5 * (Tscan(25) + Tscan(26))
    deltaT(20) = Tscan(20) - .5 * (Tscan(25) + Tscan(26))
    deltaT(21) = Tscan(21) - Tscan(25)
'   compute the local viscosities visc(i) on the blade
'   the density rho(i) determined from the ideal gas law and viscosity mu(i)
'   is determined from its linearity over a wide range of pressures
'   all calculations are based on Tavg = (Tlocal + Tinf)/2
    FOR i = 1 TO 23
    rho(i) = (101.3 + pressure(i)) / (.28708 * ((Tscan(i) + Tinf) / 2 + 273.15))
    mu(i) = 4.136E-06 + ((Tscan(i) + Tinf) / 2! + 273.15) * 4.76E-08
    visc(i) = mu(i) / rho(i)
    NEXT i
' compute local velocities vel(i) on the blade (m/s)
    FOR i = 1 TO 23
            vel(i) = SQR((2 * 1000 * q * ABS(1! - Cp(i))) / rho(i))
    NEXT i
' compute local Reynolds numbers on the blade (based on distance from leading edge).

    FOR i = 1 TO 2             'Use Stagnation on Round-nose Blunt body
            rad = .005             'radius of blunt nose, m
            Re(i) = 2 * Vinf * rad / visc(i)
    NEXT i

    FOR i = 3 TO 23
            Re(i) = vel(i) * s(i) / visc(i)
    NEXT i
' compute local resistivity of the foil in ohm-m

    FOR i = 1 TO 23
            resistivity(i) = 2.223 * 10 ^ -10 * (Tscan(i) * 1.8 + 32) + 8.446 * 10 ^ -7
    NEXT i
'   conduction constants
    uk! = .026         'urethane foam thermal conductivity, (W/m*K)
    ak! = .0263        'air thermal conductivity (W/m*K) at 30 C
'   convection constants

    Cp! = 1005.7       'for air at 30 C, (J/kg*K)
    Pr! = .707
'   radiation constants
    eps! = .17         'emissivity for polished stainless steel at 300 K
    sigma! = 5.67E-08   'Stefan-Boltzmann constant, (W/m^2*K^4)
' compute the Nusselt and Stanton numbers for the blade, using
'   steady-state 2-D heat model (ignore spanwise and chordwise heat
'   conduction through the steel foil as << heat convection).
```

```
ATot! = .013387   'area of foil = 0.26352 m x 0.0508 m)

denoml = 0
denomt = 0
FOR i = 1 TO 10                              'Pressure side
    Qc! = uk! * deltaT(i) / deltal(i)
    Qr! = eps! * sigma! * (Tscan(i) ^ 4 - Tinf! ^ 4)
    delT! = (Tscan(i) - Tinf!)
    Qheat! = Curr! ^ 2 * resistivity(i) * 7628 * 10 ^ 3        'W/m^2
    h(i) = (Qheat! - Qc! - Qr!) / delT!
    Nu(i) = ABS(h(i)) * s(i) / ak!
    St(i) = Nu(i) / (Pr! * Re(i))
' also calculate the theoretical St# and Nu# by Kays equs 9-50 and 12-32

    IF i = 1 OR i = 2 THEN GOTO 10
    denoml = denoml + ((rho(i) * vel(i)) ^ 1.87 * (s(i) - s(i - 1)))
    Sttheorl(i) = (.418 * mu(i) ^ .5 * (rho(i) * vel(i)) ^ .435) / denoml ^ .5
    Nutheorl(i) = Sttheorl(i) * Pr * Re(i)

    denomt = denomt + (((Tscan(i) - Tinf) ^ 1.25) * vel(i) * (s(i) - s(i - 1)))
    Sttheort(i) = (.0287 * Pr ^ -.4 * ((Tscan(i) - Tinf) ^ .25) * visc(i) ^ .2) / denomt ^ .2
    Nutheort(i) = Sttheort(i) * Pr * Re(i)

    K(i) = (visc(i) / vel(i) ^ 2) * ((vel(i) - vel(i - 1)) / (s(i) - s(i - 1)))
10    NEXT i
' the theoretical calculations for node 1
    denoml = (rho(1) * vel(1)) ^ 1.87 * (s(1) - s(2))
    Sttheorl(1) = (.418 * mu(1) ^ .5 * (rho(1) * vel(1)) ^ .435) / denoml ^ .5
    Nutheorl(1) = Sttheorl(1) * Pr * Re(1)
    denomt = ((Tscan(1) - Tinf) ^ 1.25) * vel(1) * (s(1) - s(2))
    Sttheort(1) = (.0287 * Pr ^ -.4 * ((Tscan(1) - Tinf) ^ .25) * visc(1) ^ .2) / denomt ^ .2
    Nutheort(1) = Sttheort(1) * Pr * Re(1)
    K(1) = (visc(1) / vel(1) ^ 2) * ((vel(1) - vel(2)) / (s(1) - s(2)))
    K(2) = 0!

    FOR i = 1 TO 2        'Use Stagnation on Round-nose Blunt body
'        Nu(i) = .81 * ((Re(i)) ^ .5) * (Pr! ^ .4)
'        St(i) = Nu(i) / (Pr! * Re(i))
        Nu(i) = ABS(h(i)) * s(i) / ak!
        St(i) = Nu(i) / (Pr! * Re(i))
    NEXT i
    FOR i = 1 TO 2
        Re(i) = vel(i) * s(i) / visc(i)
    NEXT i

' Node 11 has no heat generation term since it is off the foil.

    Qc! = uk! * deltaT(11) / deltal(11)
    Qr! = eps! * sigma! * (Tscan(11) ^ 4 - Tinf! ^ 4)
    delT! = (Tscan(11) - Tinf!)
    h(11) = (-Qc! - Qr!) / delT!
    Nu(11) = ABS(h(11)) * s(11) / ak!
    St(11) = Nu(11) / (Pr! * Re(11))
    K(11) = (visc(11) / vel(11) ^ 2) * ((vel(11) - vel(10)) / (s(11) - s(10)))
' the calculations for Node 23
    Qc! = uk! * deltaT(23) / deltal(23)
    Qr! = eps! * sigma! * (Tscan(23) ^ 4 - Tinf! ^ 4)
    delT! = (Tscan(23) - Tinf!)
    Qheat! = Curr! ^ 2 * resistivity(23) * 7628 * 10 ^ 3        'W/m^2
    h(23) = (Qheat! - Qc! - Qr!) / delT!
    Nu(23) = ABS(h(23)) * s(23) / ak!
    St(23) = Nu(23) / (Pr! * Re(23))

    denoml = denoml + ((rho(23) * vel(23)) ^ 1.87 * (s(23) - s(1)))
    Sttheorl(23) = (.418 * mu(23) ^ .5 * (rho(23) * vel(23)) ^ .435) / denoml ^ .5
    Nutheorl(23) = Sttheorl(23) * Pr * Re(23)

    denomt = denomt + (((Tscan(23) - Tinf) ^ 1.25) * vel(23) * (s(23) - s(1)))
    Sttheort(23) = (.0287 * Pr ^ -.4 * ((Tscan(23) - Tinf) ^ .25) * visc(23) ^ .2) / denomt ^ .2
    Nutheort(23) = Sttheort(23) * Pr * Re(23)

    K(23) = (visc(23) / vel(23) ^ 2) * ((vel(23) - vel(1)) / (s(23) - s(1)))

    FOR i = 22 TO 12 STEP -1                      'Suction side
        Qc! = uk! * deltaT(i) / deltal(i)
```

```basic
        Qrl = eps! * sigma! * (Tscan(i) ^ 4 - Tinf! ^ 4)
        delT! = (Tscan(i) - Tinf!)
        Qheat! = Curr! ^ 2 * resistivity(i) * 7628 * 10 ^ 3        'W/m^2
        h(i) = (Qheat! - Qcl - Qrl) / delT!
        Nu(i) = ABS(h(i)) * s(i) / ak!
        St(i) = Nu(i) / (Pr! * Re(i))

        denoml = denoml + ((rho(i) * vel(i)) ^ 1.87 * (s(i) - s(i + 1)))
        Sttheorl(i) = (.418 * mu(i) ^ .5 * (rho(i) * vel(i)) ^ .435) / denoml ^ .5
        Nutheorl(i) = Sttheorl(i) * Pr * Re(i)

        denomt = denomt + (((Tscan(i) - Tinf) ^ 1.25) * vel(i) * (s(i) - s(i + 1)))
        Sttheort(i) = (.0287 * Pr ^ -.4 * ((Tscan(i) - Tinf) ^ .25) * visc(i) ^ .2) / denomt ^ .2
        Nutheort(i) = Sttheort(i) * Pr * Re(i)

        K(i) = (visc(i) / vel(i) ^ 2) * ((vel(i) - vel(i + 1)) / (s(i) - s(i + 1)))

    NEXT i
    ' calculate the flat plate Nu# for comparison purposes

    FOR i = 1 TO 23
        fltpltl(i) = .453 * Re(i) ^ .5 * .88917
        fltpltt(i) = .030784 * Re(i) ^ .8 * .88917
    NEXT i
' save data on disk

    OPEN "e:\steve\htxfer\temp\red" + file$ + ".dat" FOR OUTPUT AS #1
    PRINT #1, "Heat transfer results for run"; SPC(1); file$
    PRINT #1, USING "Electrical energy input = ####.# watts"; Qheat!
    PRINT #1, USING "Uinf = ##.# m/s"; Vinf!
    PRINT #1, " "
    PRINT #1, "Tap s/c   Re#      K    h   Nu#   Nutl   Nutt  Nufpl  Nufpt"
    FOR i = 1 TO 23
        PRINT USING "## #.## ##.##^^^^ ##.##^^^^ ####.# ####.# ####.## ####.# ####.#
####.# ####.#"; i; s(i) / .1143; Re(i); K(i); h(i); Nu(i); Nutheorl(i); Nutheort(i); fltpltl(i); fltpltt(i)
        PRINT #1, USING "## #.## ##.##^^^^ ##.##^^^^ ####.# ####.# ####.## ####.# ####.#
####.# ####.#"; i; s(i) / .1143; Re(i); K(i); h(i); Nu(i); Nutheorl(i); Nutheort(i); fltpltl(i); fltpltt(i)
    NEXT i
    CLOSE #1
' write the nusslet plot files "nsltHX__.dat"

'       file$ = "NsltHX" + LTRIM$(STR$(alpha)) + LTRIM$(STR$(test))
'       OPEN dir$ + file$ + ".dat" FOR OUTPUT AS #1
'       FOR i = 8 TO 2 STEP -1
'           PRINT #1, USING "##.#### , ##.##^^^^, ####.#, ####.#, ####.#, ####.# , ####.#"; -s(i) /
.1143; Re(i); Nu(i); Nutheorl(i); Nutheort(i); fltpltl(i); fltpltt(i)
'           NEXT i

' print the suction side numbers 1, 23 - 13

'       FOR i = 1 TO 1
'           PRINT #1, USING "##.#### , ##.##^^^^, ####.#, ####.#, ####.#, ####.# , ####.#"; s(i) /
.1143; Re(i); Nu(i); Nutheorl(i); Nutheort(i); fltpltl(i); fltpltt(i)
'           NEXT i

'       FOR i = 23 TO 13 STEP -1
'           PRINT #1, USING "##.#### , ##.##^^^^, ####.#, ####.#, ####.#, ####.# , ####.#"; s(i) /
.1143; Re(i); Nu(i); Nutheorl(i); Nutheort(i); fltpltl(i); fltpltt(i)
'           NEXT i
'           CLOSE #1
' write the h plot files "HHX__.dat"

'       file$ = "KHX" + LTRIM$(STR$(alpha)) + LTRIM$(STR$(test))
'       OPEN dir$ + file$ + ".dat" FOR OUTPUT AS #1
'       FOR i = 8 TO 2 STEP -1
'           PRINT #1, USING "##.### , ##.##^^^^"; -s(i) / .1143; K(i)
'           NEXT i
"
"  print the suction side numbers 1, 23 - 13

'       FOR i = 1 TO 1
'           PRINT #1, USING "##.#### , ##.##^^^^"; s(i) / .1143; K(i)
'           NEXT i

'       FOR i = 23 TO 13 STEP -1
```

```
'          PRINT #1, USING '##.### , ##.##^ ^ ^ ^'; s(i) / .1143; K(i)
'          NEXT i
'
'
'          CLOSE #1
'
'          INPUT 'press ENTER to continue'; ans$
        NEXT test
        NEXT alpha
        END


DEFINT K-L
SUB PREDUCE (file$, Uinf, Cp(), pressure(), q)

    DIM pvolts(28)

    OPEN 'e:\steve\cal\PCOEFF.dat' FOR INPUT AS #1
    INPUT #1, m, b
    CLOSE #1

    OPEN 'e:\steve\htxfer\pressure\' + file$ + 'pv.dat' FOR INPUT AS #1
    FOR i = 0 TO 28
        INPUT #1, pvolts(i)
    NEXT i
    INPUT #1, Ttun
    CLOSE #1
' convert the voltage readings into kPa pressures
    FOR i = 0 TO 28
        pressure(i) = (m * pvolts(i)) + b
    NEXT i
' calculate the tunnel q, deltah, and velocity
    q = pressure(26) - pressure(28)

    density = (101.3 + pressure(28)) / (.28708 * (Ttun + 273.15))

    deltah = q * 1000! / 249!

    Uinf = SQR(2000! * q / density)

' 'collapse the vector' by eliminating atmospheric pressure readings
    FOR i = 11 TO 20
        pressure(i) = pressure(i + 1)
    NEXT i
    FOR i = 21 TO 23
        pressure(i) = pressure(i + 2)
    NEXT i
' calculate the blade surface pressure coefficients (Cp)
    PRINT : PRINT 'calculating Cps'
    FOR i = 1 TO 23
        Cp(i) = (pressure(i) - pressure(28)) / q
        PRINT USING 'pressure## = ##.### kPa  CP## = ##.###'; i; pressure(i); i; Cp(i)
    NEXT i
    PRINT USING 'Vinf = ##.# m/s'; Uinf
'   INPUT 'press Enter to continue'; ans$
    END SUB
```

VELREDUC.BAS

```
' VELREDUC.BAS
' This program reduces the binary-stored fluctuation data
DECLARE SUB PLOT (nplot!, xmin!, xmax!, ymin!, ymax!, c0!(), C1!(), C2!())
DECLARE SUB STATS (N!, E1!(), E2!(), MEAN!(), STDDEV!())
DECLARE SUB REDUCE (N, E1(), E2(), ufile$, vfile$, calfile$)
DECLARE SUB RealFT (dat(), N, ISIGN%)
DECLARE SUB Four1 (dat(), NN, ISIGN%)
DECLARE SUB SCALES (E1(), E2(), N, MEAN!(), STDDEV!(), MICRO!(), INTEGRAL!(), df)
DEFINT I-J
'Main Program Block
        '$DYNAMIC

'       outfile$ = "e:\steve\htxfer\turb\hxturbb.dat"
        calfile$ = "e:\steve\cal\044_84b.cof"
'       OPEN outfile$ FOR APPEND AS #5

        N = 8192                'samples
        fsample = 20000!          'hertz
        dt = 1 / fsample          'seconds
        df = fsample / N          'hertz
        nbins = 1024

        DIM E1(16384), E2(16384), frequ(16384)
        DIM MEAN(2), STDDEV(2), MICRO(2), INTEGRAL!(2)
        DIM uspec(nbins), vspec(nbins), freq(nbins)
        DIM c0(nbins), C1(nbins), C2(nbins)

'       FOR test = 1 TO 6

        run$ = "hx14" + LTRIM$(STR$(test))
        ufile$ = "a:\turb\" + run$ + "e1.dat"  'these files are the binary raw
        vfile$ = "a:\turb\" + run$ + "e2.dat"  'X-wire voltage files from VELACQ.

' read in the x-wire voltages and converted to velocities

        CALL REDUCE(N, E1(), E2(), ufile$, vfile$, calfile$)
        CALL STATS(N, E1(), E2(), MEAN(), STDDEV())
' plot the first 100 u' and v'

'       nplot = 100
'       xmin = 0: xmax = nplot
'       ymin = -.25 * MEAN(1): ymax = -ymin
'       FOR i = 1 TO nplot
'           c0(i) = i
'           C1(i) = E1(i)
'           C2(i) = E2(i)
'       NEXT i
'       CALL PLOT(nplot, xmin, xmax, ymin, ymax, c0(), C1(), C2())

' obtain the FFT and energy spectrum and stored the FFT values in E1 and E2

        PRINT : PRINT "     performing FFT on u1' and ";
        halfn = N / 2
        CALL RealFT(E1(), halfn, 1)

' calculate the right side of Parseval's theorem.

        sumcheck = 2 * E1(1) ^ 2 + 2 * E1(2) ^ 2
        FOR i = 3 TO N - 1 STEP 2
        sumcheck = sumcheck + 2 * (E1(i) ^ 2 + E1(i + 1) ^ 2)
        NEXT i
        sumcheck = sumcheck / (N + 1)
        PRINT USING "the right side of Parseval's = ##.###^^^^"; sumcheck

'   use Parseval's Theorem to obtain E (n) from H(u')
'                             u'
        freq(0) = 0
        E1(0) = (2 * (E1(1) ^ 2 / N) ^ 2) / df
        FOR i = 3 TO halfn + 1          'frequ(i) are the discrete Freqs
        j = 2 * (i - 2) + 1             'E1(i) are the spectral energies
        frequ(i - 2) = (i - 2) * df
        E1(i - 2) = 2 * ((SQR(E1(j) ^ 2 + E1(j + 1) ^ 2) / N) ^ 2) / df
```

```basic
        NEXT i
        frequ(halfn) = 10000!
        E1(halfn) = (2 * (E1(2) ^ 2 / N) ^ 2) / df
'    PRINT "    performing FFT on u2'"
'    CALL RealFT(E2(), halfn, 1)
'
' use Parseval's Theorem to obtain E  (n)  from H(v')
'                         v'
'    FOR i = 3 TO halfn + 1
'      j = 2 * (i - 2) + 1              'E2(i) are the spectral energies
'      E2(i - 2) = 2 * ((SQR(E2(j) ^ 2 + E2(j + 1) ^ 2) / N) ^ 2) / df
'    NEXT i
'    E2(halfn) = E2(halfn - 1)
'
' calculate the integral of energy over the frequency for comparison to u'^2

        sumcheck = 0
        FOR i = 3 TO halfn + 1
        sumcheck = sumcheck + E1(i - 2)
        NEXT i
        sumcheck = sumcheck * (fsample / N)
        PRINT
        PRINT USING "    The energy integration = ##.########"; sumcheck

' calculate the integral scale and the microscale
        CALL SCALES(E1(), E2(), N, MEAN(), STDDEV(), MICRO(), INTEGRAL!(), df)
        TUINTENS = (((((STDDEV(1) ^ 2 + STDDEV(2) ^ 2) / 2) ^ .5) / MEAN(1)) * 100
'    PRINT #5, USING "& , ###.## , ##.### , #.##### , #.#####"; run$; MEAN(1); TUINTENS; MICRO!(1);
INTEGRAL!(1)
'    NEXT test
'    CLOSE #5
' reduce the energy spectrum file from n points to 256 points
'    nperbin = N / nbins
'    k = 0
'    FOR i = 1 TO nbins / 2
'    uspec(i) = 0!
'    vspec(i) = 0!
'    freq(i) = 0!
'    FOR j = 1 TO nperbin
'        k = k + 1
'        uspec(i) = uspec(i) + E1(k)
'        vspec(i) = vspec(i) + E2(k)
'        freq(i) = freq(i) + frequ(k)
'    NEXT j
'    uspec(i) = uspec(i) / nperbin
'    vspec(i) = vspec(i) / nperbin
'    freq(i) = freq(i) / nperbin
'    NEXT i
'
' plot the spectrum
'
'    xmin = LOG(freq(1)): xmax = LOG(freq(nbins / 2))
'    ymin = LOG(uspec(1) / 10000!): ymax = LOG(10! * uspec(1))
'    FOR i = 1 TO nbins / 2
'        c0(i) = LOG(freq(i))
'        C1(i) = LOG(uspec(i))
'        C2(i) = LOG(vspec(i))
'    NEXT i
'    CALL PLOT(nbins / 2, xmin, xmax, ymin, ymax, c0(), C1(), C2())
'
'    specfile$ = "e:\steve\dat\SPEC.DAT"
'    OPEN specfile$ FOR OUTPUT AS #1
'    FOR i = 1 TO nbins / 2
'        PRINT #1, freq(i), uspec(i), vspec(i)
'    NEXT i
'    CLOSE #1
'
'    OPEN "e:\steve\dat\logplot.dat" FOR OUTPUT AS #1
'    FOR i = 1 TO 256
'    uspec(i) = (uspec(i) * MEAN(1)) / (STDDEV(1) ^ 2 * INTEGRAL!(1))
'    freq(i) = (freq(i) * INTEGRAL!(1)) / MEAN(1)
'    PRINT #1, uspec(i), freq(i)
'    NEXT i
'    CLOSE #1
        END
```

```
REM $STATIC
DEFINT K-M
    SUB Four1 (dat(), NN, ISIGN)

    N = 2 * NN
    j = 1
    FOR i = 1 TO N STEP 2
        IF j > i THEN
            TEMPR = dat(j)
            TEMPI = dat(j + 1)
            dat(j) = dat(i)
            dat(j + 1) = dat(i + 1)
            dat(i) = TEMPR
            dat(i + 1) = TEMPI
        END IF
        m = N / 2
1   IF ((m > 2) AND (j > m)) THEN
        j = j - m
        m = m / 2
        GOTO 1
        END IF
        j = j + m
11  NEXT i
    MMAX = 2
2   IF N > MMAX THEN
        ISTEP = 2 * MMAX
        THETA = 6.28318530717959# / (ISIGN * MMAX)
        WPR = -2# * SIN(.5# * THETA) ^ 2
        WPI = SIN(THETA)
        WR = 1#
        WI = 0#
        FOR m = 1 TO MMAX STEP 2
          FOR i = m TO N STEP ISTEP
            j = i + MMAX
            TEMPR = WR * dat(j) - WI * dat(j + 1)
            TEMPI = WR * dat(j + 1) + WI * dat(j)
            dat(j) = dat(i) - TEMPR
            dat(j + 1) = dat(i + 1) - TEMPI
            dat(i) = dat(i) + TEMPR
            dat(i + 1) = dat(i + 1) + TEMPI
          NEXT i
          WTEMP = WR
          WR = WR * WPR - WI * WPI + WR
          WI = WI * WPR + WTEMP * WPI + WI
        NEXT m
        MMAX = ISTEP
    GOTO 2
    END IF
END SUB



DEFSNG I-M
    SUB PLOT (nplot, xmin, xmax, ymin, ymax, c0(), C1(), C2())
CLS
xmax = xmax - xmin
ymax = ymax - ymin
FOR i = 1 TO nplot
        c0(i) = c0(i) - xmin
        C1(i) = C1(i) - ymin
        C2(i) = C2(i) - ymin
NEXT i
SCREEN 9
LINE (0, 0)-(639, 319), 3, BF
FOR i = 0 TO 10
        Y = (1 - i / 10) * 319
        LINE (0, Y)-(639, Y)
NEXT i
x0 = (c0(1) / xmax) * 639
y0 = (1 - C1(1) / ymax) * 319
y02 = (1 - C2(1) / ymax) * 319
FOR i = 1 TO nplot
        y1 = (1 - C1(i) / ymax) * 319
        y2 = (1 - C2(i) / ymax) * 319
        x1 = (c0(i) / xmax) * 639
```

```
            LINE (x0, y0)-(x1, y1), 5
'       LINE (x0, y02)-(x1, y2)
            y0 = y1
            x0 = x1
            y02 = y2
NEXT i
INPUT "continue"; ans$
SCREEN 0
END SUB



DEFINT I-M
SUB RealFT (dat(), N, ISIGN)
    THETA = 6.28318530717959# / 2# / N
    C1 = .5
    IF ISIGN = 1 THEN
        C2 = -.5
        CALL Four1(dat(), N, 1)
    ELSE
        C2 = .5
        THETA = -THETA
    END IF
    WPR = -2# * SIN(.5# * THETA) ^ 2
    WPI = SIN(THETA)
    WR = 1# + WPR
    WI = WPI
    N2P3 = 2 * N + 3
    FOR i = 2 TO N / 2 + 1
        I1 = 2 * i - 1
        I2 = I1 + 1
        I3 = N2P3 - I2
        I4 = I3 + 1
        WRS = WR
        WIS = WI
        H1R = C1 * (dat(I1) + dat(I3))
        H1I = C1 * (dat(I2) - dat(I4))
        H2R = -C2 * (dat(I2) + dat(I4))
        H2I = C2 * (dat(I1) - dat(I3))
        dat(I1) = H1R + WRS * H2R - WIS * H2I
        dat(I2) = H1I + WRS * H2I + WIS * H2R
        dat(I3) = H1R - WRS * H2R + WIS * H2I
        dat(I4) = -H1I + WRS * H2I + WIS * H2R
        WTEMP = WR
        WR = WR * WPR - WI * WPI + WR
        WI = WI * WPR + WTEMP * WPI + WI
    NEXT i
    IF ISIGN = 1 THEN
        H1R = dat(1)
        dat(1) = H1R + dat(2)
        dat(2) = H1R - dat(2)
    ELSE
        H1R = dat(1)
        dat(1) = C1 * (H1R + dat(2))
        dat(2) = C1 * (H1R - dat(2))
        CALL Four1(dat(), N, -1)
    END IF
END SUB



DEFSNG I-M
SUB REDUCE (N, E1(), E2(), ufile$, vfile$, calfile$)
'
' subroutine to reduce hot wire data
'
        CLS
        REDIM B0(2), B1(2)
'
' read in calibration constants
'
        OPEN calfile$ FOR INPUT AS #1
        FOR i = 1 TO 2
        INPUT #1, B0(i), B1(i)
        NEXT i
```

F-32

```
        CLOSE #1
'
' read in hot wire data
'
        PRINT I    IG '    Reading in Hot Wire Data from &'; ufile$
        i = 0
        OPEN ufile$ FOR BINARY AS #1
        OPEN vfile$ FOR BINARY AS #2
        FOR j = 1 TO N
        i = i + 1
           GET #1, , E1 (j)
           GET #2, , E2(j)
        NEXT j
        CLOSE #1
        CLOSE #2
        NPOINTS = i
'
' calculate wire effective velocities
'
        PRINT : PRINT '    Calculating Wire Effective Velocities'
        FOR i = 1 TO N
        E1(i) = ((E1(i) ^ 2 - B0(1)) / B1(1)) ^ 2.22
        E2(i) = ((E2(i) ^ 2 - B0(2)) / B1(2)) ^ 2.22
        NEXT i
'
' calculate velocities in wire coordinates, then lab coordinates
'
        PRINT : PRINT '    Calculating Velocities'
        k = .15
        pi = 4! * ATN(1!)
        mu = 45!
        mu = (mu / 180!) * pi
        FOR i = 1 TO NPOINTS
        XX = (E1(i) ^ 2 - (k * E2(i)) ^ 2) / (1! - k ^ 4)
        IF XX < 0! THEN XX = X ^ 2
        X = SQR(XX)
        YY = (E2(i) ^ 2 - (k * E1(i)) ^ 2) / (1! - k ^ 4)
        IF YY < 0! THEN YY = Y ^ 2
        Y = SQR(YY)
        U = COS(mu) * X + SIN(mu) * Y
        V = -SIN(mu) * X + COS(mu) * Y
        E1(i) = U
        E2(i) = V
        NEXT i
' U(i) is now stored in E1(i), V(i) in E2(i)
END SUB



DEFINT I-J
SUB SCALES (E1(), E2(), N, MEAN!(), STDDEV!(), MICRO!(), INTEGRAL!(), df)
        sum = 0
        FOR i = 3 TO (N / 2) + 1
        sum = sum + ((i - 2) ^ 2) * E1(i - 2)
        NEXT i
        sum = sum * df ^ 3
        MICRO(1) = SQR(1 / ((sum * 2 * 3.14 ^ 2) / (MEAN!(1) ^ 2 * STDDEV!(1) ^ 2)))

        sum = 0
        FOR i = 3 TO 12
           sum = sum + E1(i - 2)
        NEXT i
        sum = sum / 10

        INTEGRAL!(1) = (MEAN!(1) / (4! * STDDEV!(1) ^ 2)) * sum
        PRINT
        PRINT USING '    the microscale    = #.######### m'; MICRO!(1)
        PRINT USING '    the integral scale = #.######### m'; INTEGRAL!(1)

'    INPUT 'press ENTER to continue'; ans$
END SUB
```

```
DEFSNG I-J
     SUB STATS (N, E1(), E2(), MEAN(), STDDEV())

' calculate the means of u' and v'
     PRINT : PRINT '     Calculating Mean and Standard Deviation'
     MEAN(1) = 0!
     MEAN(2) = 0!
     FOR i = 1 TO N
     MEAN(1) = MEAN(1) + E1 (i)
     MEAN(2) = MEAN(2) + E2(i)
     NEXT i
     MEAN(1) = MEAN(1) / N
     MEAN(2) = MEAN(2) / N

' calculate the standard deviations of u' and v' and remove the mean for FFT
     STDDEV(1) = 0!
     STDDEV(2) = 0!
     FOR i = 1 TO N
     E1(i) = E1 (i) - MEAN(1)           'removing mean for u'
     E2(i) = E2(i) - MEAN(2)           'removing mean for v'
     STDDEV(1) = STDDEV(1) + E1(i) ^ 2
     STDDEV(2) = STDDEV(2) + E2(i) ^ 2
     NEXT i
     STDDEV(1) = SQR(STDDEV(1) / N)
     STDDEV(2) = SQR(STDDEV(2) / N)

     PRINT : PRINT '     mean  std dev'
     FOR i = 1 TO 2
     PRINT USING '     +##.### +##.###'; MEAN(i); STDDEV(i)
     NEXT i

' calculate u'^2 mean to compare to the energy integral.
     sumcheck = 0
     FOR i = 1 TO N
     sumcheck = sumcheck + E1(i) ^ 2
     NEXT i
     sumcheck = sumcheck / N
     PRINT : PRINT USING '    u'^2 mean = ###.########  and '; sumcheck;

' calculate the left side of Parseval's theorem

     sumcheck = sumcheck * N
     PRINT USING 'the left side of Parseval's = ##.###^ ^ ^ ^'; sumcheck
END SUB
```

Detailed pressure transducer and x-wire calibration procedures are listed below, complete with example calibration results.

<u>Pressure Transducer Calibration</u>. The Scanivalve calibration setup is illustrated in Figure G1. Pressure is applied to Scanivalve using shop air and vacuum is applied using a vacuum hand pump. The "known" pressure is measured with a King Instruments 25" water manometer with 1.5 digits of accuracy.

Once executed, the PRESSCAL.bas pressure transducer calibration program prompts the user to trigger a voltage reading and input the associated pressure in inches of water ($inches\,H_2O$). The program converts $inches\,H_2O$ to kPa, the units required for data reduction. After all the calibration data is collected, it must be to a straight line using any curve fitting technique. The calibration steps are listed below:

1. connect the Scanivalve as shown in figure G1;

2. execute the PRESSCAL.bas program and follow the program prompts;

3. starting with atmospheric pressure, record the pressure transducer pressure and voltage using the PRESSCAL program;

4. increment the pressure and record the voltages;

5. once the upper limit of the pressure transducer range is reached, increment back down to atmospheric, recording the voltages;

6. repeat steps 3 - 5 for vacuum;

7. after recording the pressures and voltages, use any straight line curve fitting technique to determine the intercept and slope of the linear pressure transducer voltage / pressure relationship and write the constants to a files.

Using a +/- 2 psi pressure transducer, the calibration curve generated for this experiment is shown in Figure G2. The curve demonstrates the linearity of the pressure transducer over the operational range.

X-wire Calibration. The X-wires for this experiment are calibrated with known velocities generated with a standard calibration tank, illustrated in Figure G3. Shop air enters the tank, passes through baffles into the stilling chamber, then passes through a low-loss nozzle, exiting to atmosphere in a uniform jet. The low-loss/isentropic nozzle insures that total pressure will be conserved and the jet velocity V_j can be calculated based on the tank pressure:

$$V_j = \left(2 \frac{P_T - P_j}{\rho_j} \right)^{1/2}$$

where P_T is the tank pressure

P_j is the pressure of the jet

ρ_j is the density of the jet

For this calibration configuration, P_j is atmospheric pressure and ρ_j is calculated from the ideal gas law based on P_j and the tank air temperature. The tank air temperature is measured by the data acquisition system and the tank pressure is measured by the user with a 20" Miriam Micromanometer with 4 digits of accuracy. The user enters the tank pressure in $inches\,H_2O$ and the calibration program calculates V_j.

An elaborate calibration scheme is described in the works of Galassi and Acree in which the X-wire probe is 1) examined microscopically to determine the bisector angle; 2) eyeball aligned in the calibration stand probe fixture; and, 3) calibrated through both a velocity range and an angle range (by rotating the probe). After the calibration data is

collected, the data is manipulated to determine the calibration constants A and B and the correction factor k, and then the probe is removed from the calibration stand and eyeball aligned in the tunnel probe fixture.

For this experiment, a new tunnel probe fixture was fabricated which also serves as the calibration stand probe fixture, eliminating a realignment of the probe; additionally, a new probe alignment procedure was developed. Instead of measuring the bisector angle, software was incorporated which uses the data acquisition system to measure the wire1 and wire2 voltages for a fixed jet velocity. For a bisector angle of 90 degrees and identical wires, the voltages will be identical and the bisector will be aligned with the jet when the sum of the voltages is maximized. Although no X-wires are "perfect", this method was determined to be as good as eyeballing the alignment.

Another change to the X-wire calibration procedure was the elimination of the angle calibration. As mentioned, studies (Champagne, 1965) have found that, for a limited velocity and angle range, k varies linearly with 2l/d of the probe from k = 0.2 for 2l/d = 200 to k = 0.0 for 2l/d = 600 to 800. With 2l/d = 300, our TSi T1.5 probes have k = 0.15.

The new X-wire calibration procedure is:

1. configure the calibration stand as illustrated in Figure G4;

2. install the probe in the calibration stand, paying attention to the flow geometry and wire positions;

3. execute XWIRECAL.bas and follow the instructions and prompts;

4. align the probe using the "Probe Alignment" menu selection and maximizing the voltage for a fixed jet velocity;

5. calibrate the probe by selecting "Calibrate the Probe" and following the instructions;

6. calculate the probe calibration coefficients by selecting "Calculate Coefficients" and following the instructions;

7. remove the probe/probe fixture and install in TCTF.

A typical calibration curve is illustrated in Figure G5. Since no temperature compensation is applied in this calibration configuration, a new calibration must be performed for a change in temperature of more than 5 degrees F.
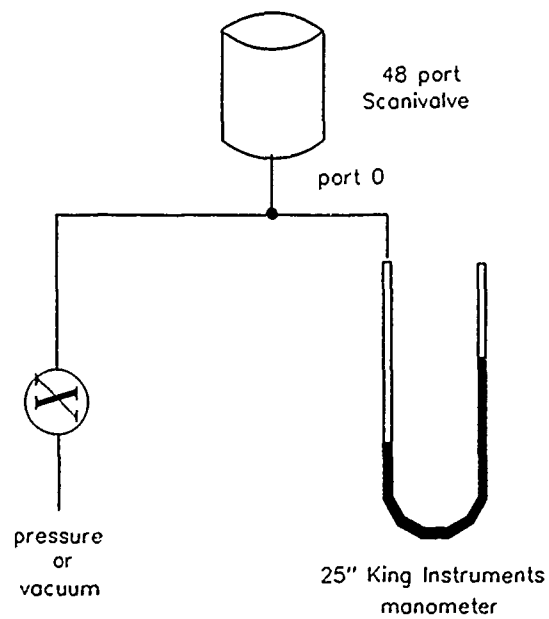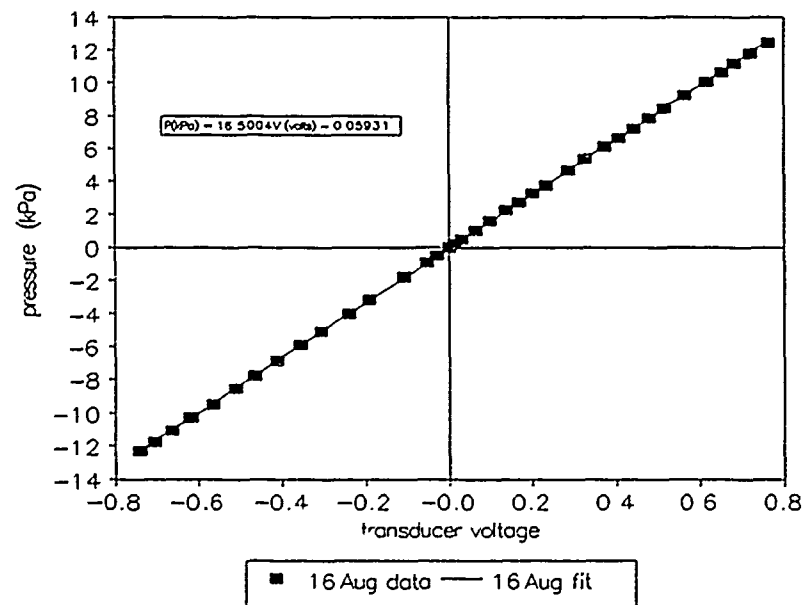
Figure G1 Pressure Calibration Setup
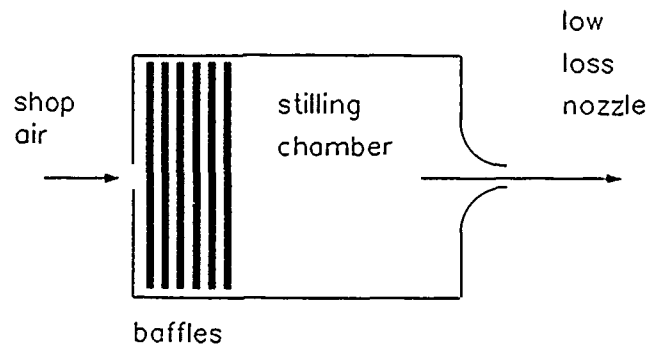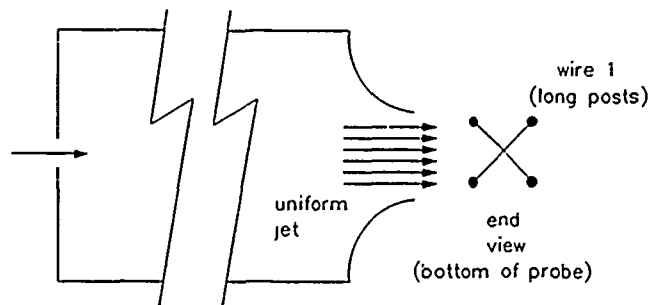

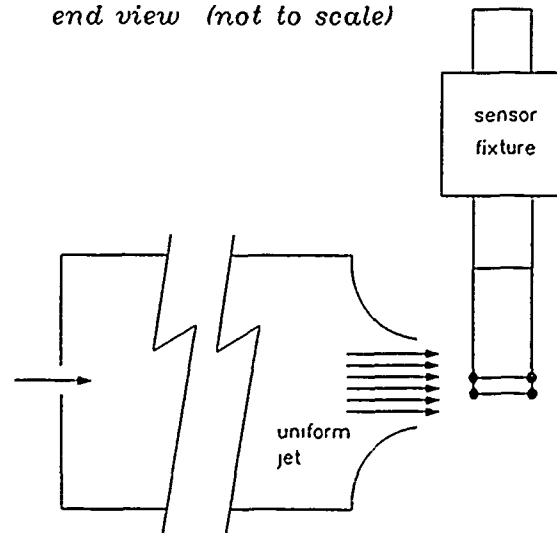Figure G2 Typical Pressure Calibration Curve

Figure G3 Hot Wire Calibration Tank

Figure G4 Hot Wire Calibration Setup
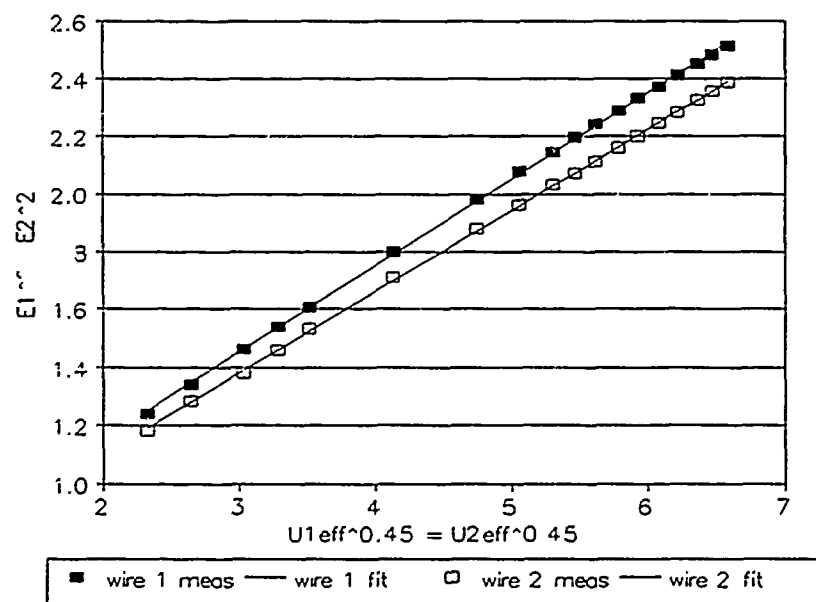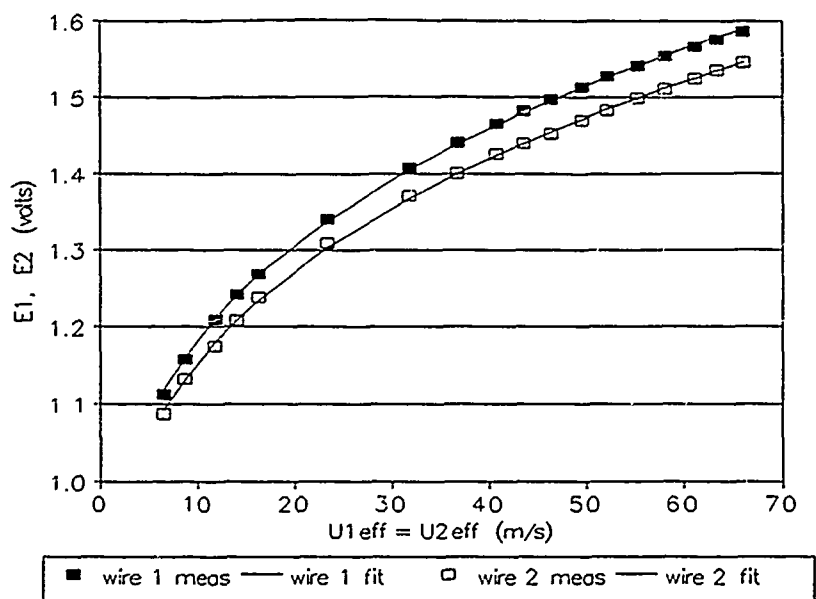
Figure G5 Typical Hot Wire Calibration Curves

REPORT DOCUMENTATION PAGE

1. AGENCY USE ONLY (Leave blank)	2. REPORT DATE	3. REPORT TYPE AND DATES COVERED
	December 1991	Master's Thesis

4. TITLE AND SUBTITLE

The Effect of the Angle of Incidence and Reynolds Number on Heat Transfer in a Linear Turbine Cascade

5. FUNDING NUMBERS

6. AUTHOR(S)

Steven G Meschwitz, Capt, USAF

7. PERFORMING ORGANIZATION NAME(S) AND ADDRESS(ES)

Air Force Institute of Technology
WPAFB OH 45433-6583

8. PERFORMING ORGANIZATION REPORT NUMBER

AFIT/GAE/ENY/91D-6

9. SPONSORING/MONITORING AGENCY NAME(S) AND ADDRESS(ES)

Dr Dick Rivir
WL/POTC WPAFB OH 45433-6583

10. SPONSORING/MONITORING AGENCY REPORT NUMBER

11. SUPPLEMENTARY NOTES

12a. DISTRIBUTION/AVAILABILITY STATEMENT

Approved For Public Release; Distribution Unlimited

12b. DISTRIBUTION CODE

13. ABSTRACT (Maximum 200 words)

The AFIT linear Turbine Cascade Test Facility (TCTF) was used to study the effect of small changes in the angle of incidence on turbine blade convective heat transfer. Other parameters in the study were the model Reynolds number and the freestream turbulence level. Cascade flow characterization tests were performed to determine the feasibility of the study followed by a series of tests designed to separate the effects of the angle of incidence, Reynolds number, and freestream turbulence level on the convective heat transfer. For a given freestream turbulence level or angle of incidence, there is an increase in the heat transfer coefficient for an increase in the Reynolds number. For the low freestream turbulence level (0.5%) configuration at a given Reynolds number, there is a decrease in the convective heat transfer coefficient with an increase in the angle of incidence. For the high freestream turbulence configuration (10%), at any Reynolds number, there is an increase in convective heat transfer over that for the low turbulence configuration, however, the variation in the heat transfer coefficient with the angle of incidence is not as distinct as for the low turbulence configuration.

14. SUBJECT TERMS

turbine cascade, heat transfer, turbulence

15. NUMBER OF PAGES

185

17. SECURITY CLASSIFICATION OF REPORT	18. SECURITY CLASSIFICATION OF THIS PAGE	19. SECURITY CLASSIFICATION OF ABSTRACT	20. LIMITATION OF ABSTRACT
Unclassified	Unclassified	Unclassified	Unlimited

GENERAL INSTRUCTIONS FOR COMPLETING SF 298

The Report Documentation Page (RDP) is used in announcing and cataloging reports. It is important that this information be consistent with the rest of the report, particularly the cover and title page. Instructions for filling in each block of the form follow. It is important to **stay within the lines to meet optical scanning requirements.**

Block 1. Agency Use Only (Leave Blank)

Block 2. Report Date. Full publication date including day, month, and year, if available (e.g. 1 Jan 88). Must cite at least the year.

Block 3. Type of Report and Dates Covered. State whether report is interim, final, etc. If applicable, enter inclusive report dates (e.g. 10 Jun 87 - 30 Jun 88).

Block 4. Title and Subtitle. A title is taken from the part of the report that provides the most meaningful and complete information. When a report is prepared in more than one volume, repeat the primary title, add volume number, and include subtitle for the specific volume. On classified documents enter the title classification in parentheses.

Block 5. Funding Numbers. To include contract and grant numbers; may include program element number(s), project number(s), task number(s), and work unit number(s). Use the following labels:

C	- Contract	PR	- Project
G	- Grant	TA	- Task
PE	- Program Element	WU	- Work Unit Accession No.

Block 6. Author(s). Name(s) of person(s) responsible for writing the report, performing the research, or credited with the content of the report. If editor or compiler, this should follow the name(s).

Block 7. Performing Organization Name(s) and Address(es). Self-explanatory.

Block 8. Performing Organization Report Number. Enter the unique alphanumeric report number(s) assigned by the organization performing the report.

Block 9. Sponsoring/Monitoring Agency Names(s) and Address(es). Self-explanatory.

Block 10. Sponsoring/Monitoring Agency. Report Number. (If known)

Block 11. Supplementary Notes. Enter information not included elsewhere such as: Prepared in cooperation with...; Trans. of ..., To be published in .... When a report is revised, include a statement whether the new report supersedes or supplements the older report.

Block 12a. Distribution/Availablity Statement. Denote public availability or limitation. Cite any availability to the public. Enter additional limitations or special markings in all capitals (e.g. NOFORN, REL, ITAR)

DOD	- See DoDD 5230.24, "Distribution Statements on Technical Documents."
DOE	- See authorities
NASA	- See Handbook NHB 2200.2.
NTIS	- Leave blank.

Block 12b. Distribution Code.

DOD	- DOD - Leave blank
DOE	- DOE - Enter DOE distribution categories from the Standard Distribution for Unclassified Scientific and Technical Reports
NASA	- NASA - Leave blank
NTIS	- NTIS - Leave blank.

Block 13. Abstract. Include a brief (Maximum 200 words) factual summary of the most significant information contained in the report.

Block 14. Subject Terms. Keywords or phrases identifying major subjects in the report.

Block 15. Number of Pages. Enter the total number of pages.

Block 16. Price Code. Enter appropriate price code (NTIS only).

Blocks 17. - 19. Security Classifications. Self-explanatory. Enter U.S. Security Classification in accordance with U.S. Security Regulations (i.e., UNCLASSIFIED). If form contains classified information, stamp classification on the top and bottom of the page.

Block 20. Limitation of Abstract. This block must be completed to assign a limitation to the abstract. Enter either UL (unlimited) or SAR (same as report). An entry in this block is necessary if the abstract is to be limited. If blank, the abstract is assumed to be unlimited.